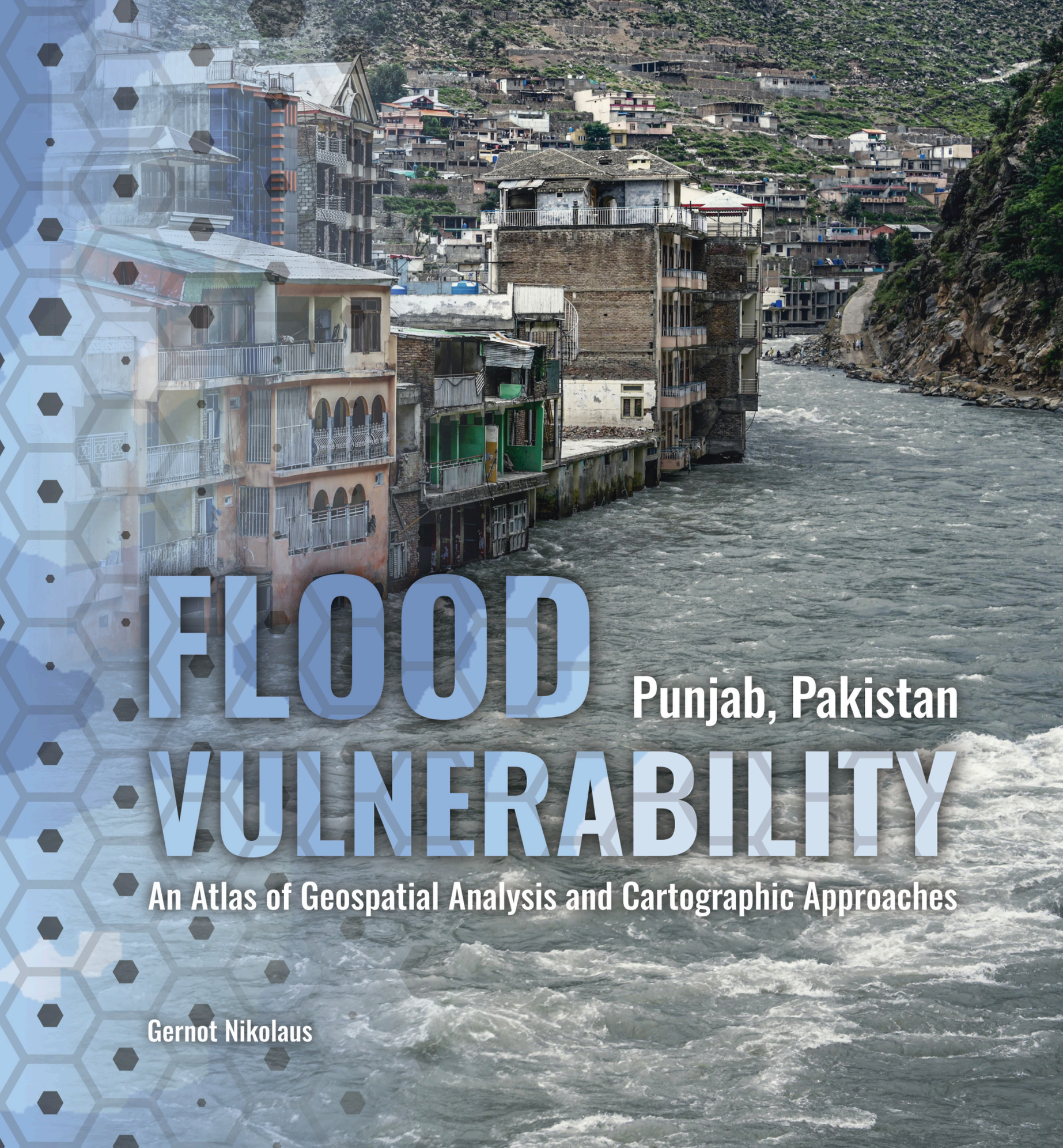

FLOOD VULNERABILITY

Punjab, Pakistan

An Atlas of Geospatial Analysis and Cartographic Approaches

Gernot Nikolaus

Flood Vulnerability in Punjab, Pakistan: An Atlas of Geospatial Analysis and Cartographic Approaches

Atlas

Author: Gernot Nikolaus
Institution: Palacký University Olomouc; University of Salzburg
Department: Department of Geoinformatics; Department of Geoinformatics, Z_GIS
Degree Program: Copernicus Master in Digital Earth
Submitted: May, 2025

Imprint

This atlas was created as part of the Master's thesis:
"Flood Vulnerability in Punjab, Pakistan: A Geospatial Analysis and Cartographic Approach"
Submitted to Palacký University Olomouc and the University of Salzburg in partial fulfillment of the requirements for the degree of Master of Science (MSc).

Copyright Notice

© 2025 Gernot Nikolaus
All rights reserved.
No part of this atlas may be reproduced, distributed, or modified in any form or by any means – electronic, mechanical, photocopying, recording, or otherwise – without the prior written permission of the author.
All maps, graphics, and analyses were created by the author unless otherwise stated.
Data sources include: Pakistan Bureau of Statistics, Sentinel-1 (via Google Earth Engine), FABDEM, OpenStreetMap, and other publicly available datasets.

Disclaimer

The author assumes no responsibility for any errors, omissions, or inaccuracies in the data, analysis, or cartographic representations presented in this atlas. The boundaries, names, and designations used in the maps do not imply any official endorsement or opinion concerning the legal status of any territory or area.
This work is intended for academic and illustrative purposes only. While every effort has been made to ensure accuracy, the author cannot guarantee the completeness or reliability of the information presented.
Use of this atlas and its contents is at the user's own risk.

Edition: First Edition – April 2025
Version: 1.0

Letter from the author

This atlas was compiled as part of my master's thesis 'Flood Vulnerability in Punjab, Pakistan: A Geospatial Analysis and Cartographic Approach".

Floods are one of the most severe catastrophic events, demanding human lives, leading to displacement, and the destruction of homes, infrastructure, and livelihoods. Climate change exacerbates the frequency and intensity of such hazards - not only floods, but also others, such as droughts, sea level rise, and wildfires.

While climate change is a global issue, it mainly affects the Global South. Millions of people are already forced to migrate due to hunger, conflict, and environmental collapse. Everyone has the right to a safe, dignified life - something many of us take for granted because of the privileges we have been given.

I believe climate change is one of the greatest challenges of our era - and we are running out of time. One of the barriers we face is the narrow-mindedness, denail, and indifference, especially those who think they are not affected. But we are all connected, and the suffering of others is not something we can afford to ignore.

The geospatial analysis was conducted, maps were created, and the atlas was compiled to support flood mitigation in Punjab, Pakistan, but also to raise awareness of climate impacts globally, through the lens of flooding. My hope is that it fosters understanding, empathy, and action.

Let us stop thinking only of ourselves, and instead be open to others - regardless of where they come from, their ethnicity, impairment, gender, sexual orientation, religion, or any other characteristics that make them who they are. We all share this planet, and we must care for it - and for each other - together.

Gernot Nikolaus

Content

Introduction **08**

How to Read 10

Flood Vulnerability 12

Methodologies in Flood Vulnerability Assessment 13

Study Area 14

The Flood Vulnerability Index 16

Flood-Prone Component **20**

Distance to the River 24

Drainage Density 26

Elevation 28

Land Use Land Cover 30

Slope 32

Topographic Wetness Index 34

Flood-Prone Component 36

Flood-Prone Component at Tehsil level 38

Population Susceptibility Component **42**

Dependent Population 44

Disabled Population 46

Female Population 48

Population Density 50

Population Susceptibility Component 52

Population Susceptibility Component at Tehsil level 54

Coping Capacity Component **58**

Distance to Health Facilities 60

Literacy Rate 62

Coping Capacity Component 64

Coping Capacity Component at Tehsil level 66

Flood Vulnerablity Index **70**

Flood Vulnerability Index 72

Flood Vulnerability Index at Tehsil level 74

Flood Vulnerability Index interpolated per 50 km^2 76

Flood Vulnerability Index interpolated per 10 km^2 77

Flood Vulnerability, a holistic view of FPC, PSC, and CCC 78

Flood Vulnerability, a holistic view at FPC and people's vulnerability 80

Flood Vulnerability per 10 km^2 81

Discussion **84**

Conclusion **86**

References **88**

Introduction

Flooding is one of the greatest dangers globally, which not only destroys infrastructure and damages the economy, but also claims human lives (Bates et al., 2008; Kundzewicz et al., 2014; Rentschler, Salhab and Jafino, 2022; Chen et al., 2024). Pakistan, especially the Punjab region, is affected frequently by floods, due to its high population density, agricultural activities, and the presence of five major rivers (Rahman et al., 2017; Waseem and Rana, 2023; Chen et al., 2024). Yearly flood events are exacerbated by climate change (Aldous et al., 2011; Arnell and Gosling, 2013; Kundzewicz et al., 2014; Youssef et al., 2021) thus demanding for effective flood assessments and effective mitigation strategies.

To address flooding globally, researchers have turned to flooding models in combining remote sensing data, Geographical Information System (GIS) techniques, and various flood drivers, to assess the flood challenge in a study area (Gigović et al., 2017; Hoque et al., 2019; Burayu, Karuppannan and Shuniye, 2023; Hossain and Mumu, 2024; Ibrahim et al., 2024; Roy and Dhar, 2024; Ullah et al., 2024). While remote sensing provides important data about topographic conditions, the GIS environment gives the opportunity to store and process this data. Depending on the study and the area, different parameters are chosen and their influence on the study's model is determined.

The flood danger and the large number of people affected in the Punjab province was the motivation for this study. Although global research on flooding exists, only a few studies concentrate on Pakistan, and fewer on the highly affected Punjab region. Studies in Punjab mainly focus on the assessment of areas that are prone to floods and where flooding occurs, but the population is not taken into account.

As flood events not only affect the landscape, but also communities, it is important to investigate flooding from a multi-dimensional perspective. Such a perspective is used in this master's thesis by developing a flood vulnerability framework. This framework consists of three components which are used to highlight areas most vulnerable to flooding. While one component considers physical and environmental factors, the others reflect the affected population. Another motivation lies in the mapping of the results. Recognizing that good visualizations, which effectively communicate the results, are missing in existing flood research, this study also focuses on creating visually appealing maps. Different mapping techniques are developed and evaluated in user testing to come to a visualization which works for different users.

All results of the master's thesis are compiled into this atas, making the outcomes tangible and accessible not only for informing a decision but also for the general or local population.

The full thesis text ca be accessed via the QR code or at https://gernotnikolaus.github.io/MasterThesis_FloodVulnerabilityPunjab. The digital version of the atlas is also available there.

How to Read

This atlas presents a geospatial analysis of flood vulnerability in Punjab, Pakistan. It is designed for both academic and dessicion-makers, as well as the general public.

The atlas is divided into thematic sections corresponding to the components of the analysis: Flood-Prone Component (FPC), Population Susceptibility Component (PSC), Coping Capacity Component (CCC), and the Flood Vulnerability Index (FVI). Each components has its own parameters which are analyzed, discussed, and presented in maps and figures (Figure 1.1).

As the aim of the atlas was intended to provide for both, the general public, as well as decision-makers, a good overview of flood vulnerability in the study region, the atlas provides information in different details.

Seeing this symbol, the text provides more detailed information, how the map, or the parameter was processed.

Seeing this symbol, the text provides more information of the results of the analysis.

Seeing this symbol, the text provides a quick summary of the processing steps and the results.

Furthermore, color schemes are consistent throughout the atlas and correspond to the respective components for easier navigation and interpretation.

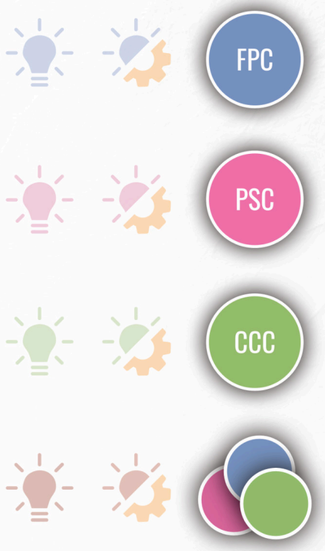

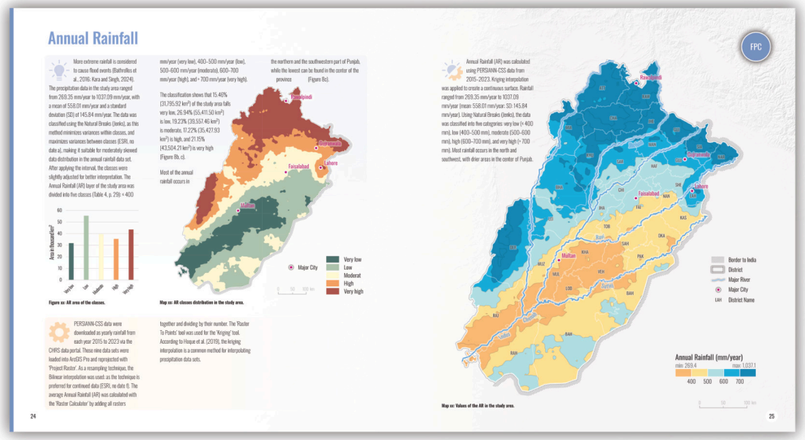

Figure 1.1: Analysis of the Annual Rainfall parameter.

After each parameter within a component is discussed, the respective component maps is presented in detail. This includes visualizations using administrative boundaries, along with a table identifying which districts are most affected (e.g., Figure 1.2).

At the end of the atlas, the overall Flood Vulnerability Index (FVI) is visualized through various cartographic approaches, including aggregation, interpolation, and separate visualizations of each component (e.g., Figure 1.3).

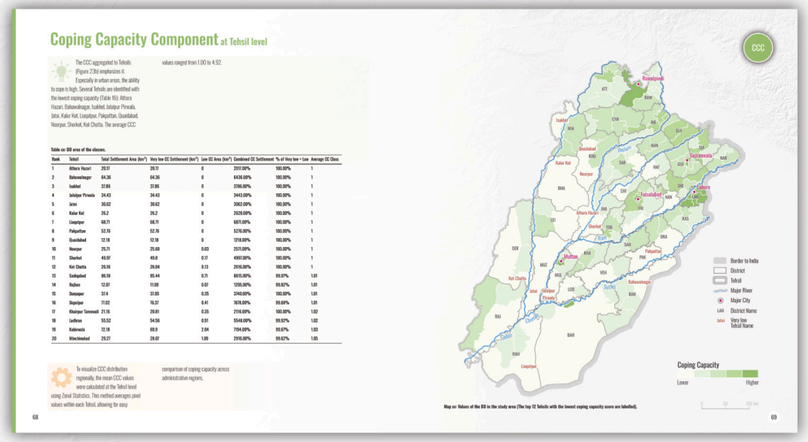

Figure 1.2: Presenting of the results of a component.

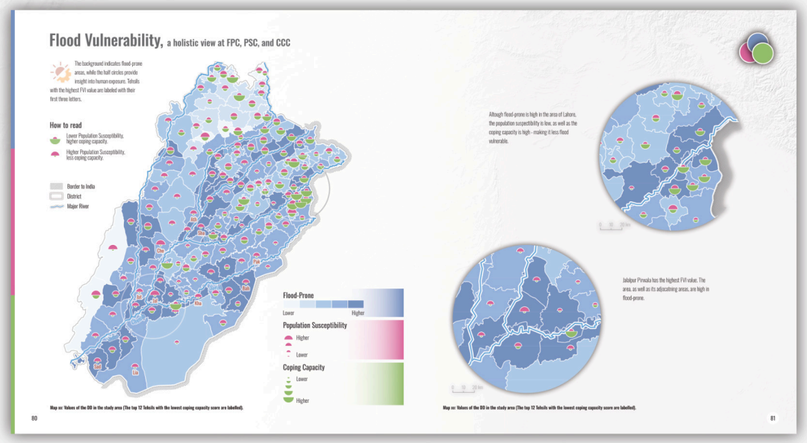

Figure 1.3: Values of the AR in the study area.

Flood Vulnerability

Floods are among the most severe disasters, affecting millions of people every year. In countries like Pakistan, where large populations live near rivers and fertile floodplains, the threat is especially high. As climate change continues to alter weather patterns, flood events are becoming more frequent and intense; and putting vulnerable communities at even greater risk.

This atlas aims to visualize and analyze flood vulnerability in Punjab, Pakistan, using a geospatial and cartographic approach. By combining scientific data with intuitive maps, the goal is to support better decision-making, improve awareness, and contribute to long-term flood mitigation efforts.

Flooding is one of the most widespread hazards, occurring across various regions and time periods, and affecting large populations worldwide (Bates et al., 2008; Kundzewicz et al., 2014; Bathrellos et al., 2018; Rentschler, Salhab and Jafino, 2022). Floods are a physical phenomenon; when rivers overtop their banks, water flows into the floodplain, which is favored for settlements because they are fertile and near water, thereby increasing the likelihood of flood-related disasters (Bathrellos et al., 2018). According to Rentschler, Salhab and Jafino (2022), 23% of the population worldwide is exposed to floodwaters exceeding 0.15 meters in depth. The majority of those exposed reside in South and East Asia, where 1.24 billion people live in areas at risk. Moreover, climate change has an impact and influence on floods, increasing both the intensity as well as the occurrence of flooding (Aldous et al., 2011; Arnell and Gosling, 2013; Kundzewicz et al., 2014; Youssef et al., 2021). According to Bates et al. (2008) flooding is influenced by various climate factors, such as precipitation and temperature patterns. Additionally, drainage also plays a significant role, as well as urbanization, and the presence of flood management structures like dams or reservoirs.

Floods pose a significant risk to both lives and livelihoods, particularly for vulnerable communities (Rentschler, Salhab and Jafino (2022). Vulnerability is a crucial component in risk management and damage assessment (Connor and Hiroki, 2005; Huang et al., 2012). However, the definition is not fixed; different definitions of the term 'Vulnerability' appear in literature, as well as different concepts of it have been created (IPCC, 2012; Nasiri, Mohd Yusof and Ali, 2016). Furthermore, its meaning evolved over time. For example, the IPCC Third Assessment Report defines vulnerability as a function of exposure, sensitivity, and adaptive capacity (IPCC, 2001). Then, the Fifth Assessment Report redefined the vulnerability's definition and excluded exposure from it (IPCC, 2014). Since then, vulnerability is seen as a function of sensitivity and the capacity to cope and adapt (IPCC, 2022). According to Proag (2014), vulnerability is "the degree to which a system, or part of a system, may react adversely during the occurrence of a hazardous event". For UNDP (2004) human vulnerability is the "human condition or process resulting from physical, social, economic and environmental factors, which determine the likelihood and scale of damage from the impact of a given hazard". Balica and Wright (2010) define vulnerability as the interaction between exposure, susceptibility, and resilience of each community in risk conditions. Nasiri et al. (2016) state that a human system is vulnerable to these three factors. Furthermore, several studies define vulnerability as a function of exposure, sensitivity, and adaptive capacity (Balica and Wright, 2009; Thomas et al., 2018). Additionally, some studies equate sensitivity with susceptibility (Nasiri, Mohd Yusof and Ali, 2016; Padhan and Madheswaran, 2023), and capacity with resilience or adaptive capacity (Balica, Douben and Wright, 2009; Padhan and Madheswaran, 2023).

Several terms appear during the definition of vulnerability: exposure, sensitivity, and capacity. The UNDRR defines exposure as the "situation of people, infrastructure, housing, production capacities and other tangible human assets located in hazard-prone areas" (UNDRR, 2009). Other studies defined it as the chance that people and/or physical items will be affected by floods (Padhan and Madheswaran, 2023). Sensitivity is the "extent to which an element of the system is exposed which in turn influences the chance of being harmed at the time of occurrence of flooding events" (IPCC, 2001). Resilience is defined as "the capacity of a system, community or society to resist or to change in order that it may obtain an acceptable level in functioning and structure." (UNDP, 2004).

Methodologies in Flood Vulnerability Assessment

The assessments of flood vulnerability have become increasingly important in understanding and mitigating flood risks. While different approaches for assessing flood risk exist, such as hydrologic and hydraulic modeling, as well as the use of artificial intelligence and machine learning (Kumar et al., 2023), the use of Geographic Information Systems (GIS), remote sensing (RS), and Multi-Criteria Decision Analysis (MCDA) provides an approach to evaluating both, the spatial extent and the vulnerability of a population to flooding events, as proven in several studies (Gigović et al., 2017; Hoque et al., 2019; Burayu, Karuppannan and Shuniye, 2023; Hossain and Mumu, 2024; Ibrahim et al., 2024; Roy and Dhar, 2024; Ullah et al., 2024).

GIS and remote sensing data have become important tools for flood disaster monitoring and management (Kabenge et al., 2017). GIS provides a framework for integrating, analyzing, and visualizing spatial data, such as data on topography, land use, precipitation, river networks, and historical flood records (Kabenge et al., 2017; Hoque et al., 2019; Ullah et al., 2024). While satellite imagery may be used to identify flood-prone areas and to evaluate flood extents (Kabenge et al., 2017), with digital elevation models (DEM), derived from remote sensing, areas where flooding most likely occurs during flooding events can be identified (Coveney and Roberts, 2017). According to Kumar et al. (2023), generally, the steps of a remote sensing and GIS-based flooding model exist of the following: data acquisition, preprocessing, flood modeling, and forecasting future floods. First, the data for the respective studies required is gathered, remote sensing data preprocessed, e.g., radiometric calibration, as well as the data processed in the GIS environment, e.g., geo-referenced. With image analysis methods, such as thresholding or image segmentation, floods are detected, and affected areas are identified. Flood maps are developed to draw a picture of the range and intensity of flooding. This flood mapping technique helps to identify flood-prone areas and to create strategies for flood mitigation (Sanders et al., 2020). To enhance the model's accuracy, their input parameters are calibrated (Jahandideh-Tehrani et al., 2020). Using data from field observation or other data sources, the flooding mapping results are validated, to improve their accuracy further (Molinari et al., 2019), ensuring that the models represent real-world flood events, and are able to predict future floods and provide early warnings to vulnerable populations (Kumar et al., 2023).

The Multi-Criteria Decision Analysis (MCDA) is a method that helps decision-makers to make well-informed decisions when dealing with complex criteria (Evers, Almoradie and de Brito, 2018). The combination of MCDA and GIS has become increasingly popular for evaluating different factors in flood modeling (Hossain and Mumu, 2024); one widely used MCDA technique is the Analytical Hierarchy Process (AHP) as shown in several studies (Hoque et al., 2019; Aydin and Sevgi Birincioğlu, 2022; Burayu, Karuppannan and Shuniye, 2023; Kara and Singh, 2024; Ullah et al., 2024; Zhran et al., 2024). The AHP method involves breaking down the flood problem into a hierarchy of parameters and then conducting pairwise comparisons among them. Through expert judgment, relative weights are assigned to each criterion, which reflects their importance in influencing flooding. According to Ouma and Tateishi (2014) the AHP consists of four steps: creating the decision hierarchy, determining the relative importance of factors, calculating their weighting, and checking the consistency with the consistency ratio.

According to Kumar et al. (2023), future flood models that leverage remote sensing data and GIS hold great potential in analyzing and managing flood risk more effectively. The quality and availability of geospatial data are increasing, making it possible for better flood modeling. The combination of GIS and AHP offers advantages, particularly in flood vulnerability analysis. GIS enables the calculation of parameters. At the same time, AHP allows for prioritizing these factors (Ouma and Tateishi, 2014).

Study Area

The study area – Punjab, Pakistan – is one of the five provinces of Pakistan (Map 1.1). According to the Pakistan Bureau of Statistic (PBS), almost 130 million people live in the region. Although it is not the largest region, it is the most populated one in Pakistan (PBS, 2023). The region spans an area of 205,345 km² and borders India on the eastern side. The PBS divides the province in their census into 36 districts, as well as 146 Tehsils; these are the administrative regions below the district level. The presence of the five major rivers – Indus, Jhelum, Chenab, Ravi as well as Sutlej – has made Punjab an agricultural center of the country, but prone to catastrophic flooding (Rahman et al., 2017).

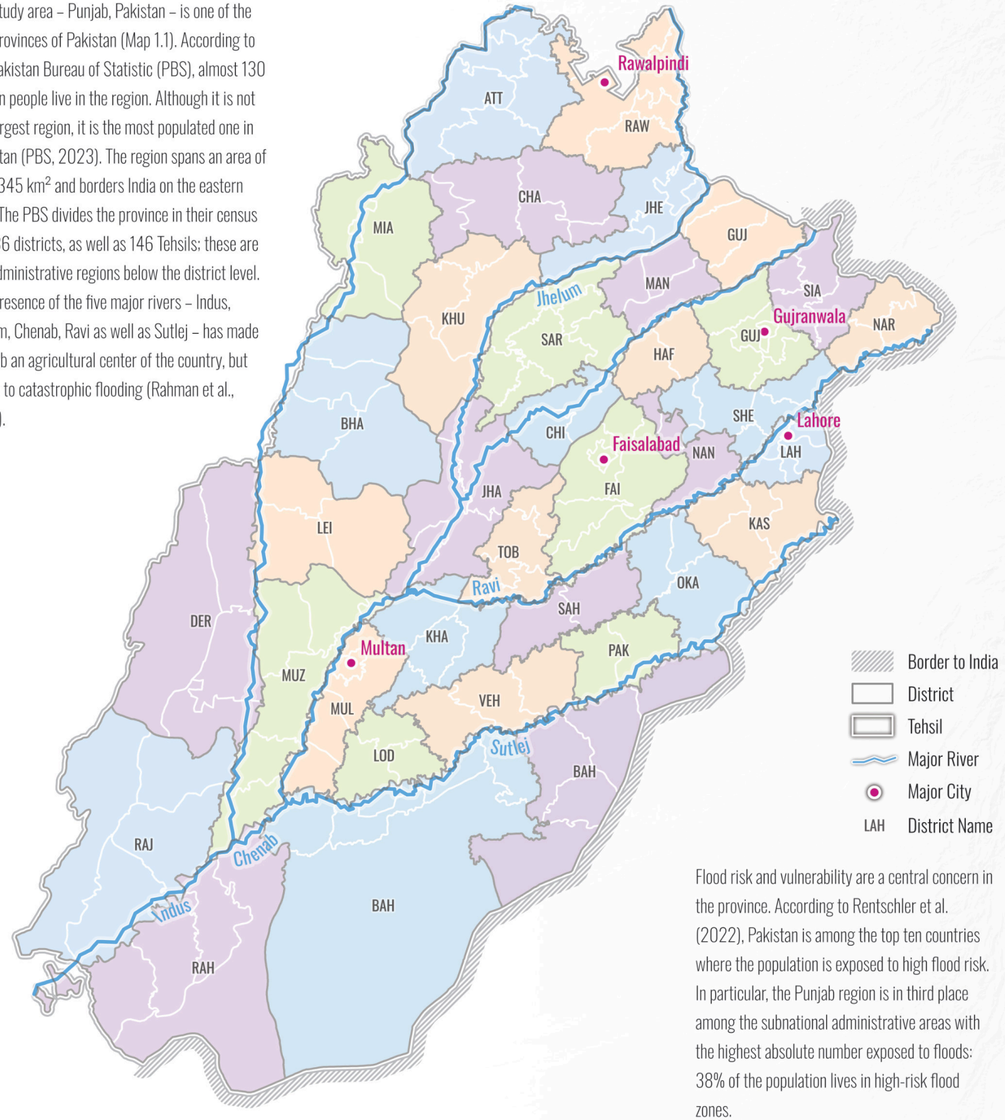

Flood risk and vulnerability are a central concern in the province. According to Rentschler et al. (2022), Pakistan is among the top ten countries where the population is exposed to high flood risk. In particular, the Punjab region is in third place among the subnational administrative areas with the highest absolute number exposed to floods: 38% of the population lives in high-risk flood zones.

0 50 100 km

Map 1.1: Study Area Punjab.

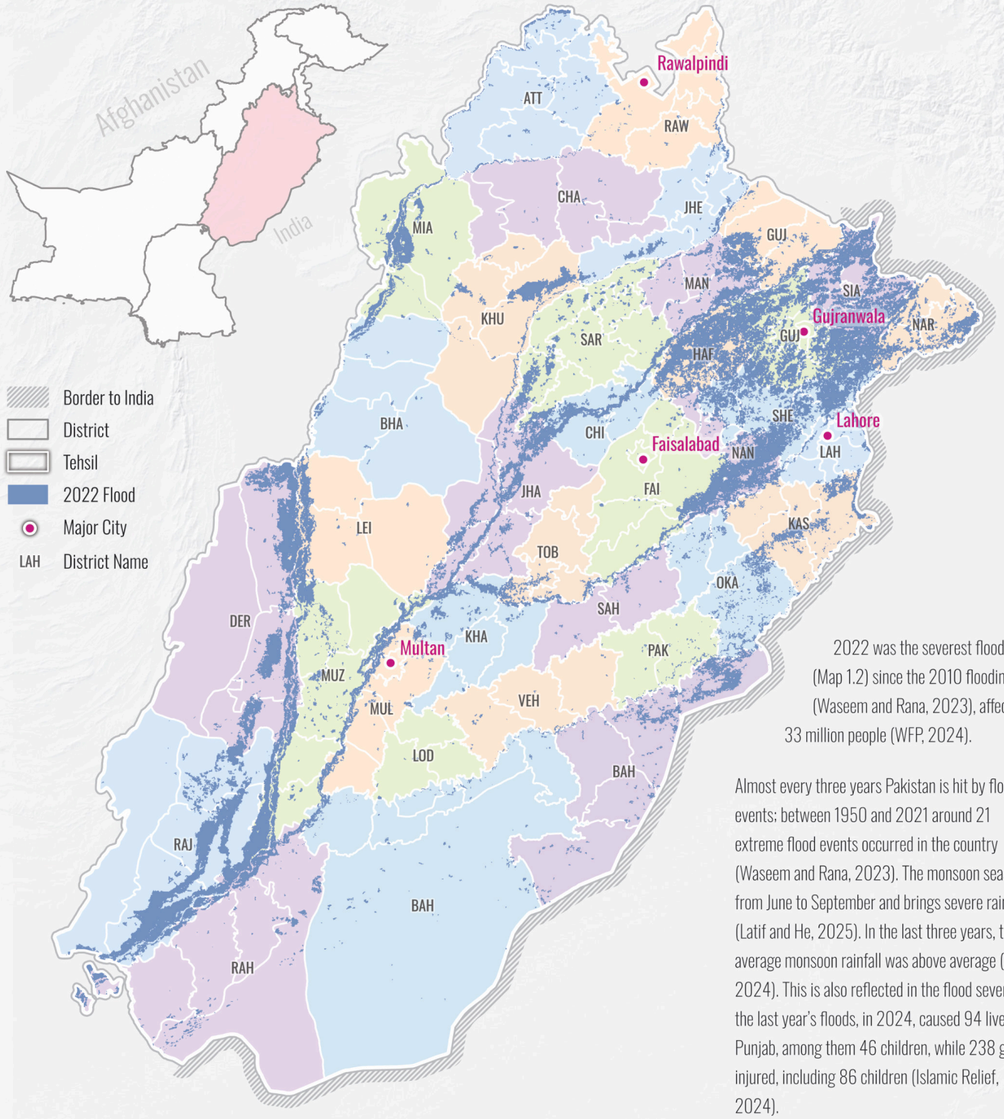

2022 was the severest flood (Map 1.2) since the 2010 flooding (Waseem and Rana, 2023), affecting 33 million people (WFP, 2024).

Almost every three years Pakistan is hit by flood events: between 1950 and 2021 around 21 extreme flood events occurred in the country (Waseem and Rana, 2023). The monsoon season is from June to September and brings severe rainfall (Latif and He, 2025). In the last three years, the average monsoon rainfall was above average (PMD, 2024). This is also reflected in the flood severity, the last year's floods, in 2024, caused 94 lives in Punjab, among them 46 children, while 238 got injured, including 86 children (Islamic Relief, 2024).

0 50 100 km

Map 1.2: Extent of the 2022 Flood in Punjab.

The Flood Vulnerability Index

Different datasets were used for the different parameters used in this study (Table 1.1). PERSIANN-CSS (Precipitation Estimation from Remotely Sensed Information using Artificial Neural Networks - Cloud Classification System) data was used for the Annual Rainfall, downloaded via the CHRS data portal (CHRS, no date). The Drainage Density, Elevation, Slope, and Topographic Wetness Index were obtained from the FABDEM (Forest And Buildings removed Copernicus 30m DEM). FABDEM is a product from the Copernicus GLO 30 Digital Elevation Model (DEM), delivering a resolution of 1 arc-second grid spacing (approximately 30m at the equator), whereas errors of buildings and vegetation were removed (Hawker et al., 2022). The WorldCover V2 2021 was used for the Land Use Land Cover (Zanaga et al., 2022). Health facilities were downloaded provided by the Humanitarian OpenStreetMap Team via the Humanitarian Data Exchange portal (HDX, no date a); the same applies to the river stream data (HDX, no date b). The census data of 2023 was accessed at the Pakistan Bureau of Statistics website (PBS, 2023), and downloaded as PDFs.

Table 1.1: Data sources.

Data Type	Output Criteria	Data Source	Period, Time, Version	Resolution
Sentinel-1	Previous Flood for validation	Google Earth Engine	2021-2024	10 m
ESA WorldCover 10m	Land Use Land Cover	WorldCover	2021	10 m
FABDEM (Forest And Buildings removed Copernicus DEM)	Drainage Density, Elevation, Slope, TWI	Google Earh Engine	2023	30 m
OpenStreetMap	Distance to river	HOT OSM	Modified: 8 January 2025	0.04° x 0.04°
PERSIANN-CCS	Annual Rainfall	CHRS	2015-2023	(4km)
Census	Dependent Population, Disabled Population, Female Population	Pakistan Bureau of Statistics	2023	Admin3 (Tehsil)
	Population Density, Literacy Rate			
OpenStreetMap	Distance to Health Facilities	HOT OSM	Modified: 8 January 2025	Lat., Long

The different criteria were selected based on the literature review, studies as well as consulting with experts (Table 1.2). As literature has shown that flood vulnerability is a multidimensional concept that includes environmental, demographic, and socioeconomic factors, a Flood Vulnerability Index (FVI) was compiled, using three parts (Figure 1.4): Flood-Prone Component (FPC), Population Susceptibility Component (PSC), and Coping Capacity Component (CCC).

This framework explicitly incorporates human vulnerability factors to flood-prone parameters, ensuring a holistic perspective on flood impacts. Furthermore, recognizing the lack of communication, this study employs mapping approaches that prioritize clarity and usability. Based on user testing, different visualization techniques were evaluated, merging the three components together, or visualizing them separately, to determine effective ways to represent flood vulnerability.

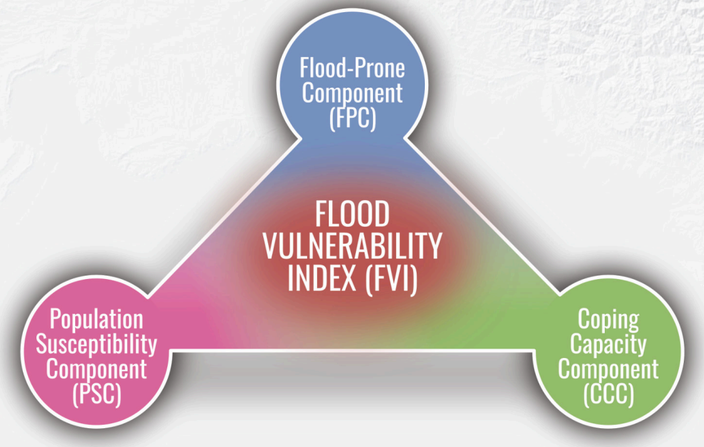

Figure 1.4: Flood Vulnerability Index and its components.

Table 1.2: Parameters of the components.

Components of FVI	Criteria
Flood-Prone Component (FPC)	Annual Rainfall (mm/y)
	Distance to River (m)
	Drainage Density (m/km²)
	Elevation (m)
	Land Use Lanc Cover
	Slope (°)
	TWI
Population Susceptibility Component (PSC)	Dependent Population (%)
	Disabled Population (%)
	Female Population (%)
	Population Density (km²)
Coping Capacity Component (CCC)	Distance To Health Facilities (m)
	Literacy Rate (%)

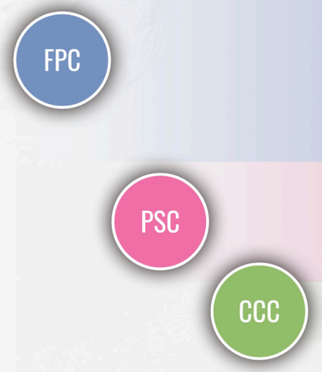

FPC

Flood-Prone Component

Annual Rainfall
Distance to the River
Drainage Density
Elevation
Land Use Land Cover
Slope
Topographic Wetness Index
Flood-Prone Component
Flood-Prone Component at Tehsil level

One component of the Flood Vulnerability Index (FVI) Model is the Flood-Prone Component (FPC). As vulnerability is determined by physical and natural factors (Hoque et al., 2019), the FPC represents the physical and environmental factors influencing flood occurrence. According to (Ullah et al., 2024), the mapping of flood-prone areas is a crucial method for flood management and risk reduction planning, as it helps in generating more effective results. To assess the exposure of the study area to flooding, seven environmental and hydrological parameters were integrated that influence the occurrence of floods (Table 1.2): Annual Rainfall (AR), which represents the precipitation of rainfall, considering that more extreme rainfall is a driver of flooding (Bathrellos et al., 2016; Kara and Singh, 2024); the Distance to the River (DR) which is the proximity to channels influencing flood-prone (Fernández and Lutz, 2010); the Drainage Density (DD) measures the extent of drainage networks affecting runoff concentration and therefore with higher drainage to a higher flooding (Subbarayan and Saravanan, 2020); the Elevation (EL) as lower elevation experiences higher flood risk (Sanyal and Lu, 2006; Rahman et al., 2019; Allafta and Opp, 2021); the Land Use Land Cover (LULC) – classifying objects, such as buildings, vegetation, and cropland – determining surface permeability and potential water retention capacity (Price, Jackson and Parker, 2010; Owuor et al., 2016; Mojaddadi et al., 2017; Ogato et al., 2020a; Allafta and Opp, 2021; Chen et al., 2024; Ullah et al., 2024); the Slope (SL) as flat surfaces are more at risk (Gigović et al., 2017); and the Topographic Wetness Index (TWI) quantifies the topography and soil moisture (Roy and Dhar, 2024).

Annual Rainfall

More extreme rainfall is considered to cause flood events (Bathrellos et al., 2016; Kara and Singh, 2024). The precipitation data in the study area ranged from 269.35 mm/year to 1037.09 mm/year, with a mean of 558.01 mm/year and a standard deviation (SD) of 145.84 mm/year. The data was classified using the Natural Breaks (Jenks), as this method minimizes variances within classes, and maximizes variances between classes (esri, no date a), making it suitable for moderately skewed data distribution in the annual rainfall data set. After applying the interval, the classes were slightly adjusted for better interpretation. The Annual Rainfall (AR) layer of the study area was divided into five classes: ≤ 400 mm/year (very low), 400–500 mm/year (low), 500–600 mm/year (moderate), 600–700 mm/year (high), and > 700 mm/year (very high).

The classification shows that 15.46% (31,795.92 km^2) of the study area falls very low, 26.94% (55,411.50 km^2) is low, 19.23% (39,557.46 km^2) is moderate, 17.22% (35,427.93 km^2) is high, and 21.15% (43,504.21 km^2) is very high (Figure 2.1, Map 2.1).

Most of the AR occurs in the northern and the southwestern part of Punjab, while the lowest can be found in the center of the province (Map 2.2).

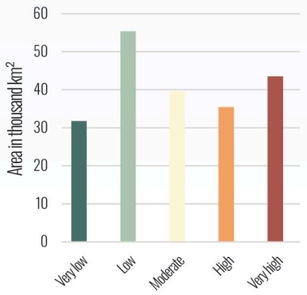

Figure 2.1: Distribution of Annual Rainfall classes by area (km^2).

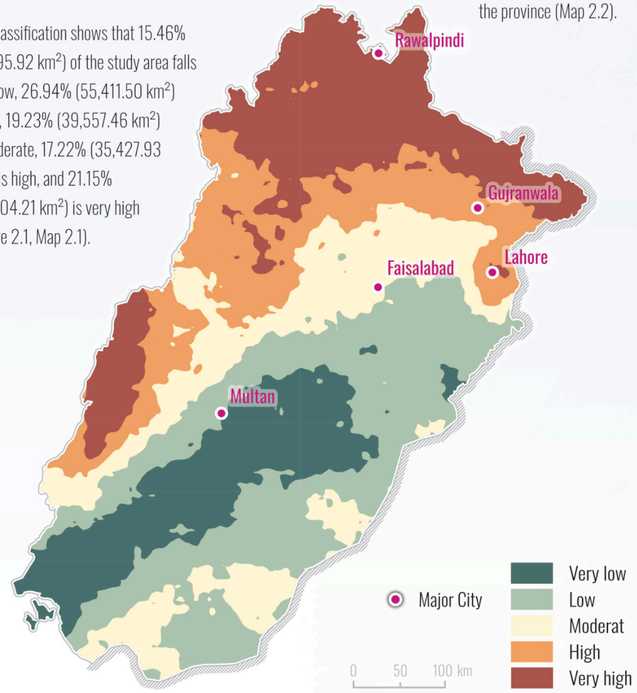

Map 2.1: Annual Rainfall classes distribution in the study area.

PERSIANN-CSS data were downloaded as yearly rainfall from each year 2015 to 2023 via the CHRS data portal. These nine data sets were loaded into ArcGIS Pro and reprojected with 'Project Raster'. As a resampling technique, the Bilinear interpolation was used; as the technique is preferred for continued data (esri, no date f). The average Annual Rainfall (AR) was calculated with the 'Raster Calculator' by adding all rasters together and dividing by their number. The 'Raster To Points' tool was used for the 'Kriging' tool. According to Hoque et al. (2019), the kriging interpolation is a common method for interpolating precipitation data sets.

FPC

Annual Rainfall (AR) was calculated using PERSIANN-CSS data from 2015–2023. Kriging interpolation was applied to create a continuous surface. AR ranged from 269.35 mm/year to 1037.09 mm/year (mean: 558.01 mm/year; SD: 145.84 mm/year). Using Natural Breaks (Jenks), the data was classified into five categories: very low (≤ 400 mm), low (400–500 mm), moderate (500–600 mm), high (600–700 mm), and very high (> 700 mm). Most rainfall occurs in the north and southwest, with drier areas in the center of Punjab.

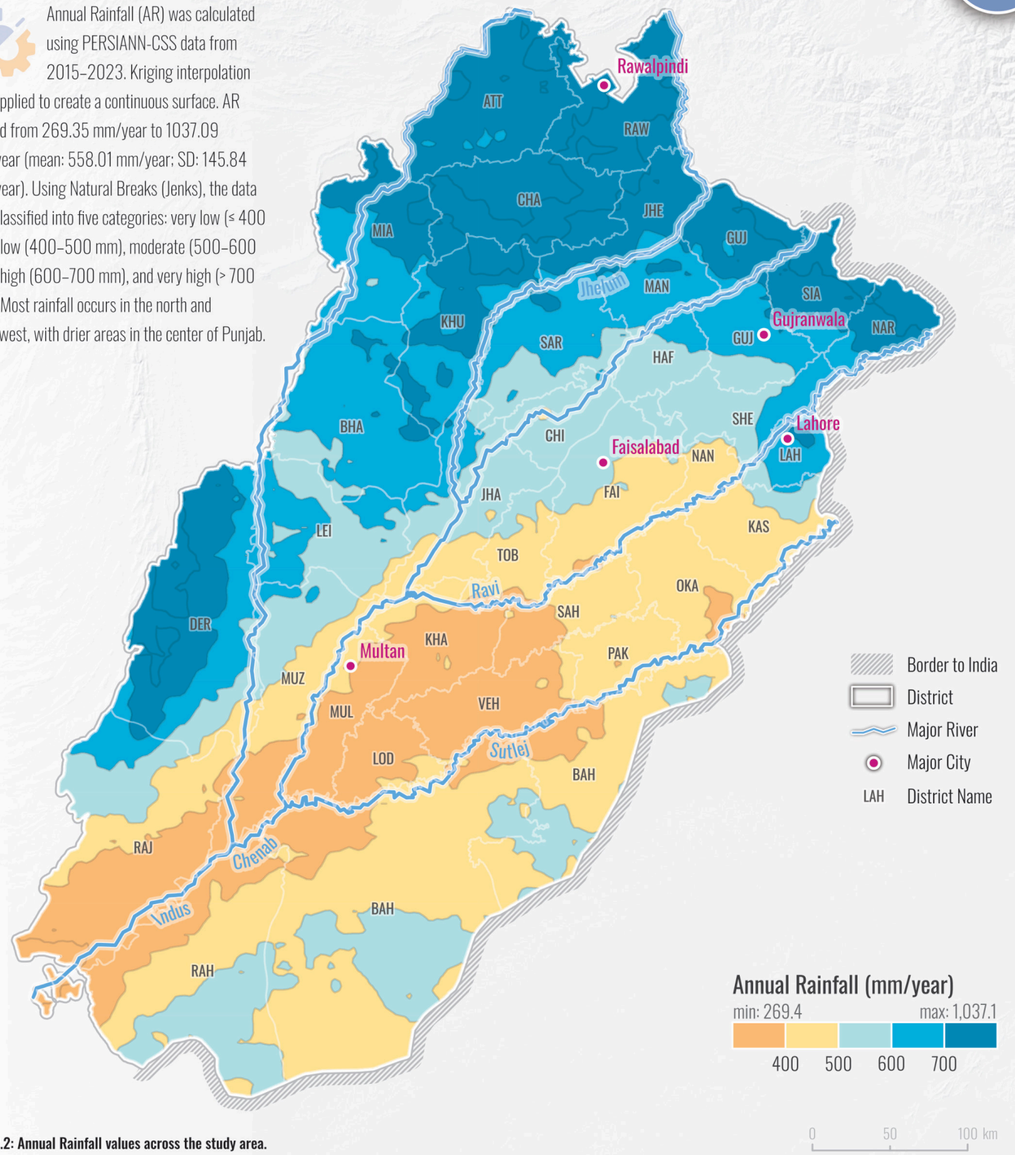

Map 2.2: Annual Rainfall values across the study area.

Distance to the River

The Distance to the River (DR) ranged from 0 m to 86,103.05 m, with a mean of 5657.92 m, and a SD of 10,351.99 m, indicating very skewed data in the lower distance. The dataset was classified on intervals with manual classes, in accordance with other literature (Hoque et al., 2019: Ullah et al., 2024). A closer distance to waterbodies means a higher risk (Fernández and Lutz, 2010), the distance to the river layer was classified into five groups: ≤ 1000 m (very low), 1000–3000 m (low), 3000–6000 m (moderate), 6000–10,000 m (high), > 10,000 m (very high).

12.75% (26,222.92 km^2) of the study area is very low, 8.62% (17,728.13 km^2) is low DR, 18.56% (38,177.38 km^2) is moderate, 31.65% (65,109.38 km^2) is high, and 28.42% (58,459.22 km^2) very high (Figure 2.2, Map 2.3).

The higher classes can be found as a result of the five major rivers, and additionally a lot of channels and streams, especially in crop field areas. These areas are mostly in the northeastern and southwestern parts of the region, which are characterized by farmland (Map 2.4).

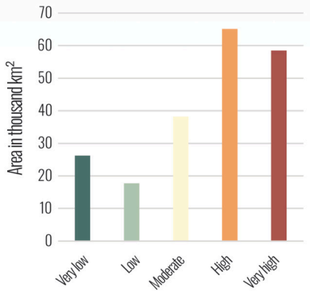

Figure 2.2: Distribution of Distance to the River classes by area (km^2).

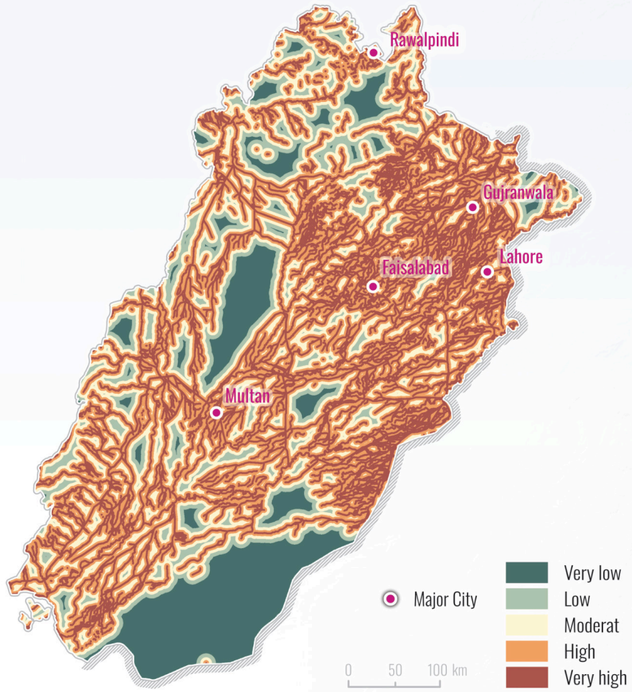

Map 2.3: Distance to the River classes distribution in the study area.

River and drainage channel data were used to calculate the proximity of the Distance to the River (DR) layer, in accordance with a study by Ghorbani et al. (2015). The distance to the river layer was calculated with 'Distance Accumulation', calculating the distance for each cell in the raster to the input layer (esri, no date b). After calculation, the layer was clipped to the study area.

FPC

Distance to the River (DR) was calculated using OSM river and drainage data via the 'Distance Accumulation' tool. The distances ranged from 0 to 86,103.05 m (mean: 5657.92 m; SD: 10,351.99 m), showing a skew toward smaller distances. Based on literature, the data was manually classified into five risk levels: very low (≤ 1000 m), low (1000–3000 m), moderate (3000–6000 m), high (6000–10,000 m), and very high (> 10,000 m). The highest risk zones are closest to rivers and concentrated in the northeast and southwest, aligning with agricultural zones.

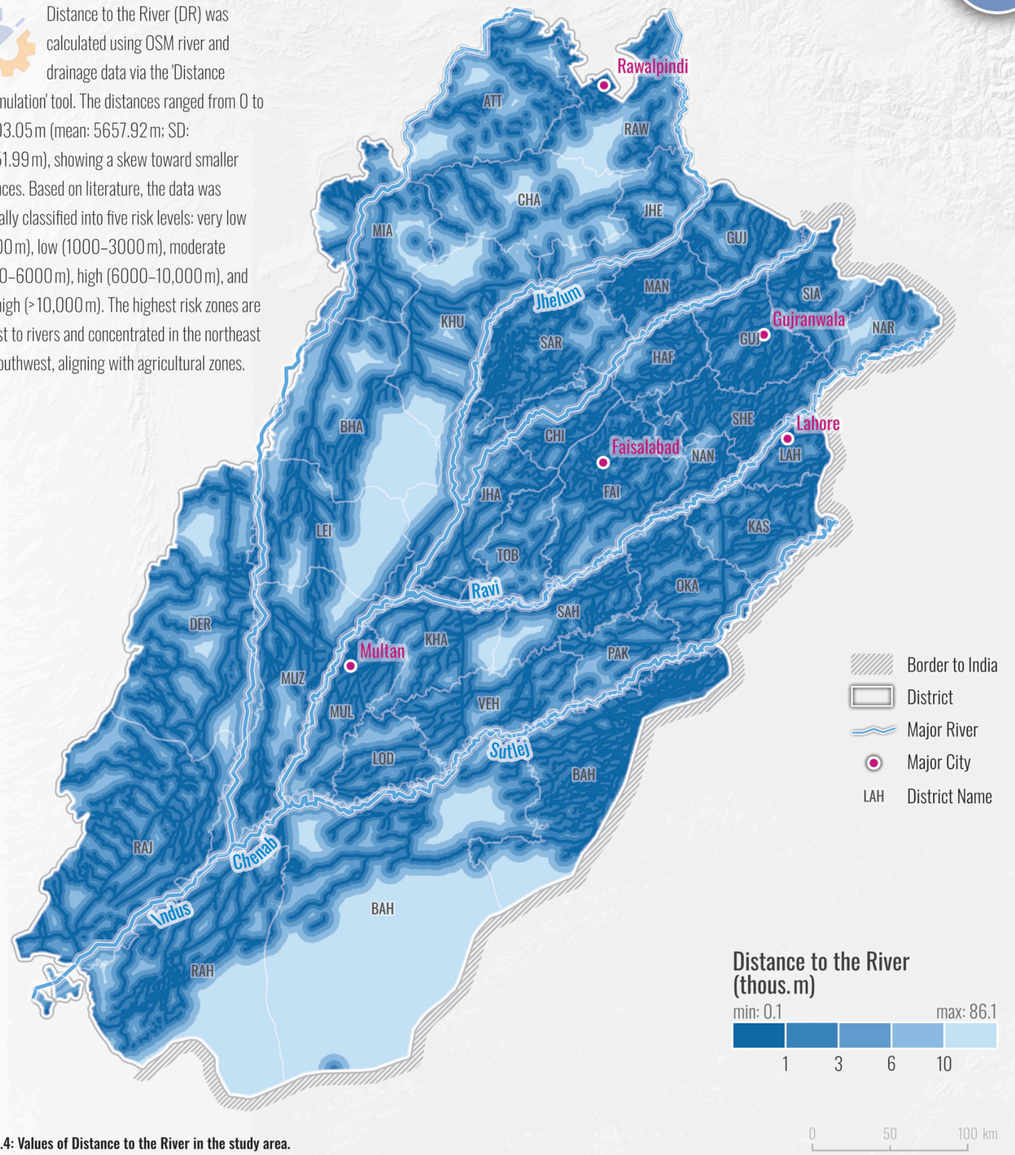

Map 2.4: Values of Distance to the River in the study area.

Drainage Density

Higher drainage leads to higher surface runoff (Subbarayan and Saravanan, 2020). The Drainage Density (DD) values ranged from 0 to 122.07 m/km^2, with a mean of 31.29 m/km^2 and a SD of 26.99 m/km^2. This indicated a skewed distribution towards lower density values; therefore, to ensure balanced classification and meaningful differentiation across the areas, the quantile method was used. This interval method classifies the data into equal-sized categories (esri, no date a), addressing skewness in the distribution and making meaningful flood vulnerability levels. For better understanding and interpretation, the values were slightly rounded. The DD in the study area was divided into five classes: ≤ 6.34 m/km^2 (very low), 6.34–27.76 m/km^2 (low), 27.76–39.25 m/km^2 (moderate), 39.25–56.96 m/km^2 (high), > 56.96 m/km^2 (very high).

The classification describes 29.75% (61,193.51 km^2) of the study area as very low, 15.00% (30,849.03 km^2) as low, 18.43% (37,918.43 km^2) as moderate, 18.61% (38,285.65 km^2) as high, and 18.21% (37,450.41 km^2) as very high (Figure 2.3, Map 2.5).

The DD layer captures mostly the five major river basins (Map 2.6).

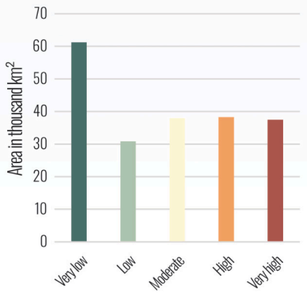

Figure 2.3: Distribution of Drainage Density classes by area (km^2).

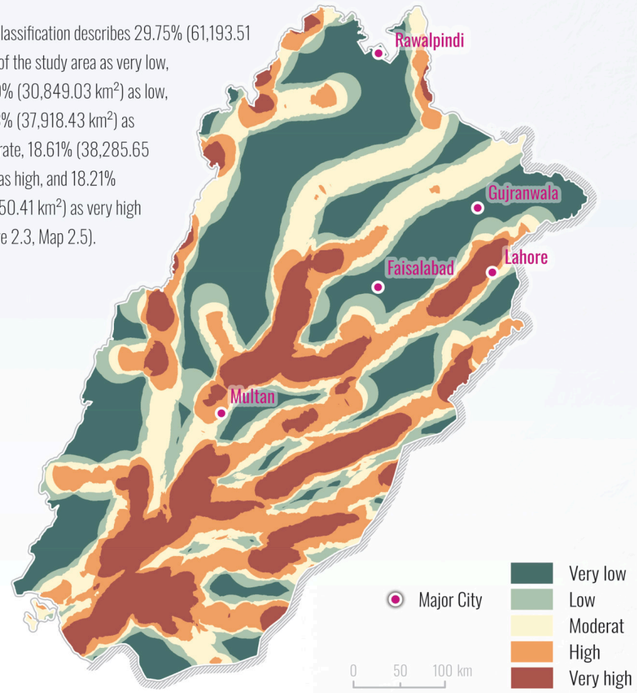

Map 2.5: Distribution of Drainage Density classes in the study area.

The Drainage Density is calculated with the equation below (Hossain and Mumu, 2024).

$$DD = \frac{\text{total length of drainage channels}}{\text{total area}}$$

The Elevation (EL) profile, which was created for the elevation map as described below was used in the calculation process. The DEM was filled with 'Fill', and then the 'Flow Direction' and the 'Flow Accumulation' were run. With the 'Raster Calculator Tool', equal or greater than 1% of the highest value of the Flow Accumulation layer is extracted and saved into a new layer. Then, the 'Stream Order' and the 'Stream to Feature' are executed. Finally, the 'Line Density' tool was executed.

FPC

Using processed DEM data, drainage features were extracted and converted into line density. Drainage Density (DD) values ranged from 0 to 122.07 m/km^2 (mean: 31.29 m/km^2; SD: 26.99 m/km^2). Classified using quantiles, the five categories are: very low (≤ 6.34), low (6.34–27.76), moderate (27.76–39.25), high (39.25–56.96), and very high (> 56.96 m/km^2). High DD, associated with higher runoff potential, is mainly found in the five major river basins.

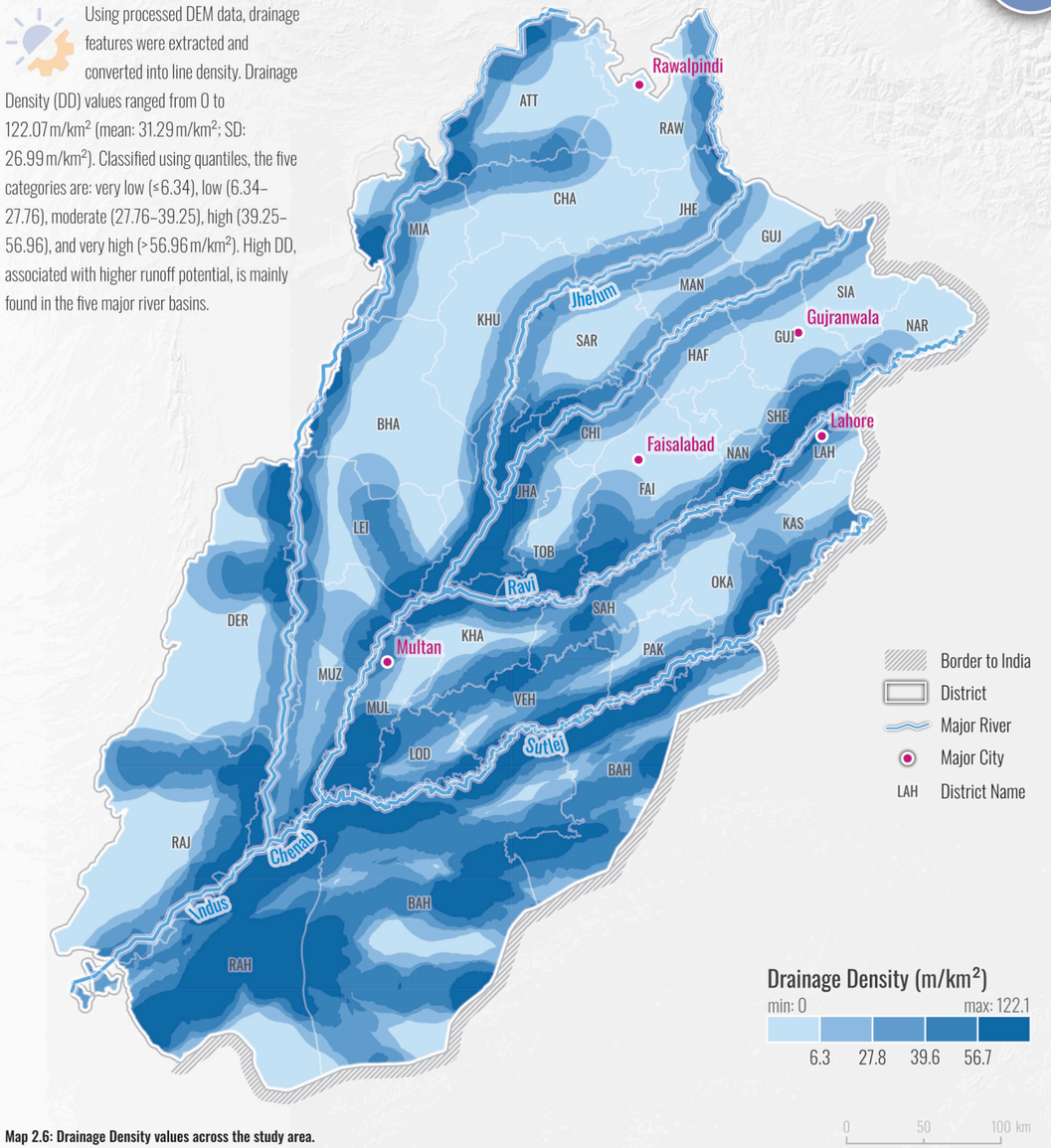

Map 2.6: Drainage Density values across the study area.

Elevation

The Elevation (EL) ranged from 68.50 to 2323.25 m above sea level, with a mean elevation of 222 m and a standard deviation of 193.60 m. Indicating very skewed data in the low elevation. Low-elevated regions are at a higher flood risk (Sanyal and Lu, 2006; Rahman et al., 2019; Allafta and Opp, 2021). The values were manually classified into five classes, focusing on low elevation ranges: ≤ 150 m (very high), 150–200 m (high), 200–300 m (moderate), 300–400 m (low), and > 400 m (very low).

The classification describes 11.27% (23,179.51 km^2) of the study area as very low, 3.88% (7990.26 km^2) as low, 15.04% (30,937.53 km^2) as moderate, 30.18% (62,085.42 km^2) as high, and 39.62% (81,504.31 km^2) as very high (Figure 2.4, Map 2.7)

The northern and the southwestern parts of Punjab are characterized by high elevation, while the center is low elevated (Map 2.8).

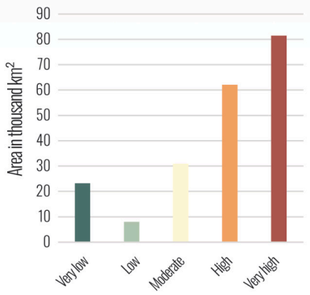

Figure 2.4: Distribution of Elevation classes by area (km^2).

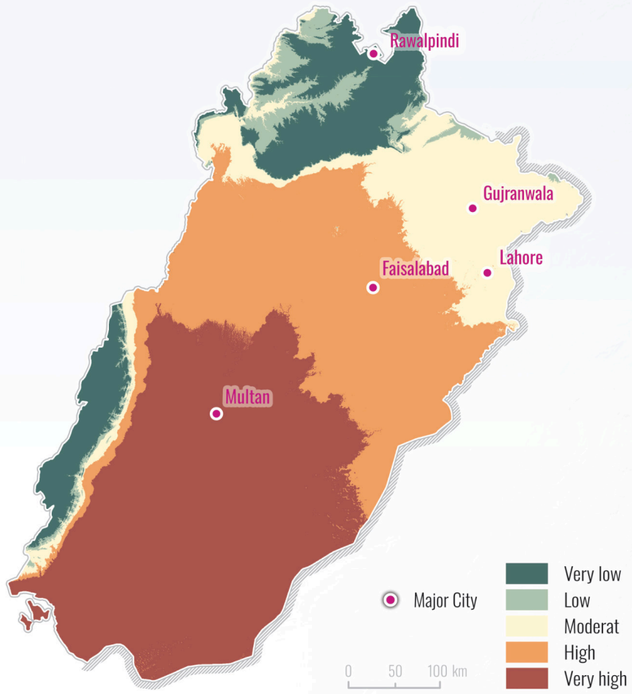

Map 2.7: Distribution of Elevation classes in the study area.

The FABDEM data was loaded into Google Earth Engine, clipped to the study area, projected on the CRS, and loaded into the GIS environment.

FPC

Elevation (EL) was derived from FABDEM and processed in GEE and GIS. Values range from 68.5 to 2323.25 m, with a mean of 222 m and skewed distribution toward lower elevations. Since lower elevations are more flood-prone, the data was manually classified into five classes: very high flood risk (≤150 m), high (150–200 m), moderate (200–300 m), low (300–400 m), and very low (>400 m). Most low-lying areas are in central Punjab, while elevated regions are in the north and southwest.

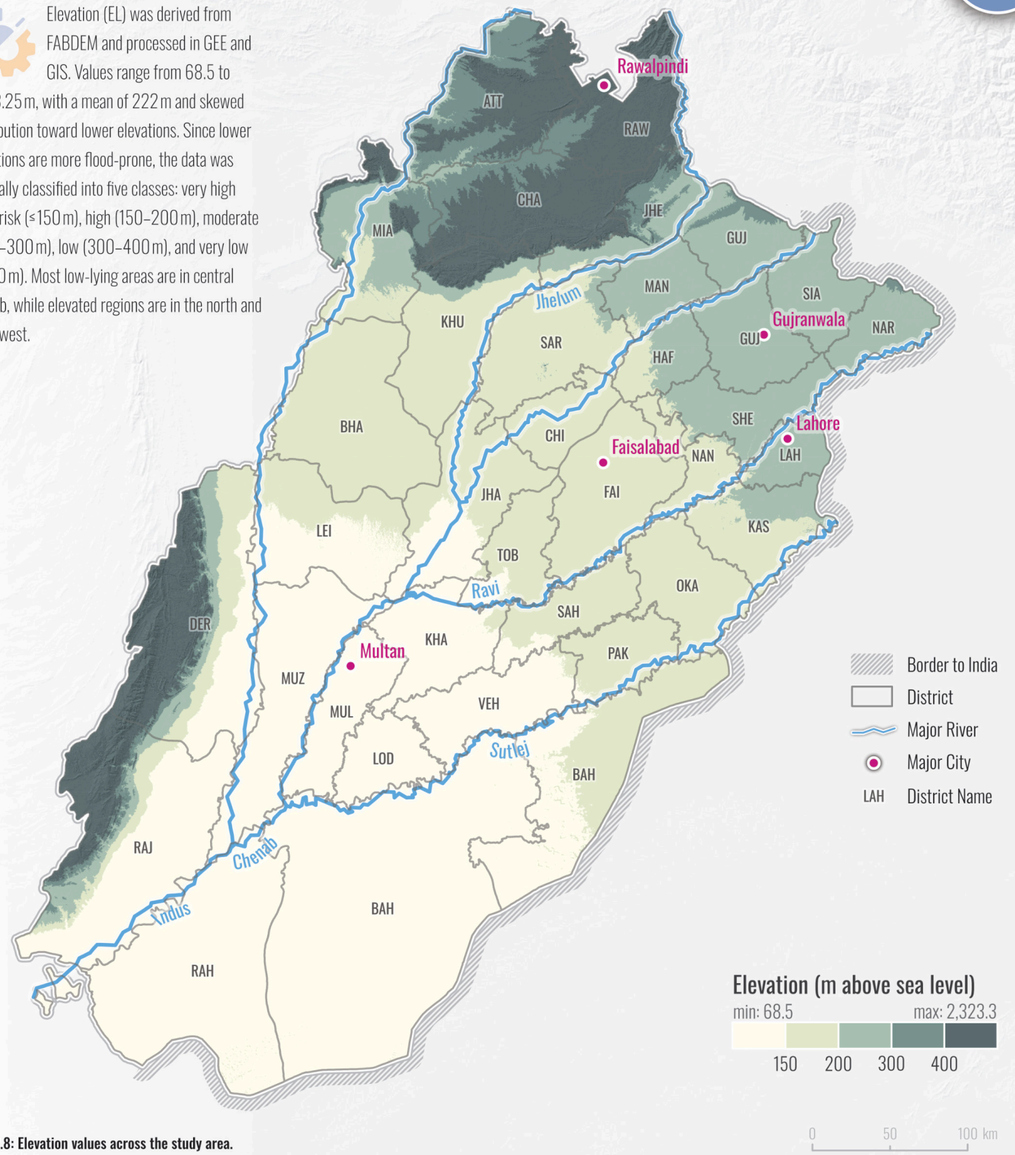

Map 2.8: Elevation values across the study area.

Land Use Land Cover

The given WorldCover layer is classified into tree cover, shrubland, grassland, cropland, built-up, bare/sparse vegetation, permanent waterbodies, and herbaceous wetland. According to Ogato et al. (2020), waterbodies are at a very high and built-up areas are at a high flood risk. Since more than half of floods in 2022 in Pakistan were cropland (Chen et al., 2024), cropland has been classified as highly vulnerable to flooding in this study. Furthermore, bare land is at a moderate risk, as precipitation hits the bare ground (Allafta and Opp, 2021), resulting in a higher risk of flood and runoff (Owuor et al., 2016), as the rain might lead to the formation of a surface crust reducing the infiltration and hydraulic conductivity (Price, Jackson and Parker, 2010). Vegetation is less vulnerable, as it can store water for a period of time (Ullah et al., 2024), and its negative correlation between vegetation density and flooding (Mojaddadi et al., 2017). Less vulnerability also applies to shrublands, due to their high roughness and seepage rates (Allafta and Opp, 2021). Considering this information, the LULC layer was classified into five classes, water bodies, herbaceous wetland (very high), built-up, cropland (high), bare/sparse vegetation (moderate), grassland (low), shrubland, and tree cover (very low).

The classification describes 14.91% (30,662.53 km^2) of the study area as very low, 4.62% (9,495.62 km^2) as low, 21.62% (44,460.48 km^2) as moderate, 57.54% (118,358.67 km^2) as high, and 1.32% (2,719.73 km^2) as very high (Figure 2.5, Map 2.9).

As Punjab is an agricultural center of the country most of the provinces are covered with cropland. Shrubland and base/sparse vegetation can be found in the southeastern and -western parts, as well as in one center area in the north-western direction. Trees are mostly in the northern part, at high elevation. Built-up areas can mostly be found in the major cities (Map 2.10.

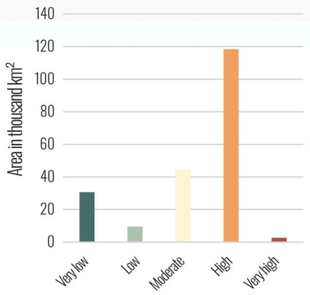

Figure 2.5: Distribution of Land Use Land Cover classes by area (km^2).

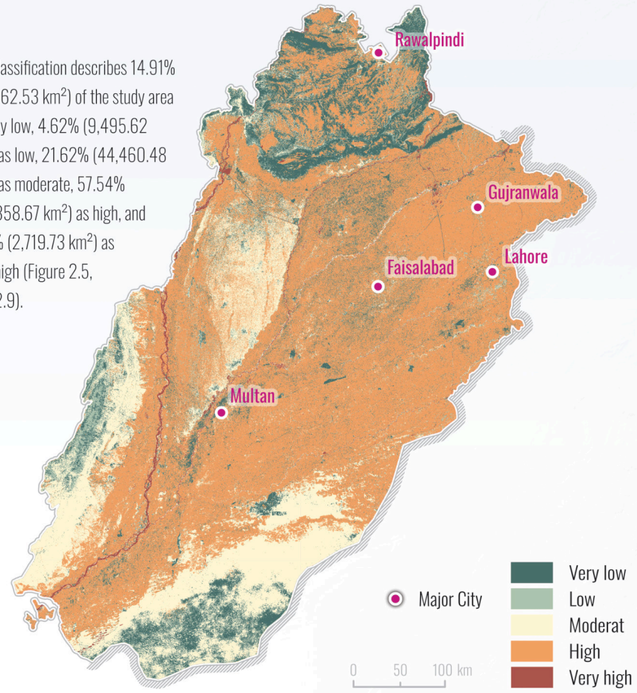

Map 2.9: Distribution of Land Use Land Cover classes in the study area.

For the Land Use Land Cover (LULC) layer, the WorldCover V2 2021 was used (Zanaga et al., 2022). The different tiles covering the study area were downloaded from the ESA WorldCover Viewer and loaded into ArcGIS Pro. While reprojecting the files to the used CRS in this study with the Project Raster tool, the cell size was resampled to 30m. As a resampling technique, the Nearest Neighbor was used, as this is best for discrete data (esri, no date f). After the 'Mosaic to New Raster' tool merged all the tiles into one, the layer was clipped to the study area, all while ensuring that the output was snapped correctly.

FPC

The Land Use Land Cover layer (LULC) was derived from WorldCover V2 2021 data. The final classification includes tree cover, shrubland, grassland, cropland, built-up areas, bare/sparse vegetation, water bodies, and herbaceous wetlands. Based on flood vulnerability, water bodies and wetlands are very high risk, built-up areas and cropland are high risk, bare/sparse vegetation is moderate risk, and vegetation (trees, shrubland, and grassland) is less vulnerable. In Punjab, cropland dominates the landscape, while shrubland and bare/sparse vegetation occur in the southern, eastern, and western parts, tree cover is found mainly in the elevated northern region, and built-up areas are concentrated around major cities. Overall, the classification indicates that 14.91% of the area is very low risk, 4.62% is low risk, 21.62% is moderate risk, 57.54% is high risk, and 1.32% is very high risk.

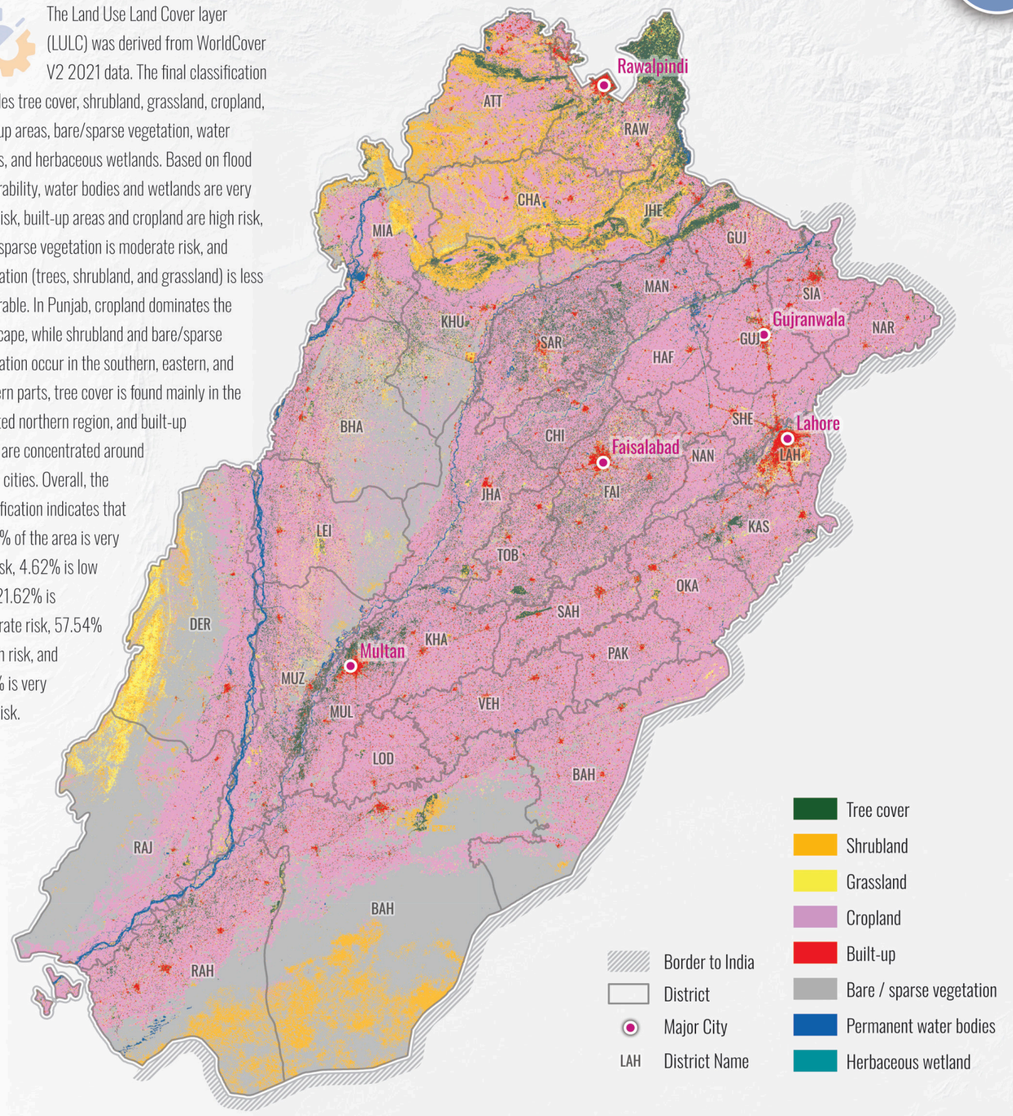

Map 2.10: Land Use Land Cover values across the study

Slope

Slope (SL) plays an important role in the rate and duration of water flow (Ogato et al., 2020a). Flatter surfaces have a higher risk, as water moves slower, collects longer, and builds up (Gigović et al., 2017). The slope ranged from 0° to 75.50°, with a mean of 1.56°, and a standard deviation of 4.72°. Natural breaks were chosen as classification intervals and slightly manually adjusted, for better interpretation and readability. Given the skewed data in the lower slope areas, as well as the fact that flat areas are at higher risk, the focus was set on shallow areas. The slope layer was classified into five classes: ≤ 1.5° (very high), 1.5°–5° (high), 5°–15° (moderate), 15°–30° (low), > 30° (very low).

According to the classification, 0.59% (1213.16 km^2) of the study area falls in very low, 2.59% (5333.28 km^2) in low, 4.52% (9298.84 km^2) in moderate, 7.63% (15,702.85 km^2) in high, and 84.66% (174,148.89 km^2) in very high classes (Figure 2.6, Map 2.11).

High degrees of SL can be found in the mountainous areas of the province, while low degrees are in the flat land (Map 2.12).

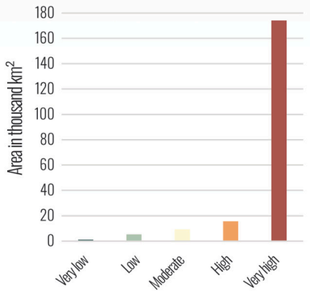

Figure 2.6: Distribution of Slope classes by area (km^2).

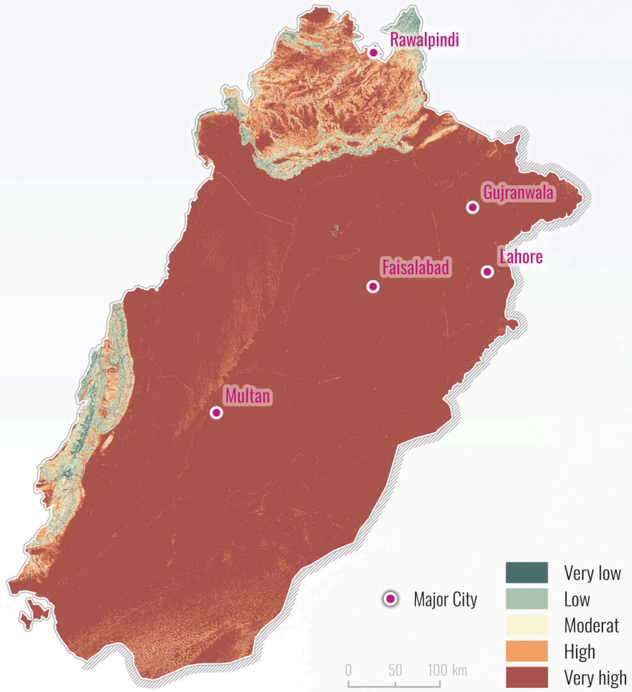

Map 2.11: Distribution of Slope classes in the study area.

Slope (SL) was created with the FABDEM data in ArcGIS Pro. With 'Fill' artificial sinks were removed (esri, no date c). Degrees were used as the output measurement, and the geodesic method for calculation, as this will give a more precise output on a larger region (esri, no date g).

Slope (SL) was derived from FABDEM using ArcGIS Pro, calculated in degrees with the geodesic method for higher accuracy over large areas. Since flatter areas increase flood risk due to slower water movement, classification emphasized low-slope values. The slope ranged from 0° to 75.5°, with a mean of 1.56°. Using Natural Breaks (manually refined), it was classified into five categories: very high risk (≤1.5°), high (1.5°–5°), moderate (5°–15°), low (15°–30°), and very low (>30°). Most of the study area (84.66%) falls in the very high-risk category, indicating predominantly flat terrain, especially in the central and southern regions. Steeper slopes are found in the mountainous north.

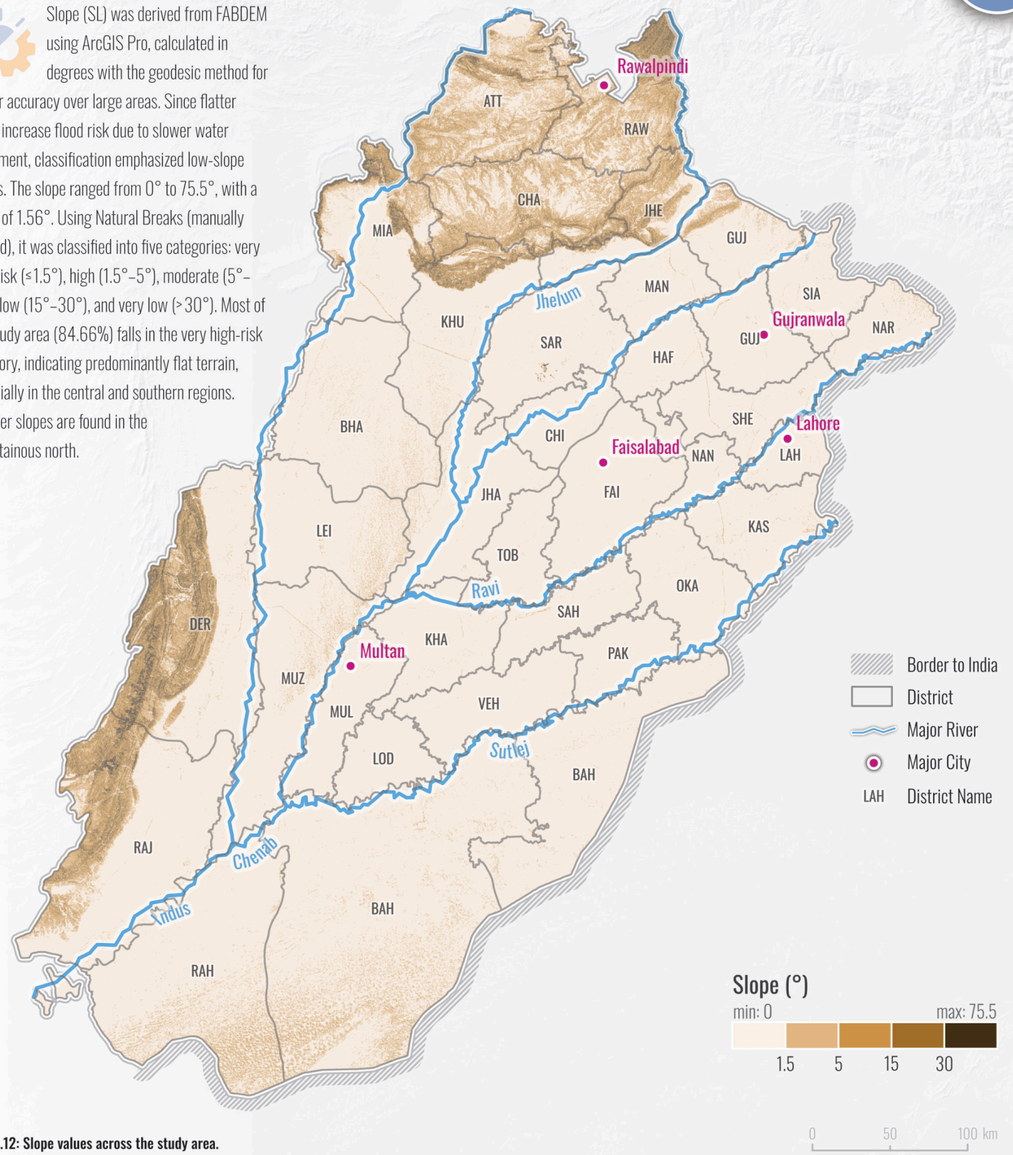

Map 2.12: Slope values across the study area.

Topographic Wetness Index

The Topographic Wetness Index (TWI) ranged from -1.35 to 34.55, with a mean of 7.88, and a standard deviation of 3.69. TWI quantifies the topography of hydrological processes and the variability in terrain in soil moisture. While the index does not have a unit, higher values mean a higher potential for flooding (Roy and Dhar, 2024). By using quantiles, each class represents a reasonable distribution of the values, from minimal water retention to higher water accumulation. The values were slightly rounded for better interpretation. The layer was classified into five classes: ≤ 5.12 (very low), 5.12–6.67 (low), 6.67–7.94 (moderate), 7.94–10.75 (high), > 10.75 (very high).

The classification describes 19.49% (40,093.62 km^2) of the study area as very low, 19.88% (40,900.81 km^2) as low, 21.94% (45,128.56 km^2) as moderate, 20.07% (41,283.85 km^2) as high, and 18.61% (38,290.19 km^2) as very high (Figure 2.7, Map 2.13).

Higher TWI values can be found at waterbodies and rivers, while lower are in the higher elevated areas of the province (Map 2.14).

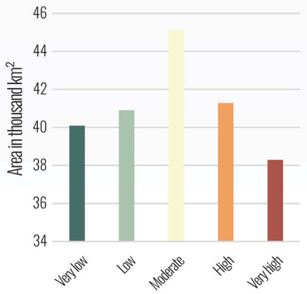

Figure 2.7: Distribution of Topographic Wetness Index classes by area (km^2).

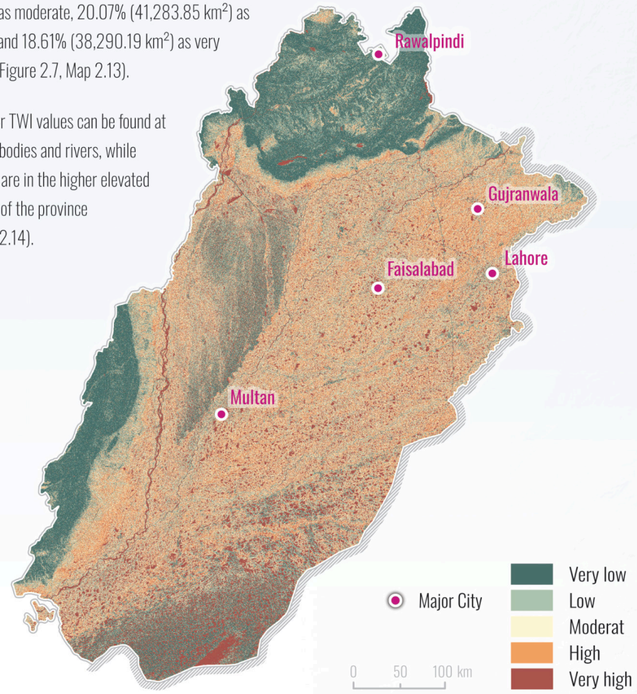

Map 2.13: Distribution of Topographic Wetness Index classes in the study area.

The Topographic Wetness Index (TWI) quantified the topography of hydrological processes and the variability in terrain in soil moisture (Roy and Dhar, 2024). The layer TWI was created with the FABDEM data in ArcGIS Pro. First, the layer was filled with the Fill tool, to remove sinks or depression which could cause errors in the flow of water. Then, the Flow Direction tool was run to create the flow direction for each raster cell (esri, no date e), followed by the Flow Accumulation tool (esri, no date d). Then the tangent of the new slope radians layer was calculated again with the Raster Calculator. Finally, the Topographic Wetness Index was calculated with the equation below (Beven and Kirkby, 1979),

$$TWI = \ln\left(\frac{a}{\tan(b)}\right)$$

where a is the flow accumulation and b is the slope in radians (Roy and Dhar, 2024). While the index does not have a unit, higher values mean a higher potential for flooding (Roy and Dhar, 2024). In the end, the raster was clipped to the study area. All steps ensured, creating the layers on the snap raster.

FPC

Topographic Wetness Index (TWI) was calculated using FABDEM data to assess soil moisture variability and flood potential. The process included filling sinks, generating flow direction and accumulation, and applying the TWI formula. The index, ranging from -1.35 to 34.55, was classified into five quantile-based classes, from very low to very high wetness. Higher TWI values, indicating greater flood potential, were mainly found near waterbodies and rivers, while lower values appeared in elevated areas.

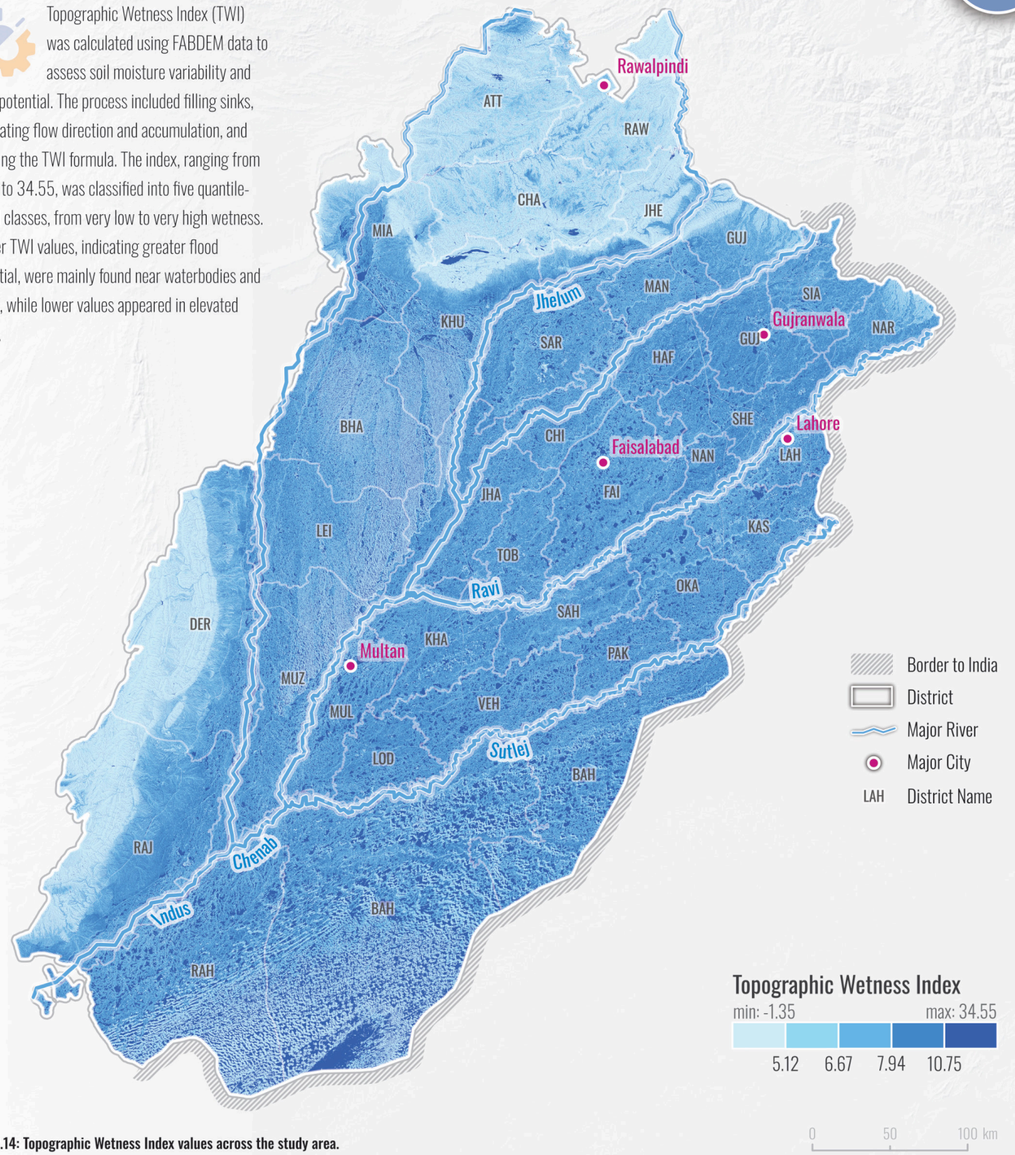

Map 2.14: Topographic Wetness Index values across the study area.

Flood-Prone Component

Using the parameters and the respective weights derived from the AHP, the overlay analysis generated the Flood-Prone Component (FPC) Map. The output of the FPC ranged from 1 (very low flood-prone) to 5 (very high flood-prone); while 8.22% (16,889.62 km^2) in low, 48.74% (100,266.5 km^2) in moderate, 42.72% (87,882.86 km^2) in high, and 0.32% (654.96 km^2) is very high flood-prone areas in the study area in the FPC pixel map (Figure 2.8, Map 2.15).

The validation of the FPC showed that the previous flood occurred in 71.22% of very high and high vulnerability classified areas: 26.47% were in the moderate vulnerability class, while 2.31 % were in the low vulnerability class.

The results indicate that almost half of the study area falls within the moderate flood-prone category, while a smaller portion of ~43% is classified as high and very high. This confirmed the high flood of catastrophic susceptibilities in the Punjab region. The high classes can especially be found near river basins, characterized by high drainage density, high proximity to rivers, flat terrain, and low slopes. While areas, characterized by high elevation, higher slope, and no river basins are classified as low, as well as moderate. Moderate areas are also especially found in flat terrain and lower slopes, However, the topographical characteristics of riverine areas in particular make them higher flood-prone areas.

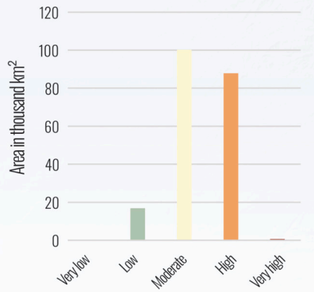

Figure 2.8: Distribution of FPC classes by area (km^2).

The Flood-Prone Component (FPC) was assessed using the Analytical Hierarchy Process (AHP) to determine the relative importance of seven key parameters: annual rainfall (AR), distance to river (DR), drainage density (DD), elevation (EL), land use land cover (LULC), slope (SL), and topographic wetness index (TWI). This technique, commonly used in flood vulnerability studies, involves expert judgment and a structured pairwise comparison method based on Saaty's 1–9 importance scale.

A survey was conducted to gather expert opinions, including responses from eight professionals in Pakistan and five climate risk analysts from the United Nations University – Institute for Environment and Human Security (UNU-EHS). Respondents compared the importance of each parameter relative to the others, and the results were used to construct pairwise comparison matrices. The geometric mean of the responses was used to complete the matrix for the FPC (Table 2.1).

The normalized values and final weights (Table 2.2) revealed that Drainage Density (0.21), Land Use Land Cover (0.18), and Annual Rainfall (0.15) were considered the most influential parameters contributing to flood susceptibility. Other parameters, including Distance to the River (0.13), Elevation (0.12), Topographic Wetness Index (0.11), and Slope (0.10), were seen as less significant but still relevant.

To ensure consistency, the matrix was tested using eigenvalue-based methods. The process included normalization of the matrices, calculation of weighted sums, consistency vectors, and the maximum eigenvalue value, confirming the logical consistency of expert judgments. The resulting consistency ratio (CR) of 0.04 confirmed the internal consistency and validity of expert assessments. Flood-prone areas were validated using Sentinel-1 SAR data (Copernicus Sentinel data, 2021-2024). The data was refined to exclude slopes > 3° and detect floods using a –3 dB threshold. Overlaps with FPC classes were analyzed to confirm accuracy.

Table 2.1: Pairwise comparison matrix for FPC.

Parameter	AR	DR	DD	EL	LULC	SL	TWI
AR	1	2	1	1	1	1	1
DR	1/2	1	1	1	1	1	1
DD	1	1	1	3	1	3	2
EL	1	1	1/3	1	1	1	1
LULC	1	1	1	1	1	3	2
SL	1	1	1/3	1	1/3	1	1
TWI	1	1	1/2	1	1/2	1	1

Table 2.2: Normalized vector for FPC.

Parameter	AR	DR	DD	EL	LULC	SL	TWI	Weight
AR	0.15	0.25	0.19	0.11	0.17	0.09	0.11	0.15
DR	0.08	0.13	0.19	0.11	0.17	0.09	0.11	0.13
DD	0.15	0.13	0.19	0.33	0.17	0.27	0.22	0.21
EL	0.15	0.13	0.06	0.11	0.17	0.09	0.11	0.12
LULC	0.15	0.13	0.19	0.11	0.17	0.27	0.22	0.18
SL	0.15	0.13	0.06	0.11	0.06	0.09	0.11	0.1
TWI	0.15	0.13	0.1	0.11	0.09	0.09	0.11	0.11

FPC

The FPC map revealed that 43.04% of the study area is highly and very highly flood-prone, 48.74% is moderately prone, and only 8.22% is low-prone. Validation with Sentinel-1 flood data showed that over 71% of past floods occurred in high and very high FPC areas, confirming the map's accuracy. High-risk zones are mainly near river basins with flat terrain, high drainage density, and proximity to rivers, while elevated and sloped areas were less flood-prone.

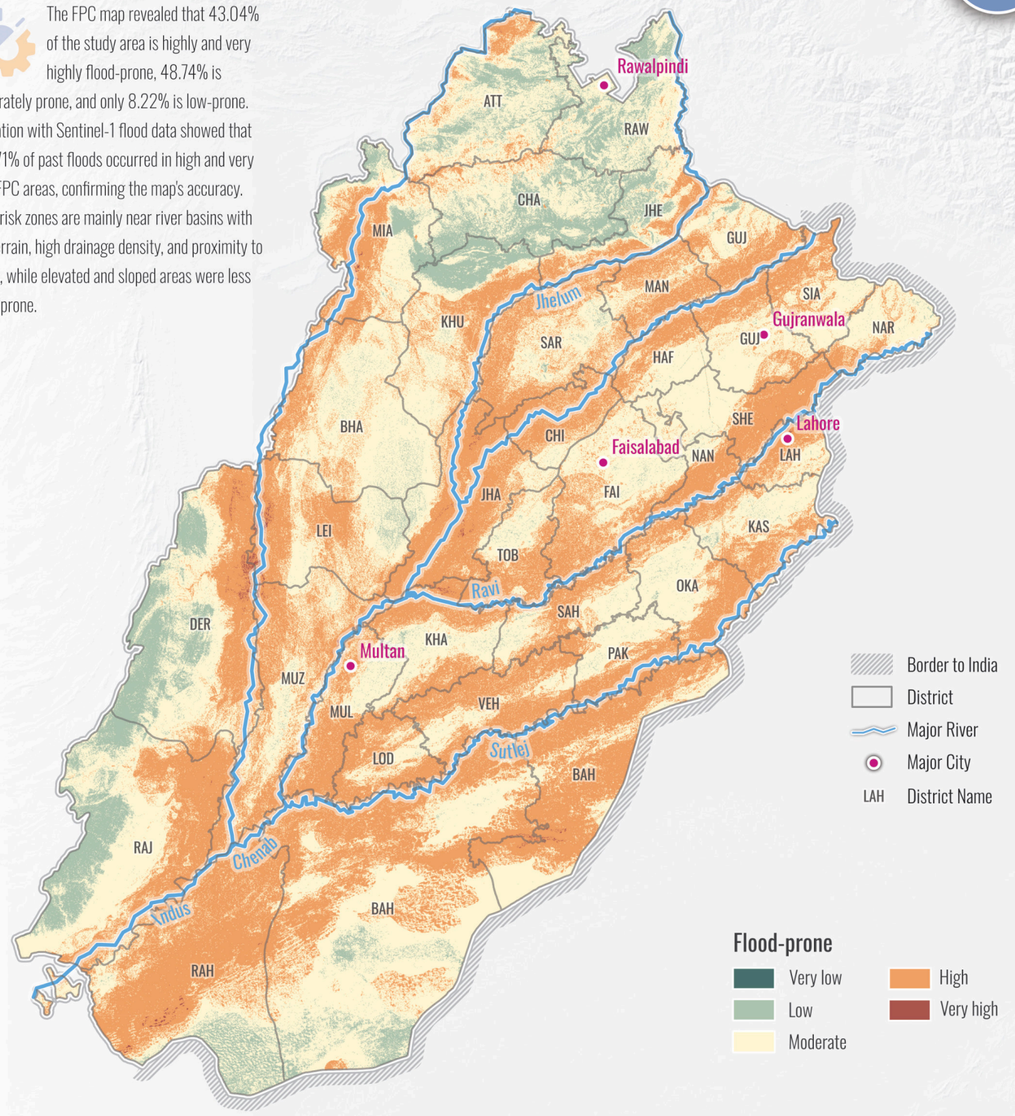

Map 2.15: Distribution of FPC classes in the study area.

Flood-Prone Component at Tehsil level

The results of the Flood-Prone Component (FPC) indicate that almost half of the study area falls within the moderate flood-prone category, while a smaller portion of ~43% is classified as high and very high. This confirmed the high flood of catastrophic susceptibilities in the Punjab region. The high classes can especially be found near river basins, characterized by high drainage density, high proximity to rivers, flat terrain, and low slopes. While areas, characterized by high elevation, higher slope, and no river basins are classified as low, as well as moderate. Moderate areas are also especially found in flat terrain and lower slopes, However, the topographical characteristics of riverine areas in particular make them higher flood-prone areas.

The FPC aggregated to Tehsils (Map 2.16) confirmed these findings. Especially areas in river basins are highly affected. Furthermore, based on the average FPC class value highest affected Tehsils are identified (Table 2.3); these values ranged from 2.26 to 3.99. Lahore City has an average FPC class value of 3.99 with 96.23% of its area classified as high and very high flood-prone. The Ahmadpur Sial and Ferozewala also show values around 3.98 with over 96% of their area in high and very high. Through these Tehsils, major rivers flow through, and almost the entire settlement area is exposed as the high percentage suggested.

Table 2.3: Tehsils with the heighest FPC.

Rank	Tehsil	Total Tehsil Area (km²)	High FP Area (km²)	Very High FP Area (km²)	Combined FP Area (km²)	% of Tehsil in High & Very High FP	Average FPC Class
1	Lahore City	237.48	222.37	6.15	228.53	96.23%	3.99
2	Ahmadpur Sial	758.67	722.73	13.1	735.83	96.99%	3.99
3	Ferozewala	576.54	553.51	3.84	557.35	96.67%	3.97
4	Muridke	832.6	782.49	0.3	782.79	94.02%	3.94
5	Khanpur	1727.94	1609.15	0.13	1609.28	93.13%	3.93
6	Bahawalpur City	385.42	355.63	0.01	355.64	92.27%	3.92
7	Sharak Pur	386.06	349.98	0.8	350.78	90.86%	3.91
8	Khairpur Tamewali	720.83	647.54	0.65	648.19	89.92%	3.9
9	Jalalpur Pirwala	878.36	784.1	0	784.1	89.27%	3.89
10	Rahim Yar Khan	2126.86	1843.92	10.99	1854.9	87.21%	3.88

To visualize FPC distribution regionally, the mean FPC values were calculated at the Tehsil level using Zonal Statistics. This method averages pixel values within each Tehsil, allowing for easy comparison of flood-proneness across administrative regions.

FPC

The FPC map averaged at the Tehsil level showed that nearly half the area is moderately flood-prone, while ~43% is high to very high. High-risk zones, mainly near river basins with flat terrain and dense drainage, include Lahore City, Ahmadpur Sial, and Ferozewala - each with over 96% of their area highly flood-prone.

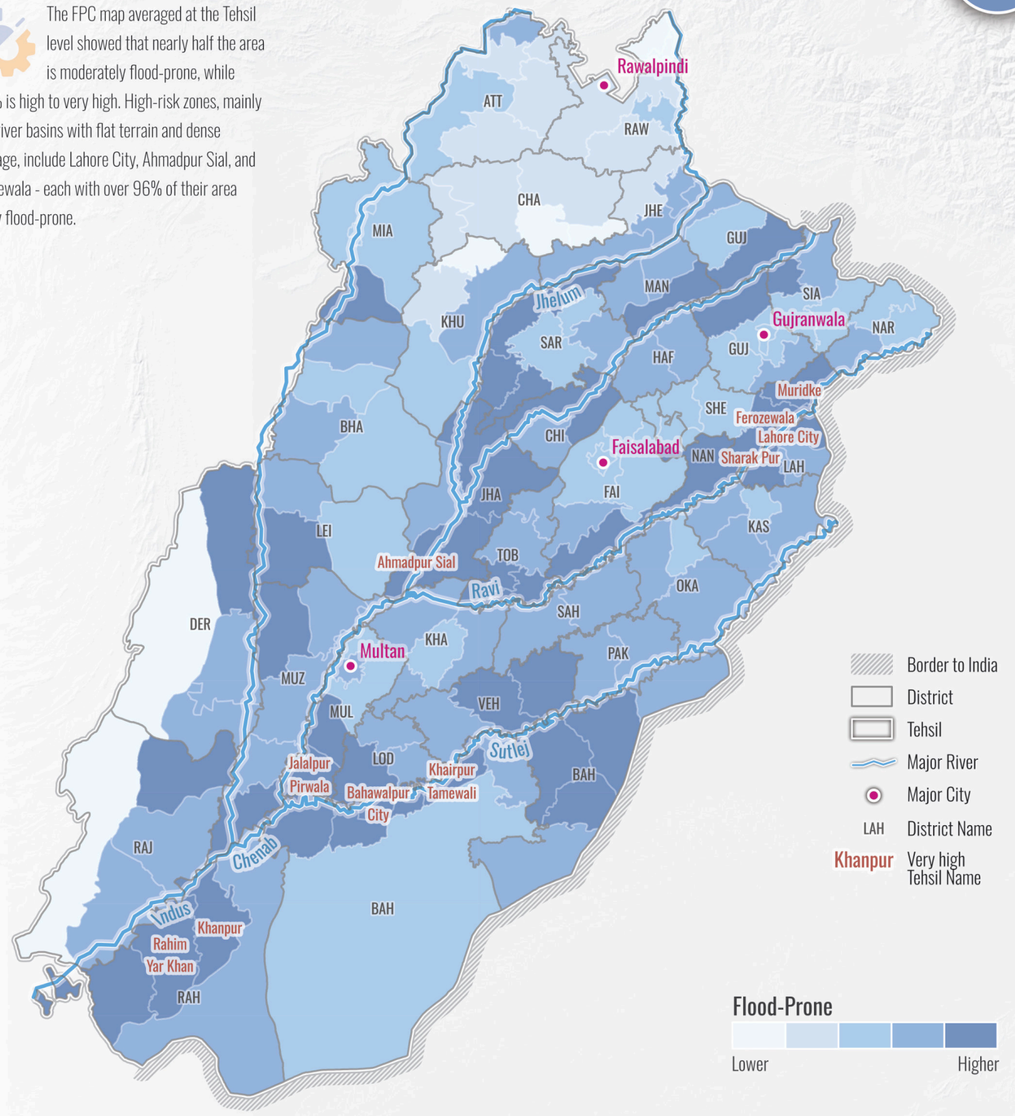

Map 2.16: FPC aggregated to Tehsils (The top 10 Tehsils with the highest flood-prone score are labelled).

PSC

Population Susceptibility Component

Dependent Population
Disabled Population
Female Population
Population Density
Population Susceptibility Component
Population Susceptibility Component at Tehsil level

While there has been extensive research into physical vulnerability, social vulnerability aspects have only been given more attention in recent years (Ajtai et al., 2023). Social vulnerability can be influenced by factors such as age, medical conditions, education, gender, race and ethnicity, income, residential property (Cutter, Boruff and Shirley, 2003). Therefore, another component of the study's FVI is the Population Susceptibility Component (PSC), assessing the demographic and socioeconomic characteristics that affect a population's ability to withstand floods, consisting of four parameters focusing directly on population characteristics (Table 1.2): the Dependent Population (DeP), the Disabled Population (DiP), the Female Population (FP), and the Population Density (PD). While the DeP, DiP, and FP have difficulties in emergency situations (Neumayer and Plümper, 2007; Hoque et al., 2019), higher PD is considered as a higher risk (Hoque et al., 2019). While social vulnerability consists of a broader range of socio-economic, demographic, and infrastructural factors (Cutter, Boruff and Shirley, 2003; Ajtai et al., 2023), other studies also use factors of economic and infrastructural kind, such as housing conditions and building characteristics (Fernandez, Mourato and Moreira, 2016; Hamidi et al., 2022), their exclusion in this study is due to data availability limitations. Therefore, this index is termed PSC, as it does not cover all aspects of social vulnerability but focuses on key demographic indicators to provide a human-centered approach, representing a measure of human susceptibility to flood risks in the study area, given the possibility of measuring flood vulnerability directly at the population.

In this study, the component of the Population Susceptibility Component (PSC) is based on four parameters: Dependent Population (DeP), Disabled Population (DiP), Female Population (FP), and Population Density (PD). Based on the downloaded census data, an Excel sheet was created putting all the required data together. For the DeP, the number of people under 15 and over 60 were counted and the percentage was calculated for each Tehsil. Furthermore, the amount of disabled, for DiP, and female population, for FP, was transferred and the share in each Tehsil was calculated. The PD was calculated with the total amount of the population and the area of the Tehsils. Then, this table was joined with the administrative boundaries' shapefile of the Tehsils. A map was created for each PSC parameter. As the census data was available on administrative boundaries (Tehsils), a dasymetric map was created for all PSC parameter maps. A dasymetric map is a thematic mapping technique in which statistical data is redistributed on the basis of additional spatial information to provide a more accurate representation of population distribution within administrative boundaries (Eicher and Brewer, 2001). To get this information, the Tehsil map was masked out with settlement data, derived from the LULC. A settlement layer was created based on the LULC consisting of buildings (1), and no-buildings (0); each PSC parameter map was then calculated with the equation below:

$$PSC\ paramter\ map\ masked = settlements \times PSC\ parameter\ map$$

The PSC represents human-related vulnerability, therefore, the dasymetric mapping method ensures that the analysis of PSC is only represented in settled areas. This prevents overestimation in large, sparsely populated Tehsils and provides a more realistic spatial representation of human vulnerability.

Dependent Population

The Dependent Population (DeP) is comprised of people under 15 and over 60. According to Hoque et al. (2019), these age groups are dependent, as they may not earn money and are dependent on other family members. The share of DeP ranged from 37.80% to 59.20%, with a mean of 44.77% and a SD of 3.31%. Given the skewed distribution, Natural Breaks was chosen as an interval method. The values were classified into five classes: ≤ 41.41% (very low), 41.41–43.54% (low), 43.54–45.70% (moderate), 45.70–49.11% (high), > 49.11% (very high). A lot of dependent populations are in the south-western rural areas, while in the northern part as well as in the City Tehsils it is less (Figure 15a).

Considering the dasymetric map, masked out with settlements (Figure 15c), the classification describes 15.64% (1107.68 km^2) of the study area as very low, 25.90% (1834.30 km^2) as low, 28.18% (1995.62 km^2) as moderate, 23.29% as high (1649.31 km^2), and 6.99% (494.74 km^2) as very high in inhabited places (Figure 3.1, Map 3.1).

Areas with a higher dependent population face greater challenges because babies, children, and elderly people might be more vulnerable when flooding occurs. The Tehsils with the highest values are Ahmadpur East, Alipur, Dera Ghazi Khan, Jampur, Jatoi, Koh-e-Suleman, Kot Chatta, Liaqatpur, Muzaffargarh, Rajanpur, Rajanpur (Tribal Area), Rojhan, and Taunsa (Map 3.2).

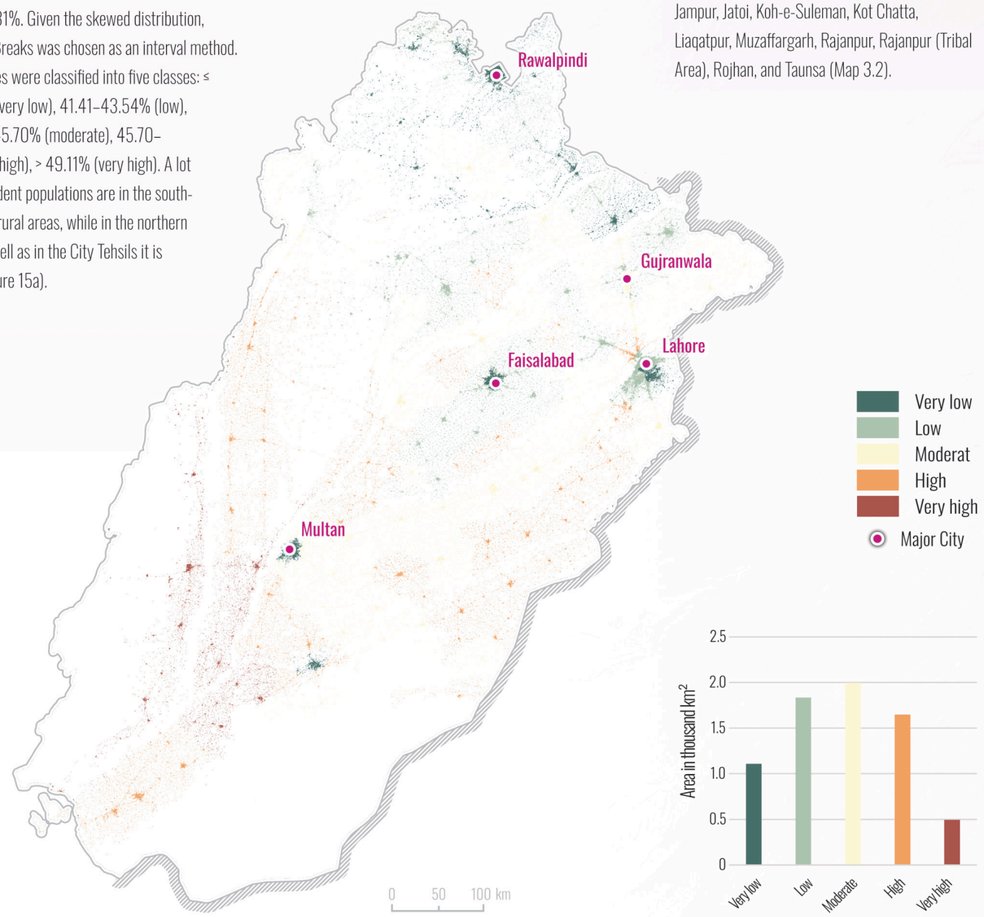

Map 3.1: Distribution of Dependent Population classes in the study area.

Figure 3.1: Distribution of Dependent Population classes by area (km^2) in inhabited places.

PSC

The Dependent Population (under 15 and over 60 years old) was calculated per Tehsil using census data. These groups are considered more vulnerable and dependent during disasters. The DeP ranged from 37.80% to 59.20%, with a mean of 44.77%. Due to skewed distribution, Natural Breaks classification was applied: ≤ 41.41% (very low), 41.41–43.54% (low), 43.54–45.70% (moderate), 45.70–49.11% (high), > 49.11% (very high). Higher dependent populations are found mainly in the rural southwest, while city Tehsils and the north show lower values. In inhabited areas, 28.18% fall in the moderate class, and 6.99% in very high. Vulnerable Tehsils include Muzaffargarh, Rajanpur, and Dera Ghazi Khan.

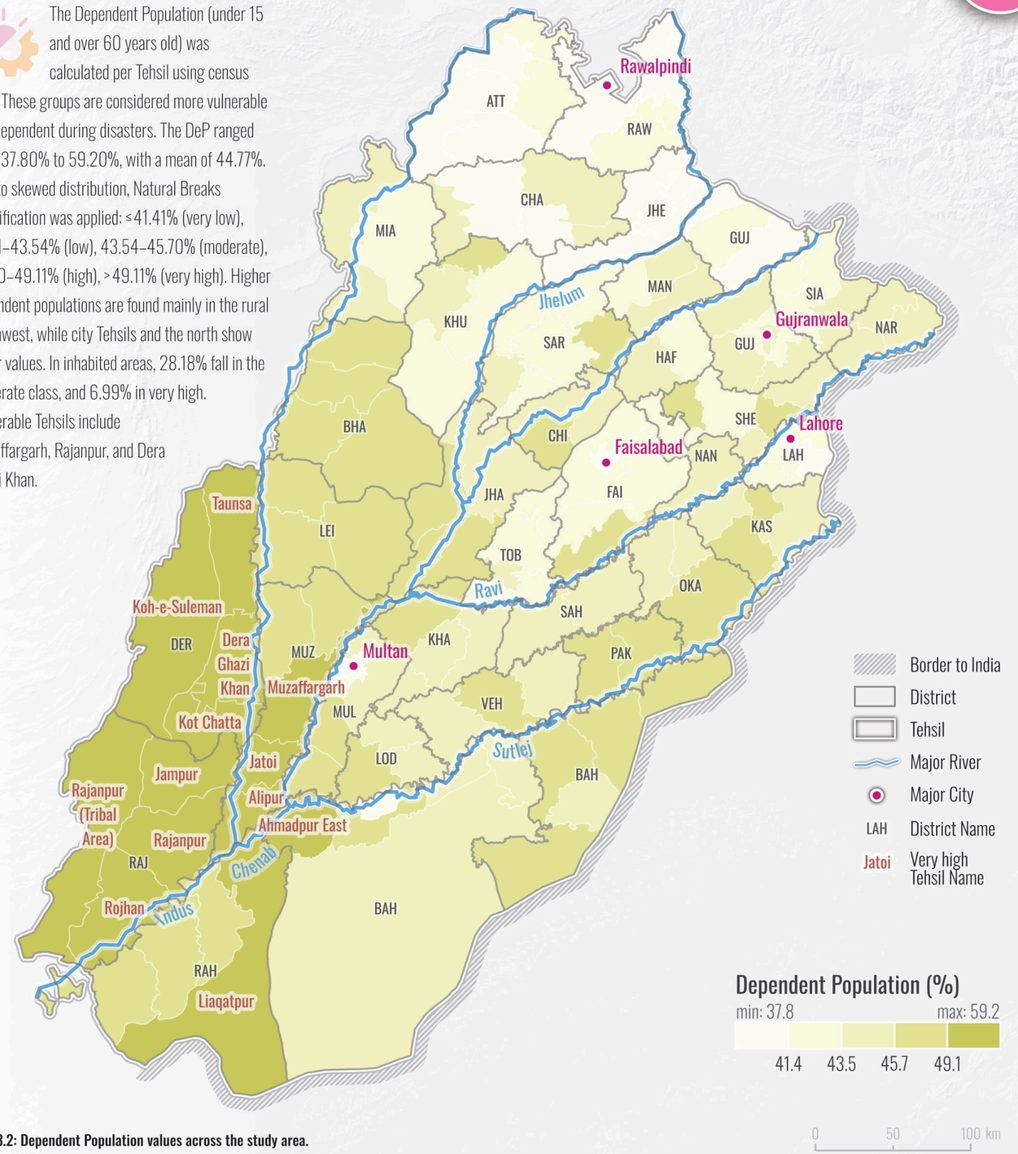

Map 3.2: Dependent Population values across the study area.

Disabled Population

Disabled populations (DiP) face challenges in emergency situations (Hoque et al., 2019). The share of DiP ranged from 1.67% to 15.73%, with a mean of 4.21% and a SD of 2.00%. Natural Breaks was chosen as an interval method. The values were classified into five classes: ≤ 2.65% (very low), 2.65–3.86% (low), 3.86–5.70% (moderate), 5.70–9.40% (high), > 9.40% (very high). The distribution of the disabled population in the Tehsils is fairly even, however, a slight distribution with a higher percentage can be seen in the north-western part. Furthermore, the highest amount is in the Tehsil in the south-west, as well as in the northern part; the Tehsil of Rajanpur (Tribal Area), as well as Kahuta (Map 3.4).

The classification describes 20.51% (1452.29 km^2) in very low, 46.10% (3264.80 km^2) in low, 24.92% (1764.74 km^2) in moderate, 8.21% (581.29 km^2) as high, and 0.26% (18.54 km^2) as very high in inhabited places (Figure 3.2, Map 3.3).

These findings suggest that, although the areas in the higher ranges are modest, some areas are characterized by very high share of disabled population, making them highly vulnerable during flood events.

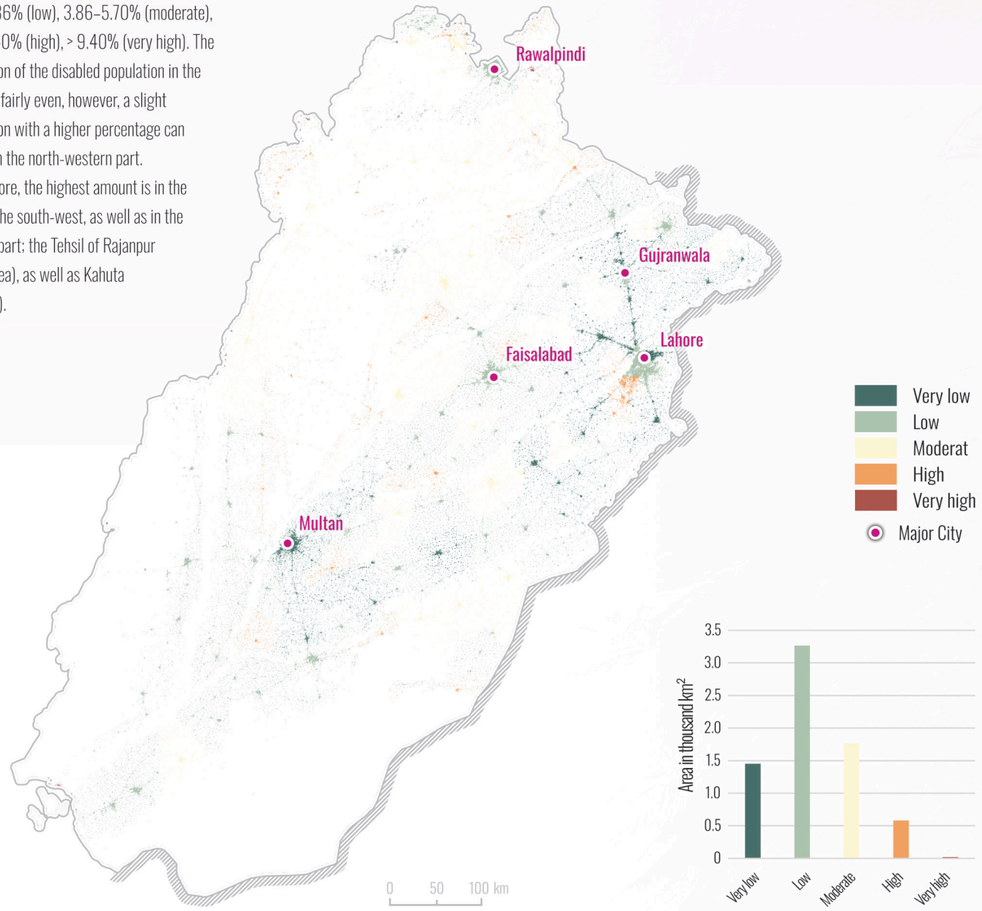

Map 3.3: Distribution of Disabled Population classes in the study area.

Figure 3.2: Distribution of Disabled Population classes by area (km^2) in inhabited places.

PSC

Disabled Population (DiP) percentages were calculated per Tehsil using census data. People with disabilities face heightened vulnerability during flood events. DiP values ranged from 1.67% to 15.73%, with a mean of 4.21%. Using Natural Breaks classification, five classes were created: ≤2.65% (very low), 2.65–3.86% (low), 3.86–5.70% (moderate), 5.70–9.40% (high), and >9.40% (very high). Most inhabited areas fall into the low (46.10%) and moderate (24.92%) categories. Higher DiP values appear in some northwestern and southwestern Tehsils, especially Rajanpur (Tribal Area) and Kahuta. Though the highest classes cover smaller areas, they mark zones of significantly increased flood vulnerability.

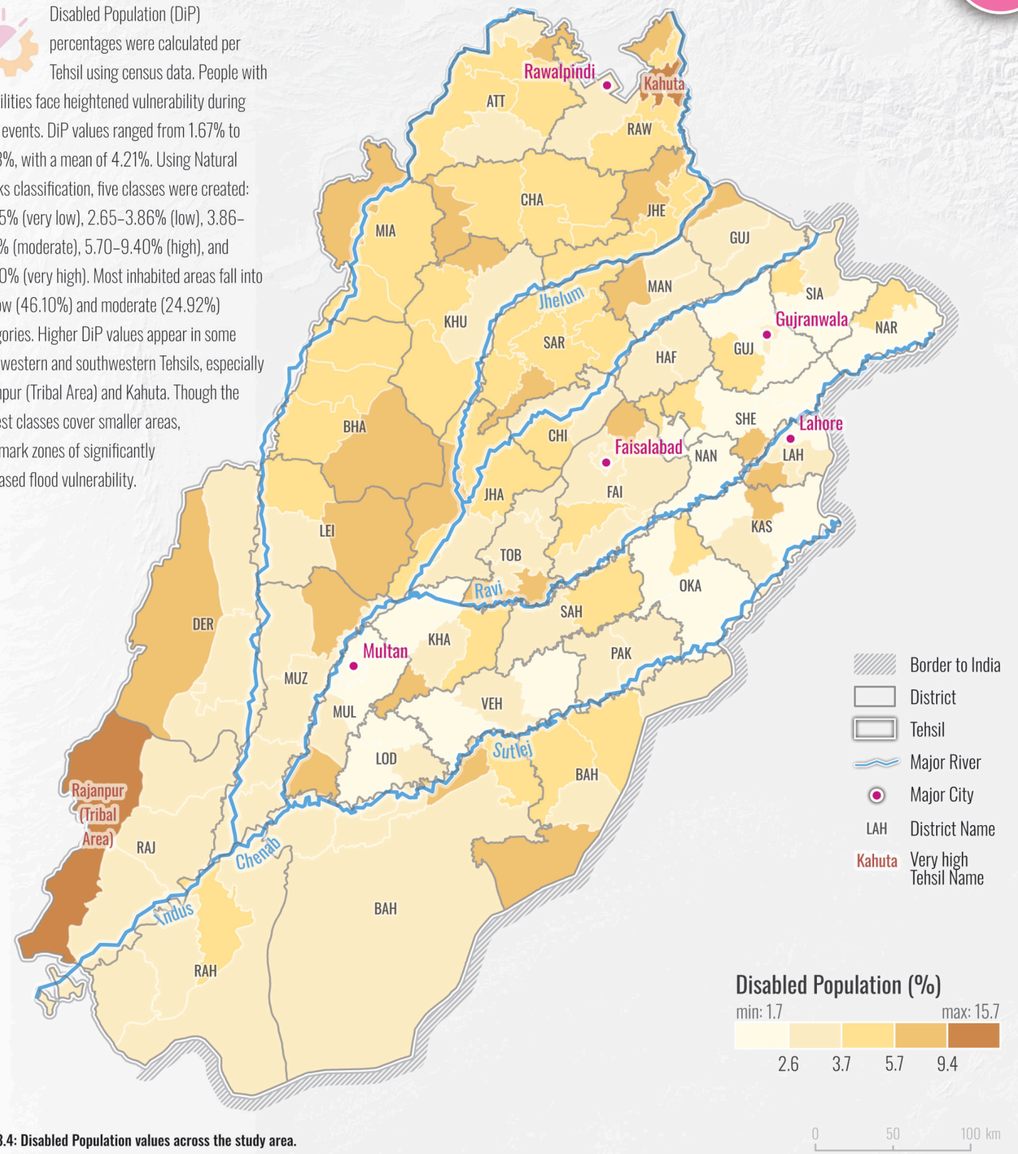

Map 3.4: Disabled Population values across the study area.

Female Population

Female population might have more difficulties in flooding situation and their mobility during evacuating, e.g., during pregnancy (Neumayer and Plümper, 2007). The share of the Female Population (FP) ranged from 46.12% to 52.02%, with a mean of 49.00% and a SD of 0.91%. Natural Breaks were chosen as an interval method. The values were classified into five classes: ≤ 48.02% (very low), 48.02–48.77% (low), 48.77–49.40% (moderate), 49.40–50.20% (high), > 50.20% (very high).

The classification describes 22.58% (1598.95 km^2) in very low, 23.56% (1668.64 km^2) in low, 30.58% (2165.22 km^2) in moderate, 20.11% (1423.83 km^2) as high, and 3.18% (225.01 km^2) as very high in inhabited areas (Figure 3.3, Map 3.5).

The higher percentage can be seen in the northern part in the Tehsils of Bhalwal, Chakwal, Gujar Khan, Jand, Kahuta, Kallar Sayaddan, Naushera (Map 3.6).

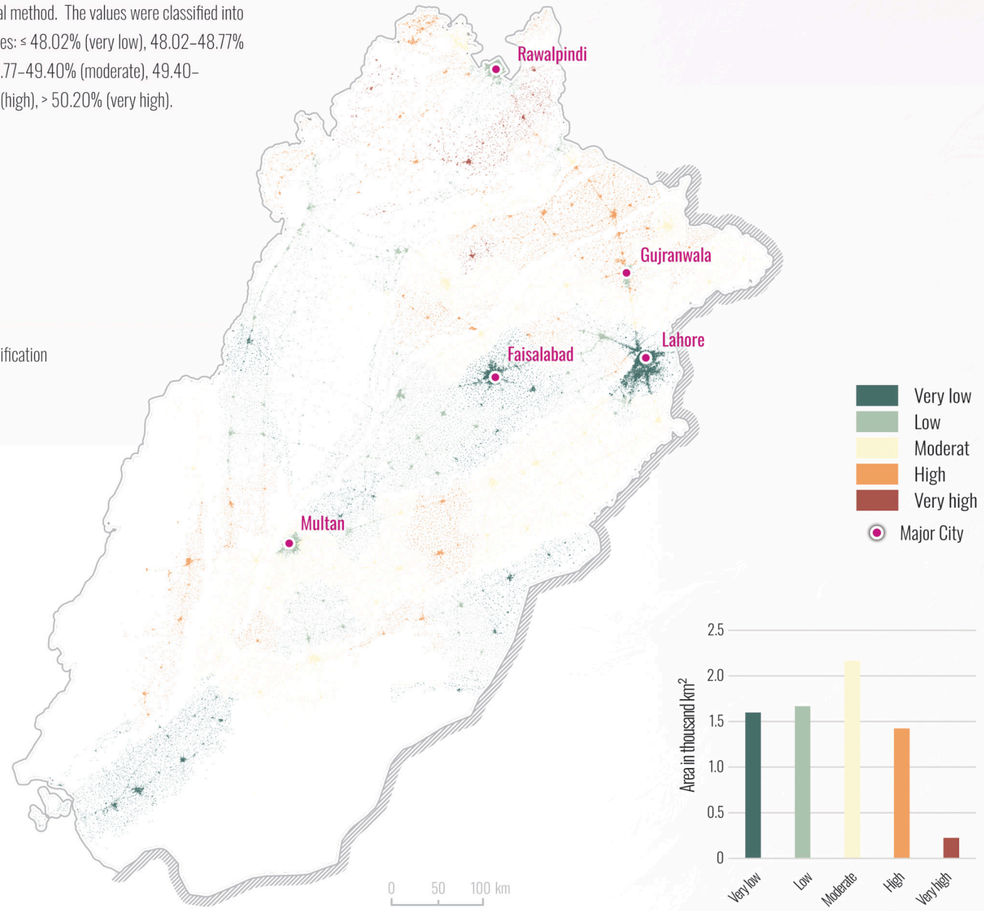

Map 3.5: Distribution of Female Population classes in the study area.

Figure 3.3: Distribution of Female Population classes by area (km^2) in inhabited places.

PSC

Census data was used to calculate the share of female population (FP) per Tehsil. Since women—particularly pregnant women—may face greater challenges during floods, higher FP percentages can indicate increased vulnerability. The FP ranged from 46.12% to 52.02%, with a mean of 49%. Using Natural Breaks, the data was classified into five categories: ≤ 48.02% (very low), 48.02–48.77% (low), 48.77–49.40% (moderate), 49.40–50.20% (high), and > 50.20% (very high). Most moderate to high values are located in northern Tehsils such as Bhalwal, Chakwal, and Kahuta.

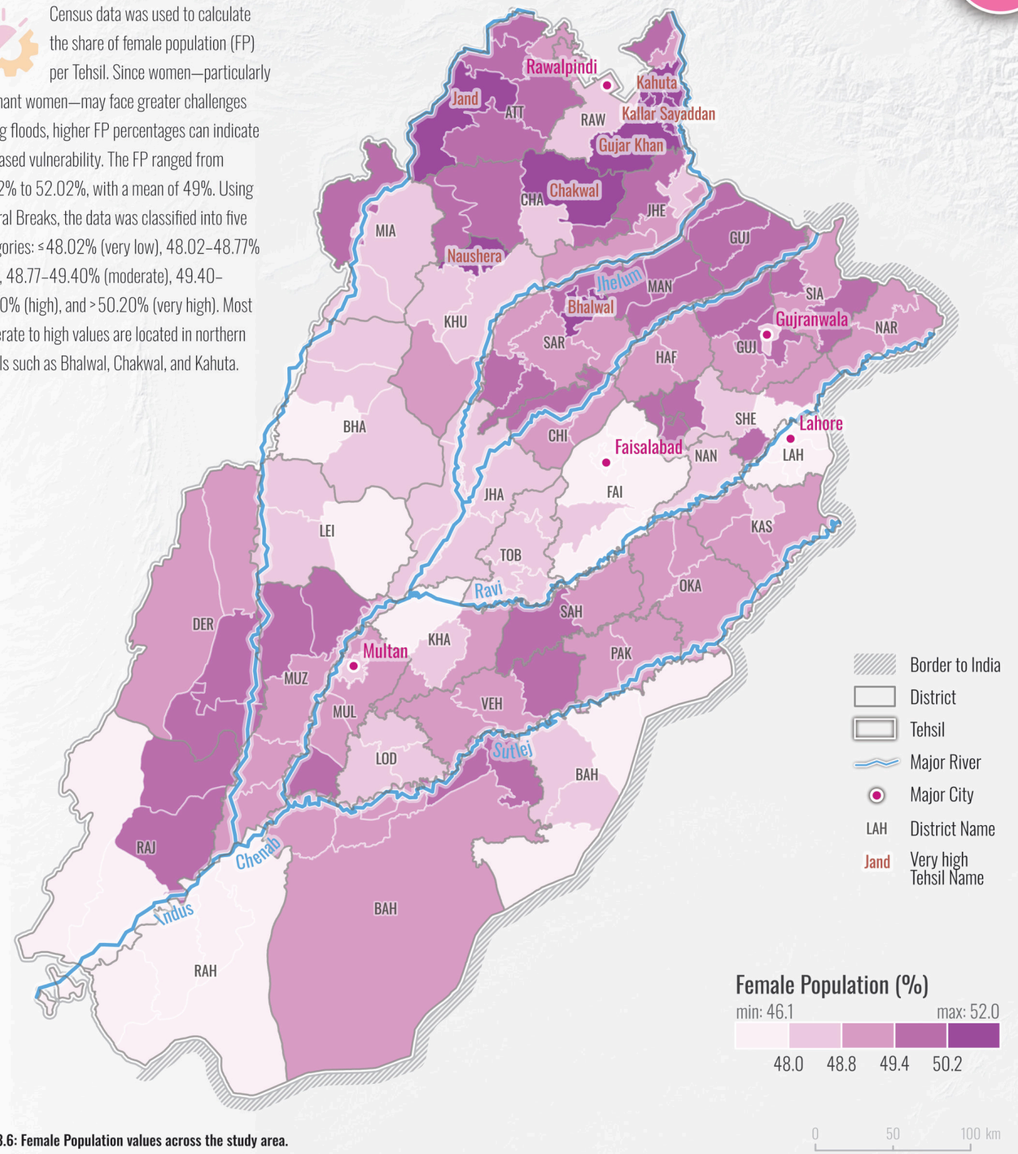

Map 3.6: Female Population values across the study area.

Population Density

Higher Population Density (PD) is considered more vulnerable (Hoque et al., 2019). The values ranged from 8.56 pop./km^2 to 18,945.59 pop./km^2, with a mean of 1276.36 pop./km^2 and a SD of 2866.66 pop./km^2. Natural Breaks was chosen as an interval method and the layer categorized into five classes: ≤ 600 pop./km^2 (very low), 600–2000 pop./km^2 (low), 2000–4000 pop./km^2 (moderate), 4000–9000 pop./km^2 (high), > 9000 pop./km^2 (very high). The classification describes 28.61% (2025.85 km^2) in very low, 53.92% (3818.63 km^2) in low, 8.74% (619.24 km^2) in moderate, 3.06% (216.62 km^2) as high, and 5.67% (401.31 km^2) as very high in inhabited places (Figure 3.4, Map 3.7).

The higher population density can be seen in the city Tehsils, especially in Faisalabad City, Gujranwala City, Model Town, and Lahore City (Map 3.8). However, since the AHP identified the PD as the least influential parameter of the PSC, its impact will be smaller than the other ones.

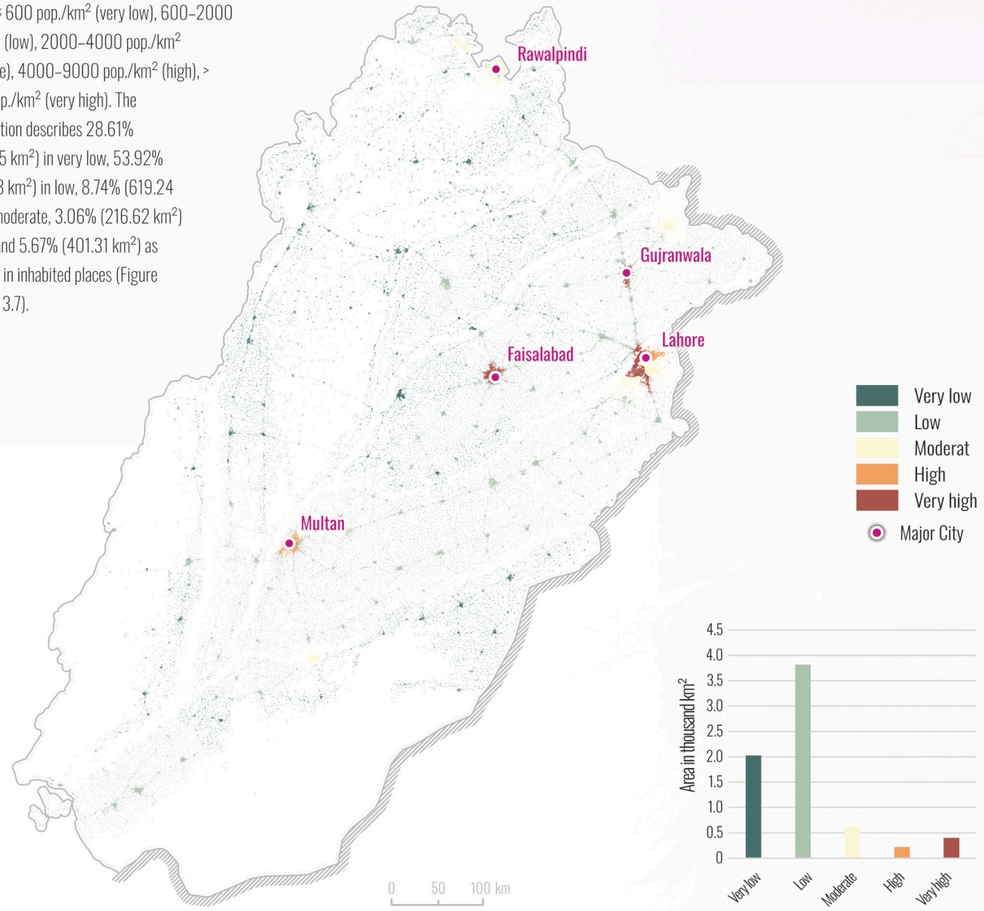

Map 3.7: Distribution of Population Density classes in the study area.

Figure 3.4: Distribution of Population Density classes by area (km^2) in inhabited places.

PSC

Population Density (PD) was calculated using census data by dividing population totals by Tehsil areas, then joined with administrative boundaries. Since denser populations are more flood-vulnerable, PD was classified using Natural Breaks into five classes: ≤ 600 (very low), 600–2000 (low), 2000–4000 (moderate), 4000–9000 (high), and > 9000 pop./km^2 (very high). Most areas fall into low (53.92%) and very low (28.61%) categories. High-density zones include urban Tehsils like Faisalabad City, Gujranwala City, Model Town, and Lahore City. Despite this, AHP ranked PD as the least influential factor in the PSC, meaning its contribution to flood vulnerability is relatively minor.

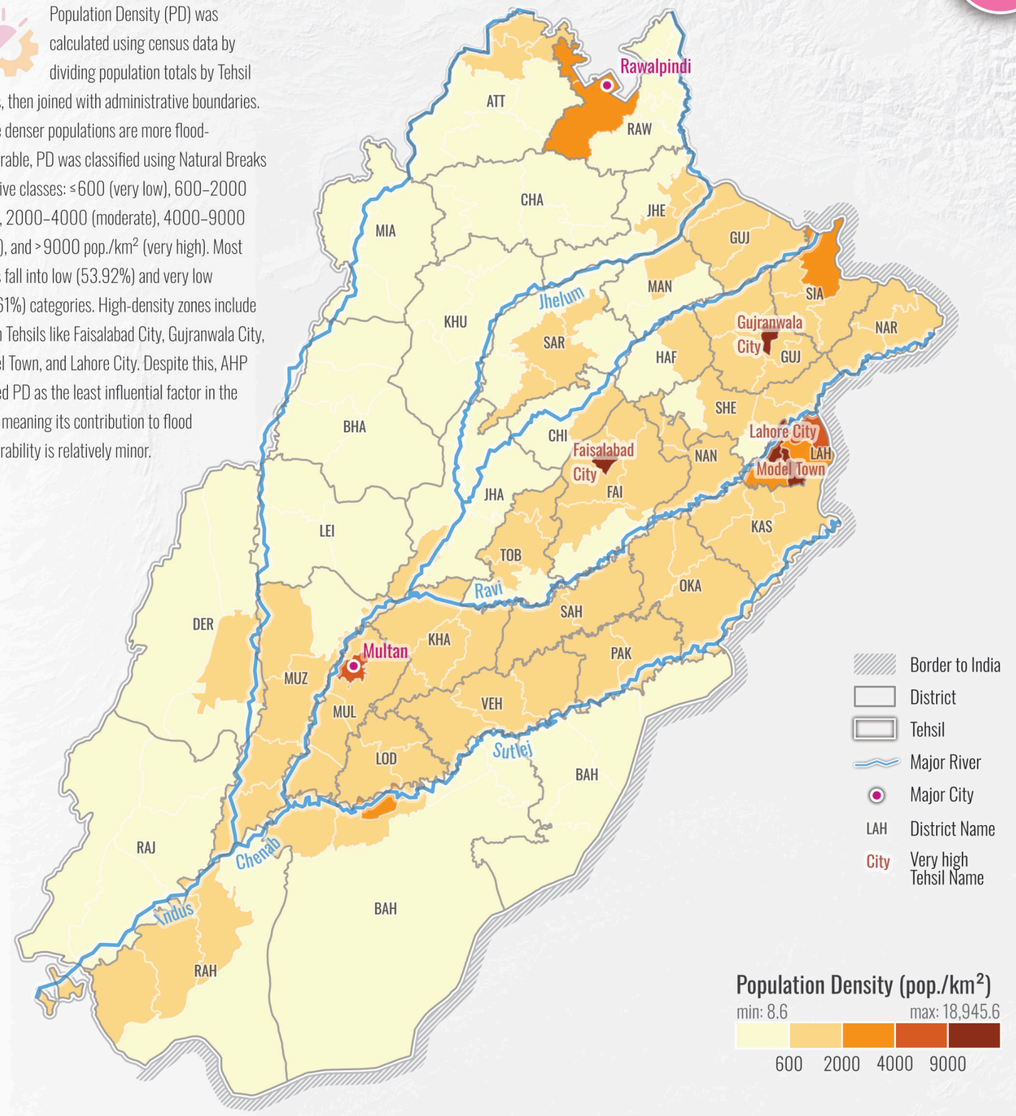

Map 3.8: Values of the PD in the study area.

Population Susceptibility Component

The Population Susceptibility Component (PSC) Map was created with overlay analyses based on its parameters and the weights. The map ranged from 1 (very low population susceptibility) to 4 (high population susceptibility); while 1.89% (133.86 km^2) in very low, 48.78% (3454.19 km^2) is low, 47.91% (3392.97 km^2) is moderate, and 1.42% (100.63 km^2) in high population susceptibilit in inhabited places in the PSC pixel map (Figure 2.5, Map 3.9).

Higher susceptibility are mostly located in rural areas, while areas with less population susceptibility are in urban areas.

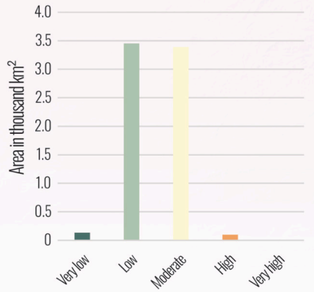

Figure 3.5: Distribution of PSC classes by area (km^2) in inhabited places.

The Population Susceptibility Component (PSC) was assessed using the Analytical Hierarchy Process (AHP) to evaluate the relative importance of four key parameters: Dependent Population (DeP), Disabled Population (DiP), Female Population (FP), and Population Density (PD). A structured pairwise comparison method, based on Saaty's 1–9 importance scale, was employed to reflect expert judgment.

Expert opinions were gathered through a survey conducted via the online tool QuestionPro. The survey was completed by eight professionals from Pakistan and five climate risk analysts from the United Nations University – Institute for Environment and Human Security (UNU-EHS).

Participants rated the importance of each parameter relative to the others, and their responses were used to construct pairwise comparison matrices. The geometric mean of the responses was applied to populate the PSC matrix (Table 3.1).

The normalized values and final weights (Table 3.2) showed that the Disabled Population (0.41) and Dependent Population (0.34) were considered the most influential indicators of population susceptibility. Female Population (0.17) and Population Density (0.08) were seen as less influential but still relevant.

To ensure the reliability of these judgments, the matrix was evaluated using eigenvalue-based consistency measures. This included the normalization of matrices, computation of weighted sums, consistency vectors, and the maximum eigenvalue value. The resulting consistency ratio (CR) of 0.04 confirmed the internal consistency and validity of expert assessments.

Table 3.1: Pairwise comparison matrix for PSC.

Parameter	DeP	DiP	FP	PD
DeP	1	1	2	4
DiP	1	1	4	4
FP	1/2	1/4	1	3
PD	1/4	1/4	1/3	1

Table 3.2: Normalized vector for CCC.

Parameter	DeP	DiP	FP	PD	Weight
DeP	0.36	0.4	0.27	0.33	0.34
DiP	0.36	0.4	0.55	0.33	0.41
FP	0.18	0.1	0.14	0.25	0.17
PD	0.09	0.1	0.05	0.08	0.08

PSC

The PSC map revealed that most inhabited areas fall within the low (48.78%) and moderate (47.91%) susceptibility classes, with only a small portion classified as high (1.42%) or very low (1.89%). Higher susceptibility is predominantly found in rural regions, driven by larger proportions of dependent and disabled populations, while urban areas tend to show lower susceptibility levels.

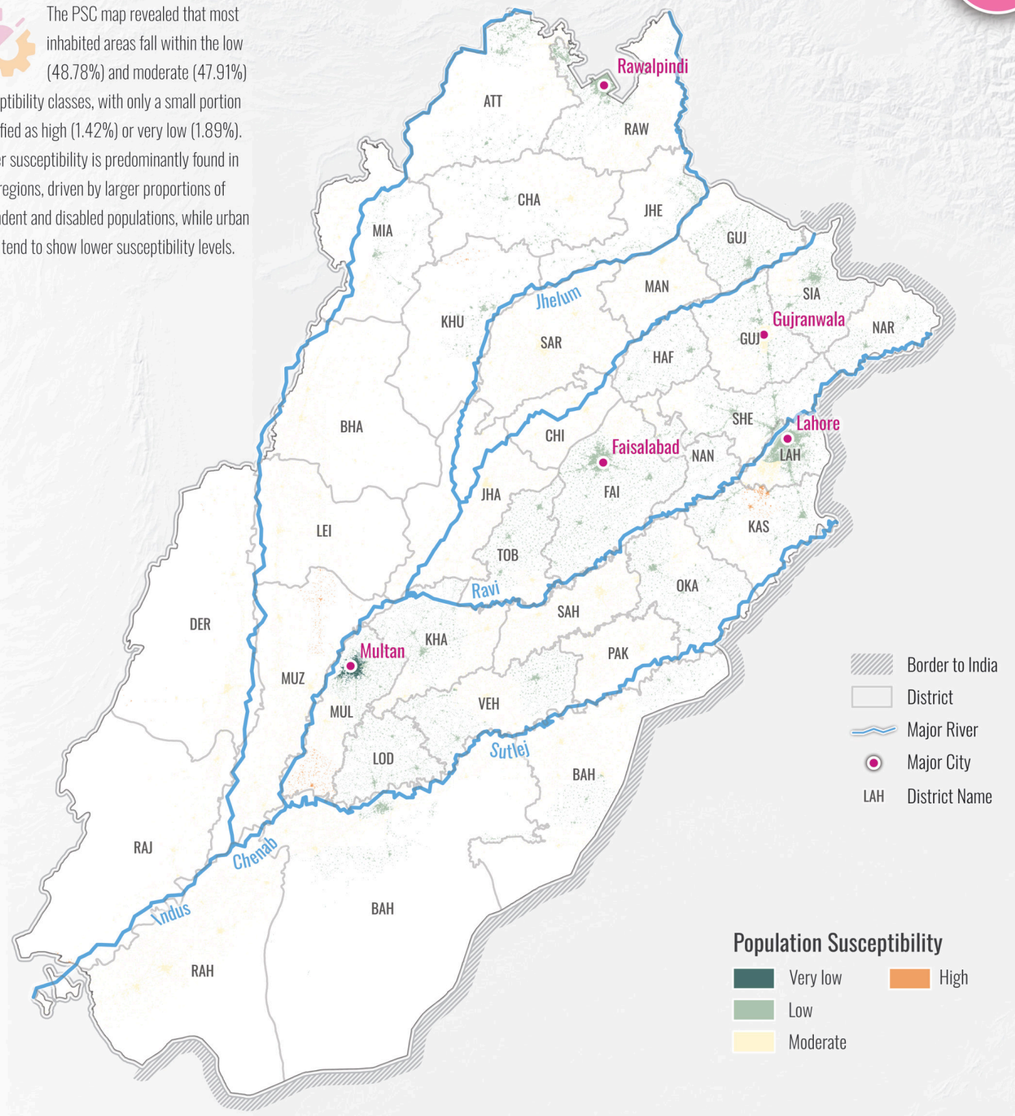

Map 3.9: PSC classes distribution in the study area in inhabited places.

Population Susceptibility Component at Tehsil level

The Population Susceptibility Component (PSC) aggregated to Tehsils (Map 3.10) showed that the Tehsils Jalalpur Pirwala, Kot Radha Kishen, Chowk Sarwar Shaheed, Naushera, Rajanpur (Tribal Area), and Koh-e-Suleman are identified as the highest population susceptibility. These Tehsils are mostly located in rural areas, while areas with less population susceptibility are in urban areas. As the AHP evaluated the population density as the lowest influential factor (8%) it makes sense, that the rural areas achieved higher values, as they are characterized by a higher percentage of dependent and disabled population.

Table 3.3, shows the values of the average PSC values, which range from 1.00 to 4.00. As the data was available as Tehsil census data, the average data values are at whole numbers when aggregating the Tehsil. However, comparing Map 3.9 and Map 3.10 the importance of dasymetric mapping becomes clear.

Dasysmetic mapping plays a crucial role in ensuring accuracy throughout the study. Without it, large Tehsils would appear highly vulnerable in the calculation of the Flood Vulnerability Index (FVI) pixel map, as every pixel of this large area would have data from the census data. While each settlement pixel within a Tehsil was assigned the same PSC value this approach offers a higher resolution and better interpretability than full-scaled aggregated data. The most accurate method would be to assign the individual pixel location the exact value based on household survey data for instance but given the unavailability of such data for the entire region, the adopted approach remains an effective and practical alternative. This is the same for the CCC, respectively.

Table 3.3: Tehsils with the heighest PSC.

Rank	Tehsil	Total Settlement Area (km²)	Moderate PS Settlement Area (km²)	High PS Settlement Area	% of High	Average PSC Class
1	Jalalpur Pirwala	34.43	0	34.43	100.00%	400.00%
2	Kot Radha Kishen	33.72	0	33.72	100.00%	400.00%
3	Chowk Sarwar Shaheed	22.18	0	22.18	100.00%	400.00%
4	Naushera	5.33	0	5.33	100.00%	400.00%
5	Rajanpur (Tribal Area)	3.49	0	3.49	100.00%	400.00%
6	Koh-e-Suleman	1.47	0	1.47	100.00%	400.00%
7	Zafarwal	27.56	27.56	0	0.00%	300.00%
8	Vehari	73.74	73.74	0	0.00%	300.00%
9	Taunsa	32.33	32.33	0	0.00%	300.00%
10	Sohawa	20.18	20.18	0	0.00%	300.00%

To visualize PSC distribution regionally, the mean PSC values were calculated at the Tehsil level using Zonal Statistics. This method averages pixel values within each Tehsil, allowing for easy comparison of population susceptibility across administrative regions.

PSC

The PSC aggregated to the Tehsil level highlighted Jalalpur Pirwala, Kot Radha Kishen, Chowk Sarwar Shaheed, Naushera, Rajanpur (Tribal Area), and Koh-e-Suleman as the most population-susceptible areas; primarily rural Tehsils with high proportions of dependent and disabled populations. Urban areas showed lower susceptibility. Due to population density being the least weighted factor in AHP, rural areas ranked higher.

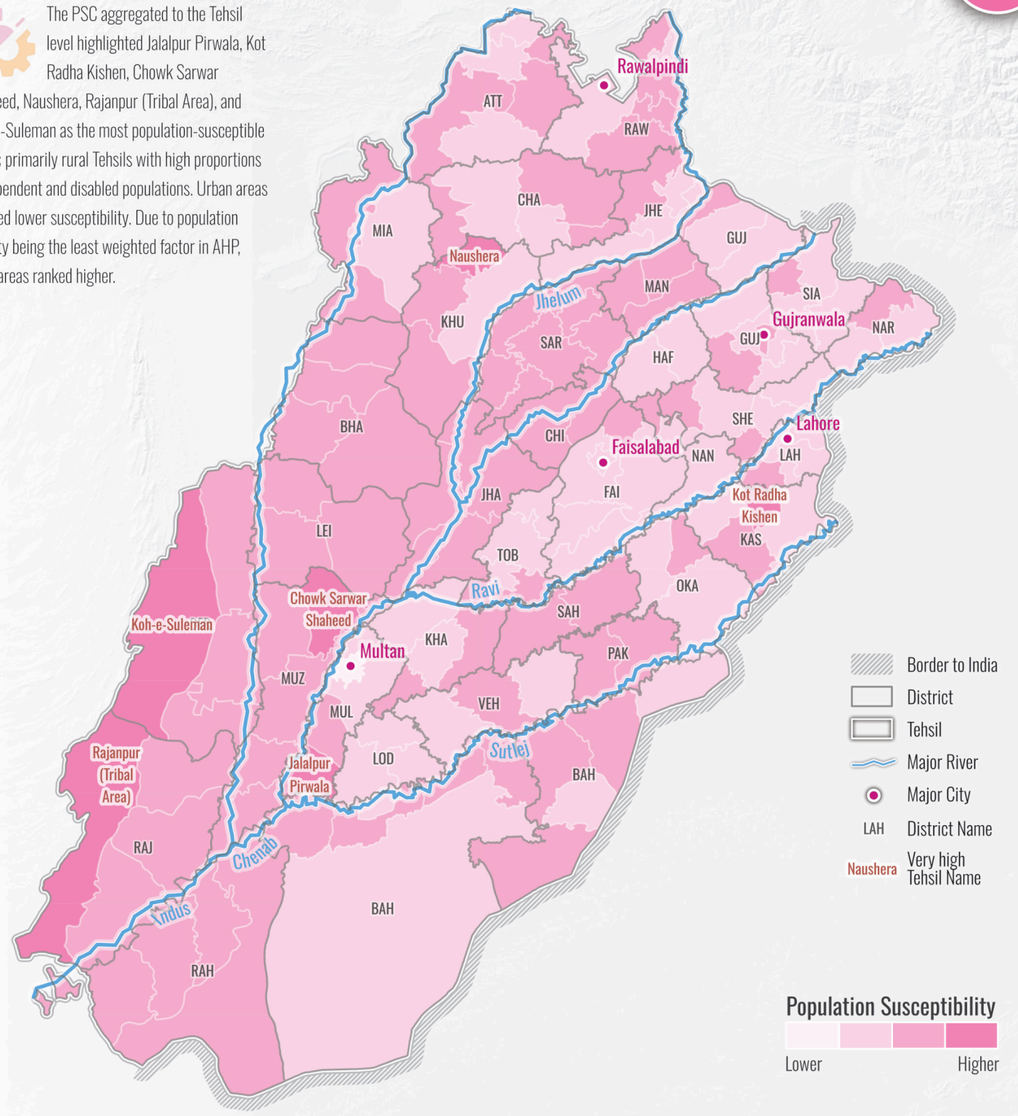

Map 3.10: PSC aggregated to Tehsils (The top 6 Tehsils with the highest flood-prone score are labelled).

CCC

Coping Capacity Component

Distance to Health Facilities

Literacy Rate

Coping Capacity Component

Coping Capacity Component at Tehsil level

The third component of the FVI is the Coping Capacity Component (CCC). According to UNISDR (2009), the coping capacity is the "ability of people, organizations, and systems, using available skills and resources, to face and manage adverse conditions, emergencies or disasters". Due to data limitations, two capacity coping parameters were chosen (Kablan, Dongo and Coulibaly, 2017; Hoque et al., 2019): the Distance to Health Facilities (DH), and the Literacy Rate (LR).

The component of the coping capacity consists of two criteria, i.e., Distance to Health Facilities (DH) and Literacy Rate (LR). The distance to health facilities was calculated with 'Distance Accumulation'. Similar to the PSC parameters, the literacy rate was derived from the 2023 census data and combined with the administrative boundaries of the Tehsils. As the census data was available on administrative boundaries (Tehsils), a dasymetric map was created for all PSC parameter maps. A dasymetric map is a thematic mapping technique in which statistical data is redistributed on the basis of additional spatial information to provide a more accurate representation of population distribution within administrative boundaries (Eicher and Brewer, 2001). To get this information, the Tehsil map was masked out with settlement data, derived from the Land Use Land Cover. A settlement layer was created based on the LULC consisting of buildings (1), and no-buildings (0); each PSC parameter map was then calculated with the equation below:

$$\text{CCC } paramter\ map\ masked = settlements \times \text{CCC } parameter\ map$$

The CCC represents human-related vulnerability, therefore, the dasymetric mapping method ensures that the analysis of CCC is only represented in settled areas. This prevents overestimation in large, sparsely populated Tehsils and provides a more realistic spatial representation of human vulnerability.

Distance to Health Facilities

The values of Distance to Health Facilities (DH) ranged from 0 m to 140,110.78 m, with a mean of 24,995.72 m and a SD of 22,050.09 m. The layer was classified in accordance with other literature (Hoque et al., 2019). The values were classified into five classes: ≤ 2000 m (very high), 2000–4000 m (high), 4000–6000 m (moderate), 6000–8000 m (low), > 8000 m (very low). Especially in the major cities of Punjab health facilities can be found (Map 4.2).

The classification describes 50.04% (3897.82 km^2) in very low, 6.77% (479.66 km^2) in low, 7.18% (508.60 km^2) in moderate, 9.76% (691.45 km^2) as high, and 21.24% (1504.12 km^2) as very high in inhabited places (Figure Figure 4.1, Map 4.1). The distribution highlights that urban areas have better connections to health facilities. Rural areas, with distances often more than 8000 m, may be more vulnerable to flood events as they may face difficulties in flood events in assessing essential emergency services.

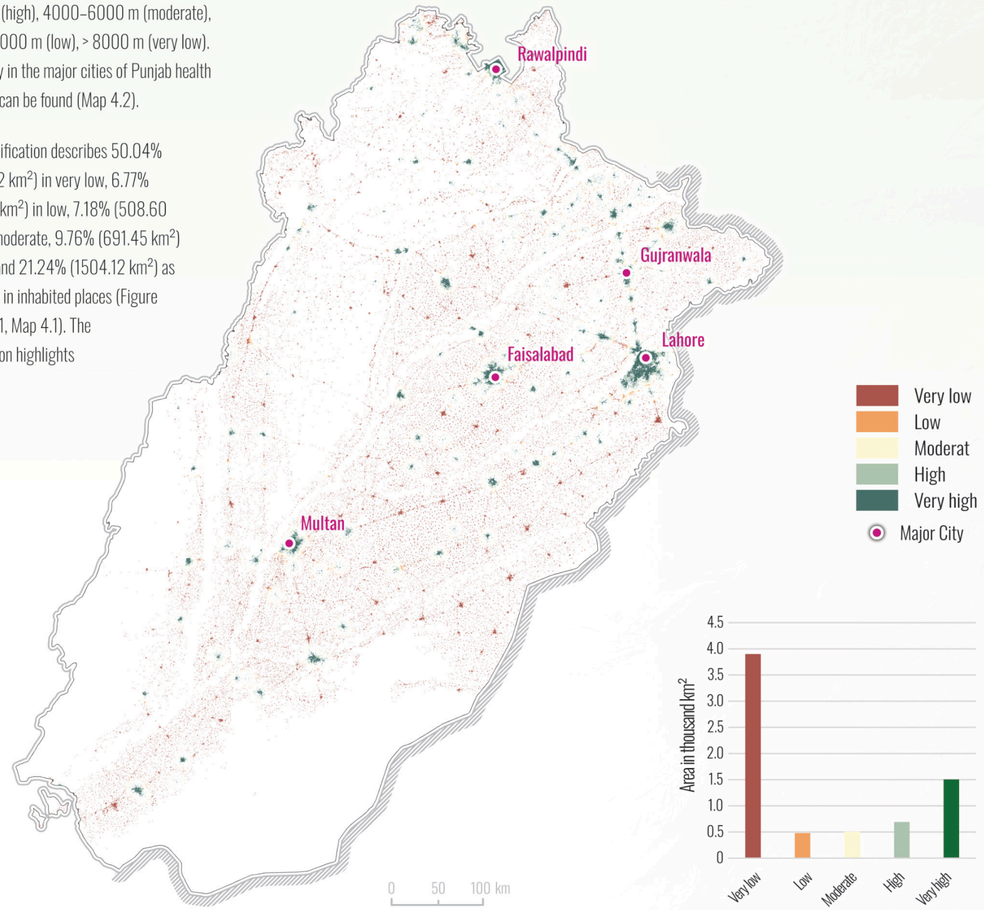

Map 4.1: Distribution of Distance to Health Facilities classes in the study area.

Figure 4.1: Distribution of Distance to Health Facilities classes by area (km^2) in inhabited places.

CCC

The Distance to Health Facilities (DH) was calculated using OSM data and the 'Distance Accumulation' tool. Distances ranged from 0 to 140,110.78 meters, with a mean of 24,995.72 meters and a standard deviation of 22,050.09 meters. Based on existing literature, the data were classified into five categories: ≤2000 m (very high accessibility), 2000–4000 m (high), 4000–6000 m (moderate), 6000–8000 m (low), and >8000 m (very low accessibility). The results show that urban areas, particularly major cities in Punjab, generally have better access to health facilities. However, 50.04% (3,897.82 km^2) of inhabited areas fall into the very low accessibility category, indicating that a large portion of the population may face difficulties accessing emergency health services during flood events. This highlights a significant vulnerability in more remote or rural regions.

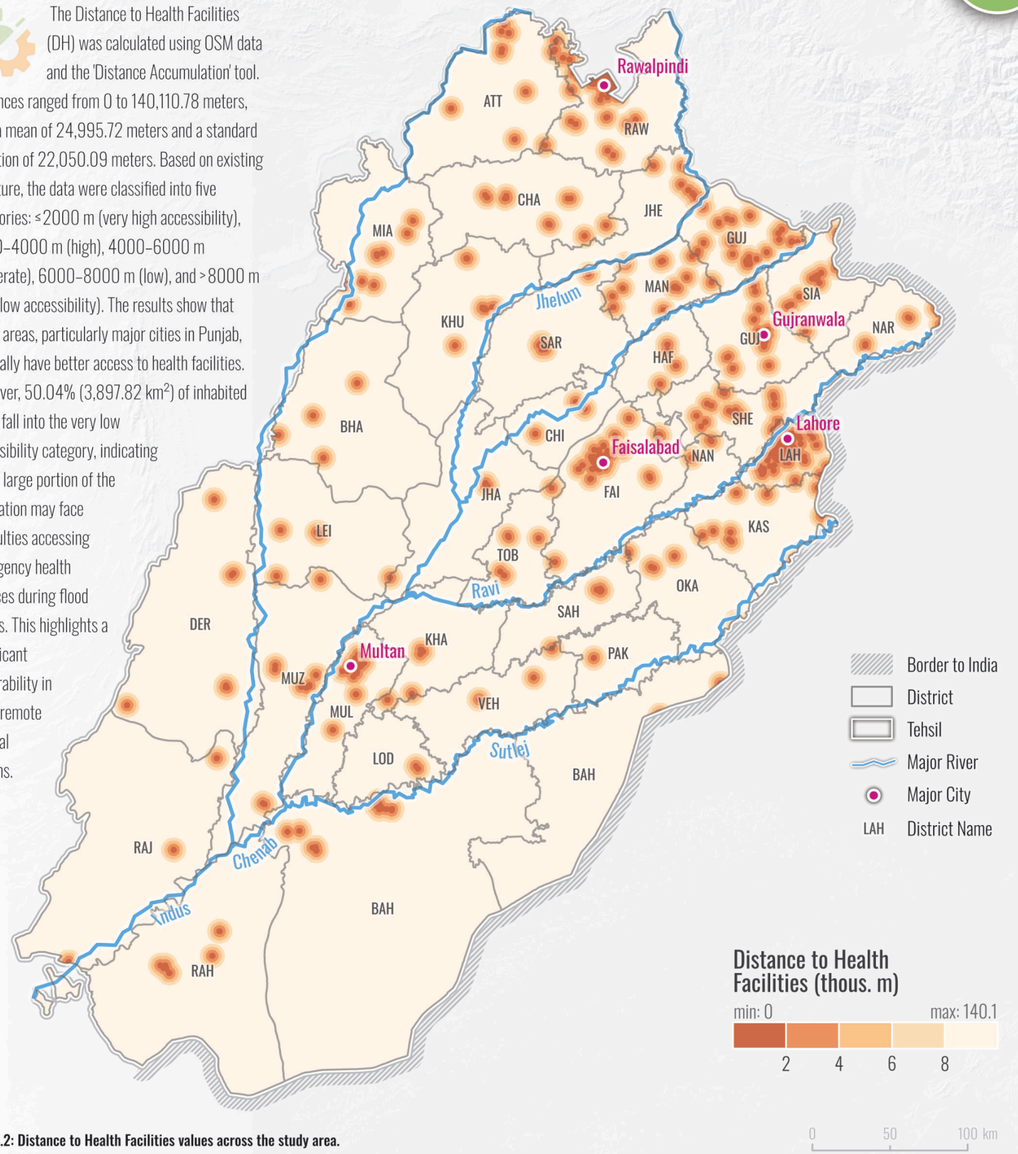

Map 4.2: Distance to Health Facilities values across the study area.

Literacy Rate

Through low literacy rate warnings can be missed (Hagenlocher et al., 2016). The values of the Literacy Rate (LR) layer ranged from 8.60% to 88.20%, with a mean of 63.94% and a SD of 13.30%. Natural Breaks were chosen as an interval method and the layer was classified into five classes: ≤ 44.05% (very low), 44.05–59.02% (low), 59.02–67.55% (moderate), 67.55–76.28% (high), > 76.28% (very high).

Low literacy rates can be found in the southwestern part of the province, and in the rural areas, while in the cities and in the northern part, high literacy rate is drawn

The classification describes 5.41% (383.26 km^2) in very low, 28.17% (1995.21 km^2) in low, 23.47% (1662.22 km^2) in moderate, 20.10% (1423.17 km^2) as high, and 22.84% (1617.79 km^2) in very high literacy rate in inhabited places (Figure 4.2, Map 4.3). The Tehsils with the lowest values are Ahmadpur East, Alipur, Jalalpur Pirwala, Jampur, Jatoi, Koh-e-Suleman, Kot Chatta, Liaqatpur, Minchinabad, Rajanpur, Rajanpur (Tribal Area), Rojhan. This distribution shows that areas with limited literacy, mainly the rural areas, may face challenges when flood warnings are communicated (Map 4.4).

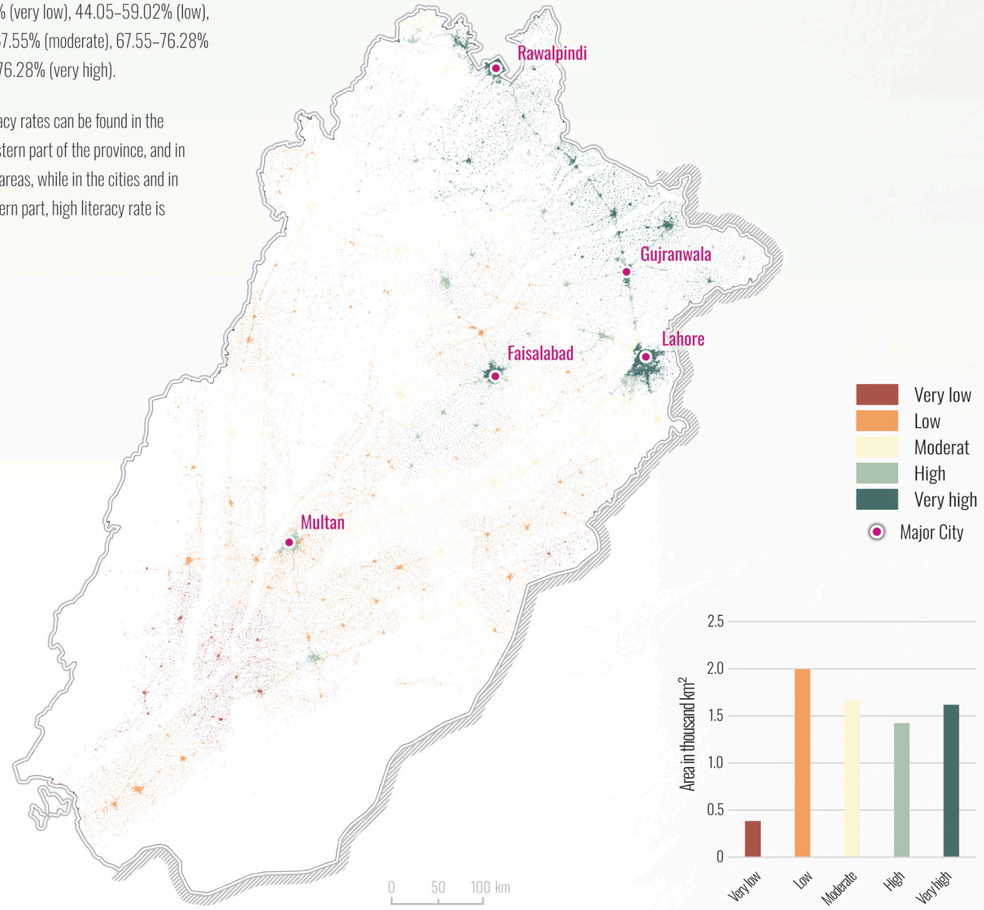

Map 4.3: Distribution of Literacy Rate classes in the study area.

Figure 4.2: Distribution of Literacy Rate classes by area (km^2) in inhabited places.

CCC

Data from the 2023 census was used to assess literacy across Tehsils. Literacy rates varied between 8.60% and 88.20%, with an average of 63.94%. Using Natural Breaks, five classes were defined: very low (≤ 44.05%) to very high (> 76.28%). Low literacy—linked to poor flood warning comprehension—is mostly found in rural and southwestern areas, while urban and northern regions show higher rates. In inhabited areas, 5.41% of land had very low literacy, while 22.84% had very high. Vulnerable Tehsils with the lowest literacy include Ahmadpur East, Alipur, Jatoi, and Rajanpur.

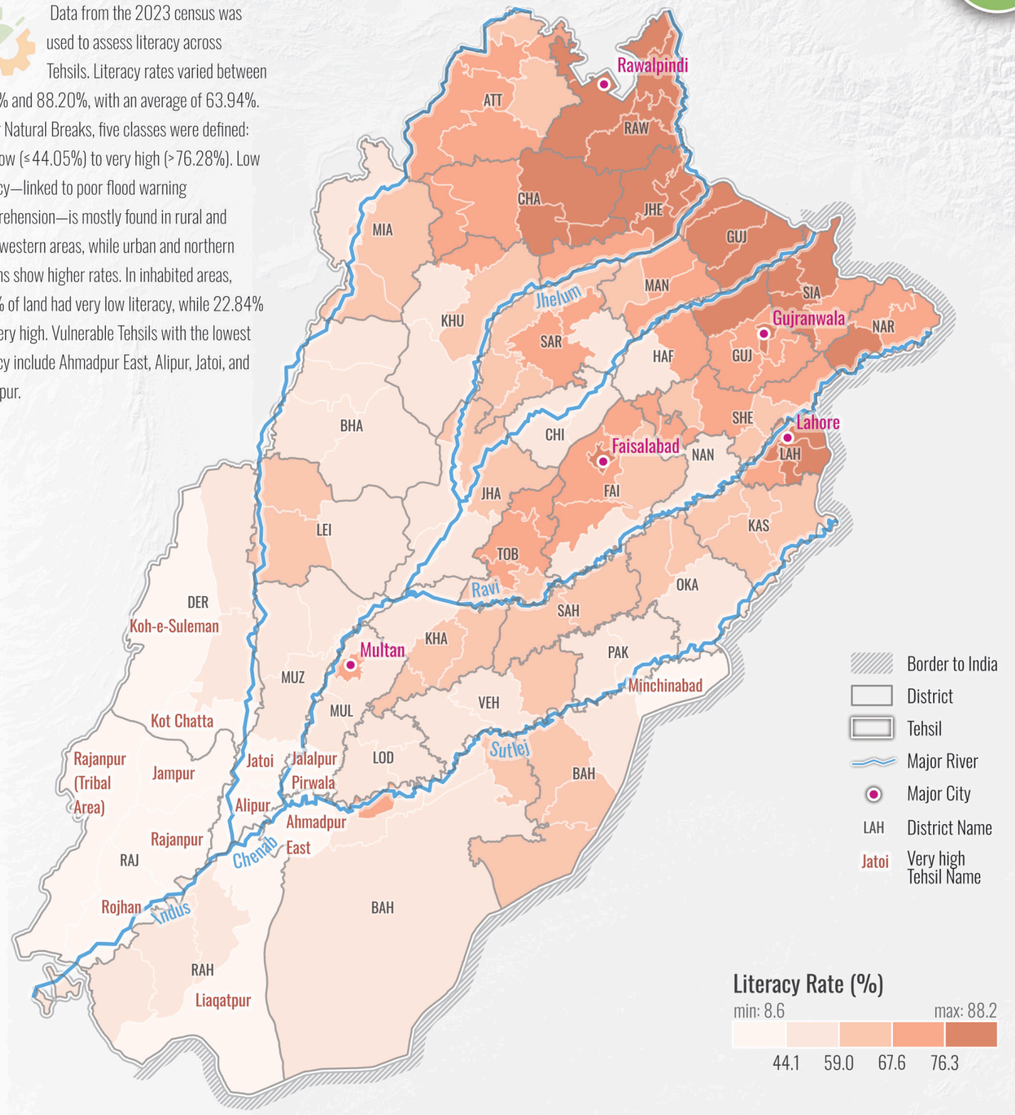

Map 4.4: Literacy Rate values across the study area.

Coping Capacity Component

The Coping Capacity Component (CCC) Map ranged from 1 (very low coping capacity) to 5 (very high coping capacity); while 26.64% (1886.33 km^2) of the study area is very low, 32.14% (2275.78 km^2) is low, 9.74% (689.99 km^2) is moderate, 15.00% (1061.94 km^2) in high, and 16.49% (1167.60 km^2) in very high coping capacity (Figure 4.3).

Urban areas are characterized by higher coping capacity, as cities have a higher presence of health facilities, and they were ranked as highest in the AHP (67%). Furthermore, the literacy rate is also higher in urban areas and to the north.

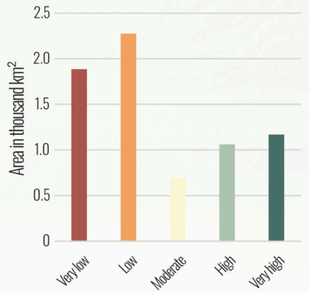

Figure 4.3: Distribution of CCC classes by area (km^2) in inhabited places.

The Coping Capacity Component (CCC) was assessed using the Analytical Hierarchy Process (AHP) to evaluate the relative importance of two key parameters: Distance to Health Facilities (DH) and Literacy Rate (LR). This structured method, based on Saaty's 1–9 scale, enabled expert-based prioritization of indicators relevant to community resilience.

Expert opinions were collected through a survey conducted via the online tool QuestionPro, involving eight professionals from Pakistan and five climate risk analysts from the United Nations University – Institute for Environment and Human Security (UNU-EHS). Participants performed pairwise comparisons of the CCC indicators, and the geometric mean of their responses was used to complete the matrix (Table 4.1).

The normalized values and final weights (Table 4.2) revealed that Distance to Health Facilities (0.67) was considered more influential than Literacy Rate (0.33) in determining coping capacity.

To ensure logical consistency, the matrix was tested using eigenvalue-based methods, including normalization, weighted sum, and consistency vector calculations. The resulting consistency ratio (CR) for the CCC matrix was 0.00, indicating perfect consistency by default.

Table 4.1: Pairwise comparison matrix for CCC.

Parameter	AR	DR	DD	EL	LULC	SL	TWI
AR	1	2	1	1	1	1	1
DR	1/2	1	1	1	1	1	1
DD	1	1	1	3	1	3	2
EL	1	1	1/3	1	1	1	1
LULC	1	1	1	1	1	3	2
SL	1	1	1/3	1	1/3	1	1
TWI	1	1	1/2	1	1/2	1	1

Table 4.2: Normalized vector for CCC.

Parameter	AR	DR	DD	EL	LULC	SL	TWI	Weight
AR	0.15	0.25	0.19	0.11	0.17	0.09	0.11	0.15
DR	0.08	0.13	0.19	0.11	0.17	0.09	0.11	0.13
DD	0.15	0.13	0.19	0.33	0.17	0.27	0.22	0.21
EL	0.15	0.13	0.06	0.11	0.17	0.09	0.11	0.12
LULC	0.15	0.13	0.19	0.11	0.17	0.27	0.22	0.18
SL	0.15	0.13	0.06	0.11	0.06	0.09	0.11	0.1
TWI	0.15	0.13	0.1	0.11	0.09	0.09	0.11	0.11

The CCC map shows that coping capacity is highest in urban areas, where access to health facilities and literacy rates are better. The majority of very high and high coping capacity zones are found in cities, with 16.49% and 15.00% of the area falling into these categories, respectively. In contrast, rural regions, especially in the south, show very low to low coping capacity, making up over half the study area.

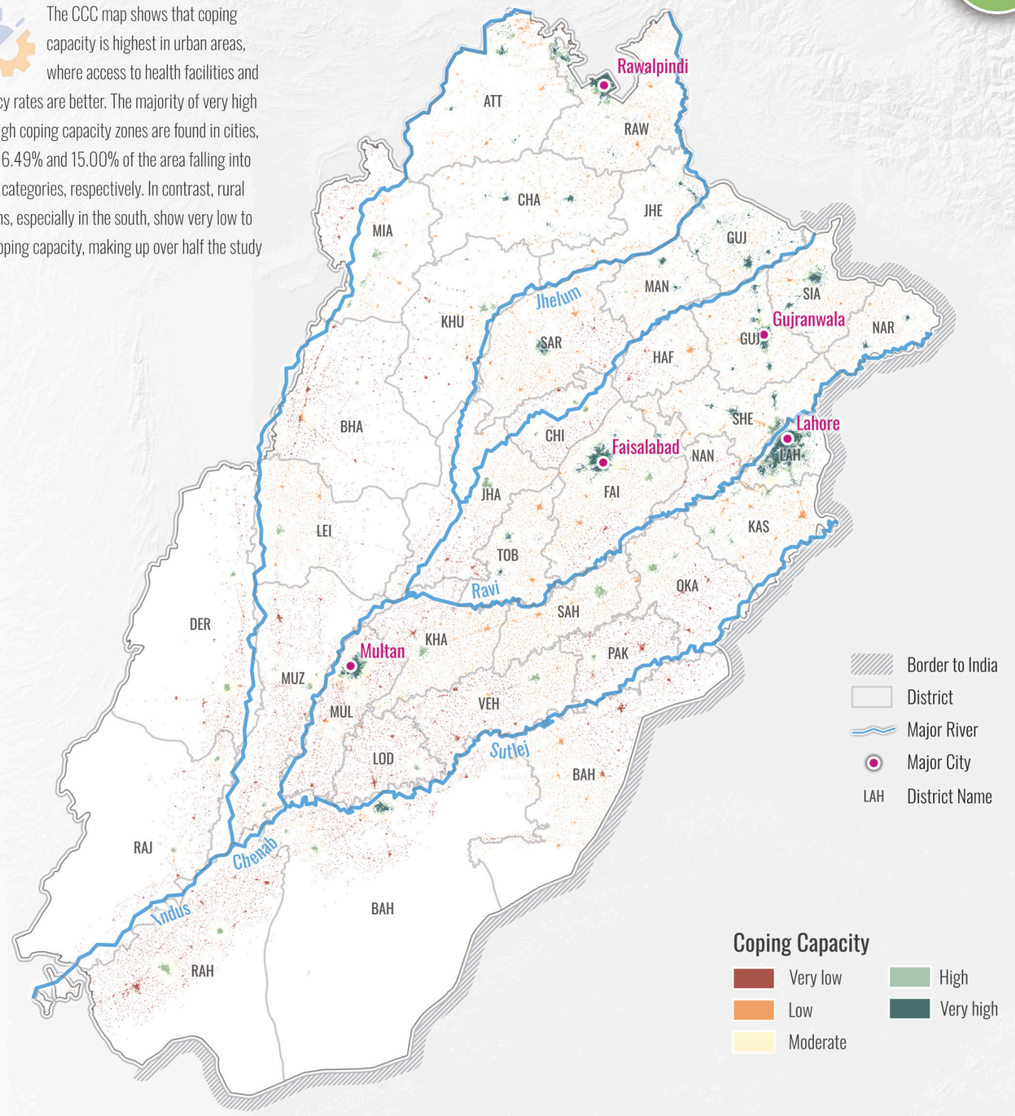

Map 4.5: Distribution of CCC classes in the study area.

Coping Capacity Component at Tehsil level

The CCC aggregated to Tehsils emphasizes the results (Map 4.6). Especially in urban areas, the ability to cope is high. Several Tehsils are identified with the lowest coping capacity (Table 4.3): Athara Hazari, Bahawalnagar, Isakhel, Jalalpur Pirwala, Jatoi, Kalur Kot, Liaqatpur, Pakpattan, Quaidabad, Noorpur, Shorkot, Kot Chatta. The average CCC values ranged from 1.00 to 4.92.

Table 4.3: CCC area of the classes.

Rank	Tehsil	Total Settlement Area (km²)	Very low CC Settlement (km²)	Low CC Area (km²)	Combined CC Settlement	% of Very low + Low	Average CC Class
1	Athara Hazari	20.17	20.17	0	2017.00%	100.00%	1
2	Bahawalnagar	64.36	64.36	0	6436.00%	100.00%	1
3	Isakhel	37.86	37.86	0	3786.00%	100.00%	1
4	Jalalpur Pirwala	34.43	34.43	0	3443.00%	100.00%	1
5	Jatoi	30.62	30.62	0	3062.00%	100.00%	1
6	Kalur Kot	26.2	26.2	0	2620.00%	100.00%	1
7	Liaqatpur	68.71	68.71	0	6871.00%	100.00%	1
8	Pakpattan	52.76	52.76	0	5276.00%	100.00%	1
9	Quaidabad	12.18	12.18	0	1218.00%	100.00%	1
10	Noorpur	25.71	25.68	0.03	2571.00%	100.00%	1
11	Shorkot	49.97	49.8	0.17	4997.00%	100.00%	1
12	Kot Chatta	26.16	26.04	0.13	2616.00%	100.00%	1
13	Sadiqabad	86.18	85.44	0.71	8615.00%	99.97%	1.01
14	Rojhan	12.07	11.99	0.07	1205.00%	99.82%	1.01
15	Dunyapur	37.4	37.05	0.35	3740.00%	100.00%	1.01
16	Depalpur	77.02	76.37	0.41	7678.00%	99.68%	1.01
17	Khairpur Tamewali	21.16	20.81	0.35	2116.00%	100.00%	1.02
18	Lodhran	55.52	54.56	0.91	5548.00%	99.92%	1.02
19	Kabirwala	72.18	69.9	2.04	7194.00%	99.67%	1.03
20	Minchinabad	29.27	28.07	1.09	2916.00%	99.62%	1.05

To visualize CCC distribution regionally, the mean CCC values were calculated at the Tehsil level using Zonal Statistics. This method averages pixel values within each Tehsil, allowing for easy comparison of coping capacity across administrative regions.

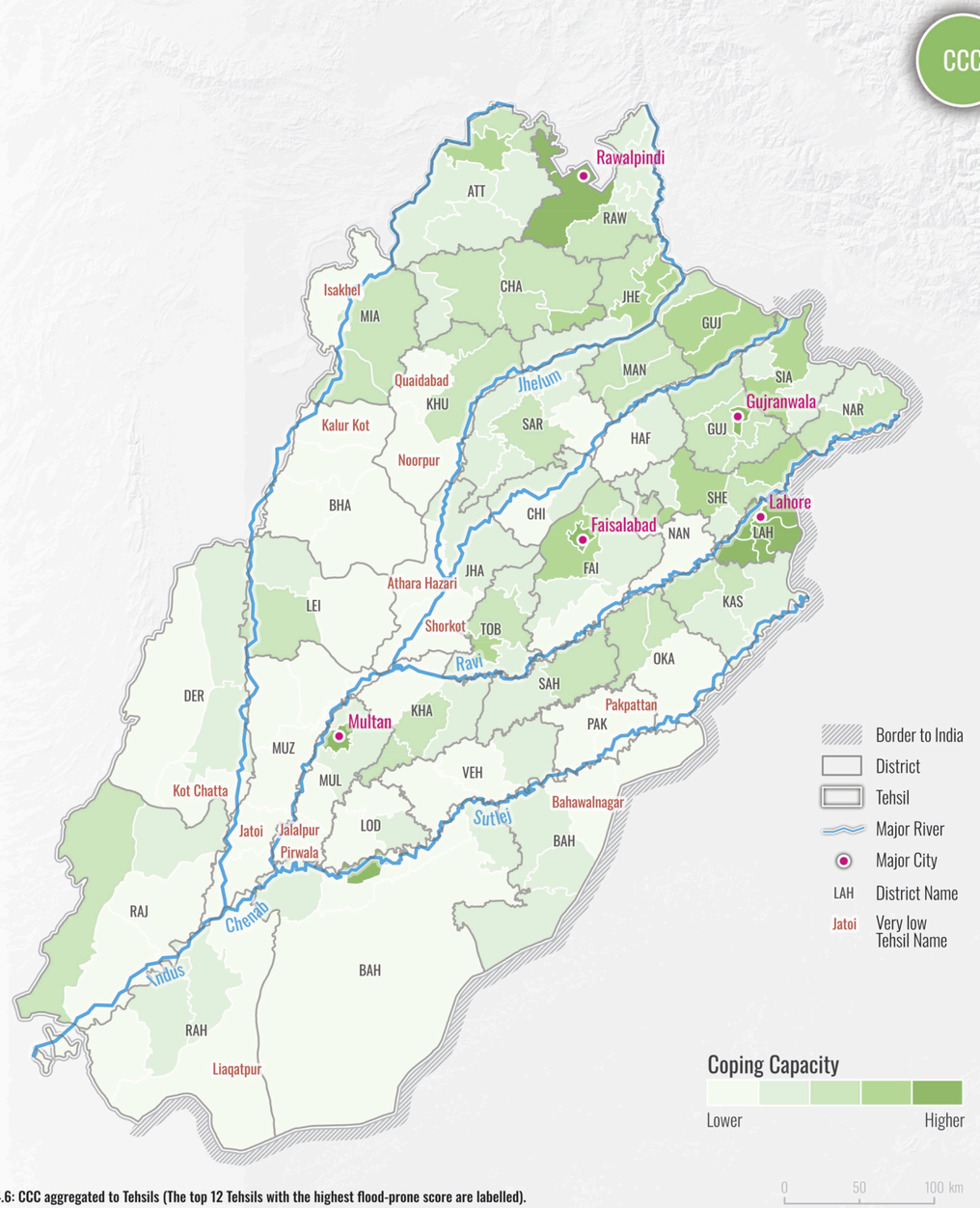

Map 4.6: CCC aggregated to Tehsils (The top 12 Tehsils with the highest flood-prone score are labelled).

FVI

Flood Vulnerablity Index

Flood Vulnerability Index

The Flood Vulnerability Index (FVI) was calculated by multiplying the Flood-Prone Component (PFC) with the Population Susceptibility Component (PSC) and dividing by the Coping Capacity Component (CCC). The FVI was classified using the Equal Interval method. The calculation of the FVI revealed that 13.28% (941 km^2) of the study area is in very high and high vulnerability areas in inhabited places in the FVI pixel map (Map 5.1). The FVI emphasizes that areas characterized by large flood-prone and large population susceptibility values, as well as low coping capacity are highly vulnerable.

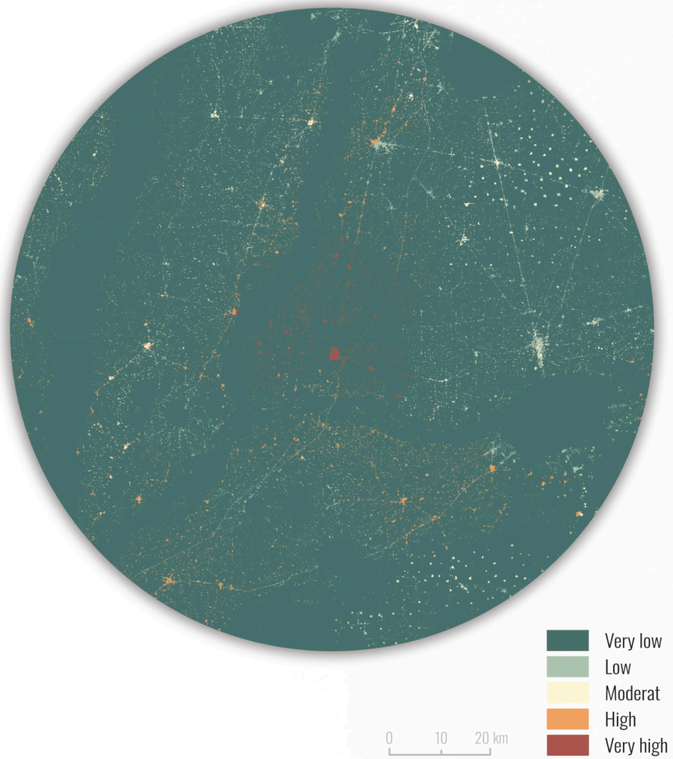

The FVI is calculated with the Equation:

$$FVI = \frac{(FPC \times PSC)}{CCC}$$

where represents the Flood Vulnerability Index, the Flood-Prone Component, the Population Susceptibility Component, and the Coping Capacity Component (CCC).

Since the PSC and the CCC outputs were masked with settlements to make sure to focus on actual human populations, a lot of Null values would exist in the results of this formula. In order to avoid computational issues and bias in the flood vulnerability calculation, areas with no data in PSC were given the lowest vulnerability class (1) to reflect the absence of population at risk. Areas with no data in the CCC were assigned with the highest coping capacity class (5) to indicate that uninhabited areas do not require coping mechanisms. This makes sure that higher FPC and PSC values indicate worse conditions (more risk), and higher CCC reduces it, respectively. The approach ensures that the FPC remains for the whole area, while PSC and CCC-related factors only apply to actual human populations, preventing distortions in the final vulnerability assessment.

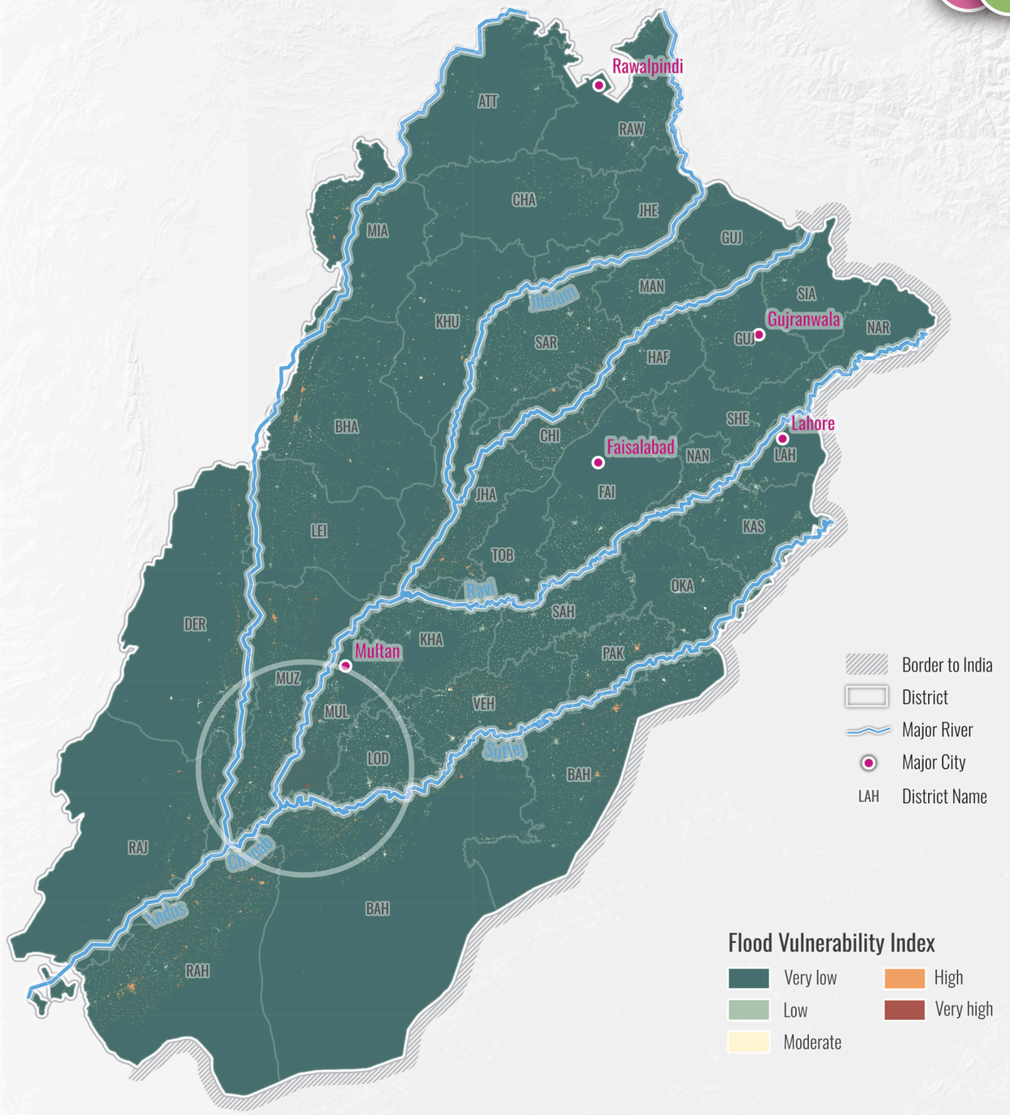

Map 5.1: Distribution of FVI classes in the study area.

Flood Vulnerability Index at Tehsil level

The FVI aggregated to Tehsils revealed that Jalalpur Pirwala is the area with the highest flood vulnerability (Map 5.6). This Tehsil has an average FPC of 3.89, an average PSC of 4.00, and an average CCC of 1.00, resulting in a raw FVI of around 15.57, which normalizes to 1.00, making it the most vulnerable.

The Tehsils identified as the most vulnerable are Jalalpur Pirwala, Shorkot, Khairpur Tamewali, Bahawalnagar, Sadiqabad, Athara Hazari, Pakpattan, Jatoi, Chowk Sarwar Shaheed, and Liaqatpur (Table 5.1). While Tehsils like Koh-e-Suleman (avg. PSC 4.00) have high population susceptibility and a lower cooping capacity (avg. CCC 1.65), their PFC is lower (avg. PFC 2.51) than other areas, making it less vulnerable when computed by the formula.

In contrast, Tehsils with higher CCC averages, like Multan City, have a high average of CCC (4.68), but low PSC (1.00) and high PFC (3.63), however, vulnerability is still low due to the high CCC. This emphasizes that even urban areas are more prone to flooding overall, due to distance to rivers, but as the ability to cope is higher and the population is less exposed, they are less affected.

The FVI and its components can also be explored in an interactive dashboard.

The website can be accessed via the QR code or at https://gernotnikolaus.github.io/FVI_Punjab/ (recommended on desktop).

Table 5.1: Tehsils with the heighest FVI.

Rank	Tehsil	Total Settl. Area (km²)	Av. PFC Settl. Tehsil	Av. PSC Settl. Tehsil	Av. CCC Settl. Tehsil	FVI norm.	Raw FVI
1	Jalalpur Pirwala	34.43	3.89	4	100.00%	100.00%	15.57
2	Shorkot	49.96	3.87	3	100.00%	73.00%	11.58
3	Khairpur Tamewali	21.16	3.9	3	102.00%	73.00%	11.51
4	Bahawalnagar	64.36	3.83	3	100.00%	72.00%	11.48
5	Sadiqabad	86.18	3.64	3	101.00%	68.00%	10.83
6	Athara Hazari	20.17	3.54	3	100.00%	66.00%	10.61
7	Pakpattan	52.76	3.49	3	100.00%	65.00%	10.46
8	Jatoi	30.62	3.47	3	100.00%	65.00%	10.41
9	Chowk Sarwar Shah	22.18	3.44	4	135.00%	63.00%	10.15
10	Liaqatpur	68.71	3.34	3	100.00%	63.00%	10.03

To visualize FVI distribution regionally, the mean FVI values were calculated at the Tehsil level using Zonal Statistics. This method averages pixel values within each Tehsil, allowing for easy comparison of flood vulnerablity index across administrative regions.

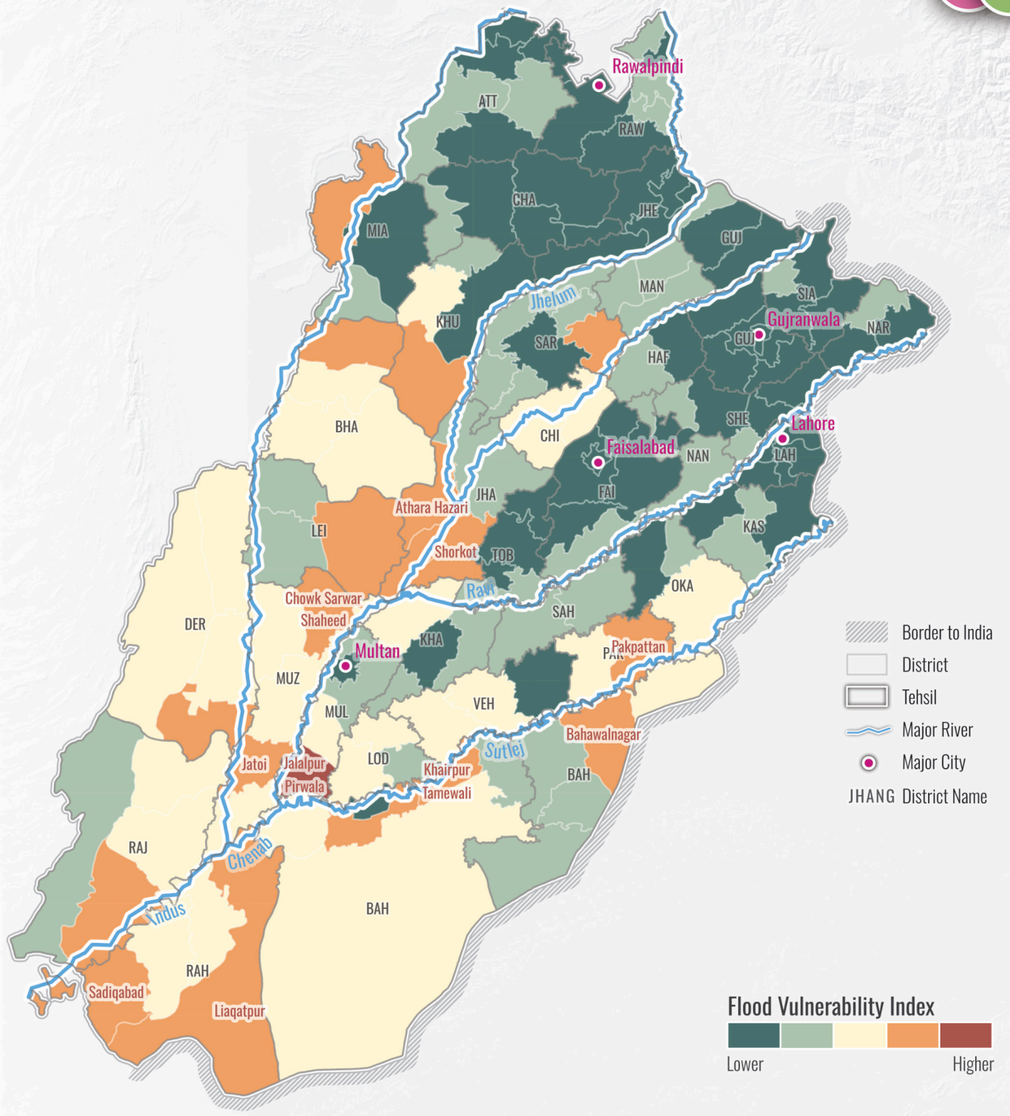

Map 5.2: FVI aggregated to Tehsils (The top 10 Tehsils with the highest flood-prone score are labelled).

Flood Vulnerability Index interpolated per 50 km²

A hexagon grid-based mapping approach was used to avoid reliance on administrative boundaries, recognizing that climate hazards cross borders. Using zonal statistics and kriging interpolation, the FVI was aggregated and visualized in a smooth, continuous pattern.

A 50 km² hexagon grid was used to map flood vulnerability highlighting critical vulnerability areas across the region.

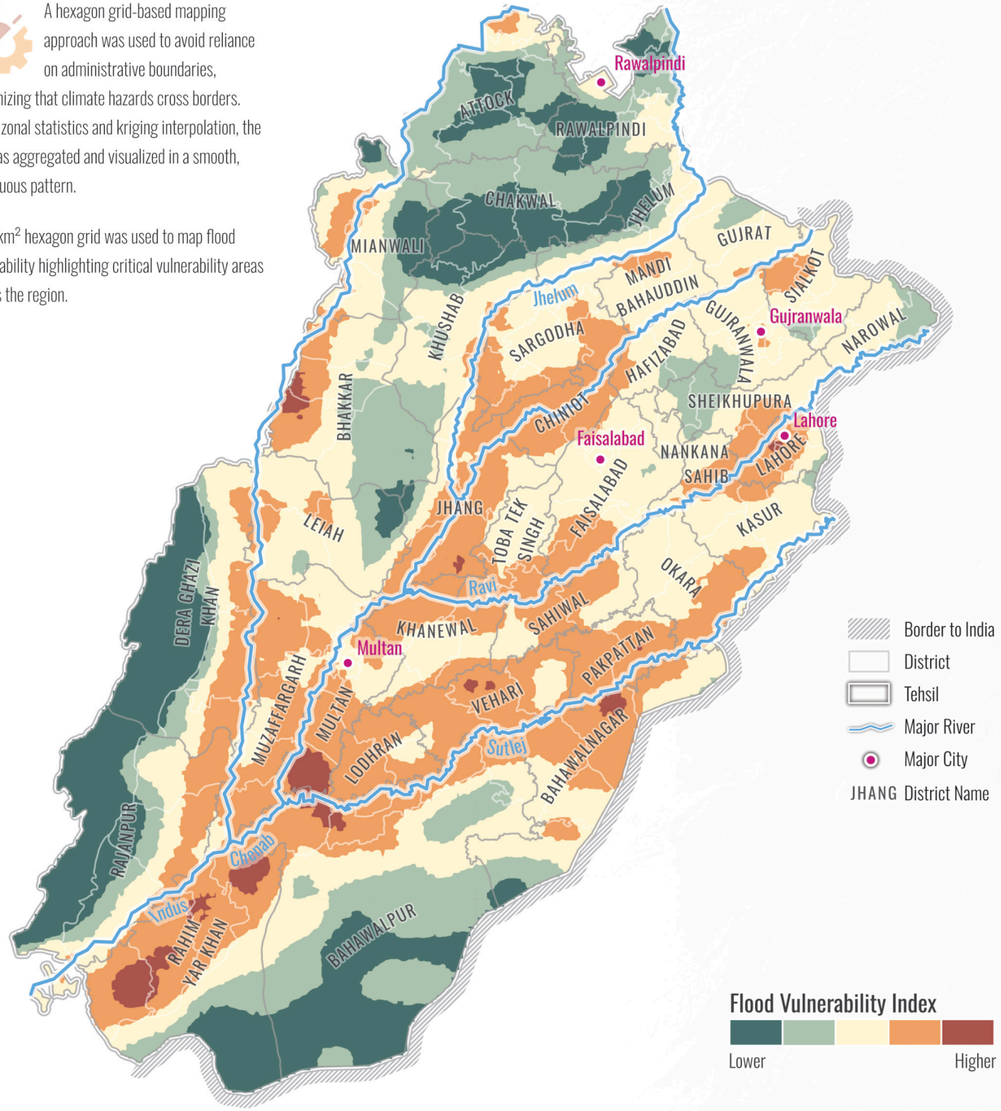

Map 5.3: FVI interpolated with a resolution of 50 km².

Flood Vulnerability Index interpolated per 10 km²

A finer 10 km² hexagon grid provided a more detailed view, enabling high-resolution spatial analysis and the identification of local vulnerability hotspot.

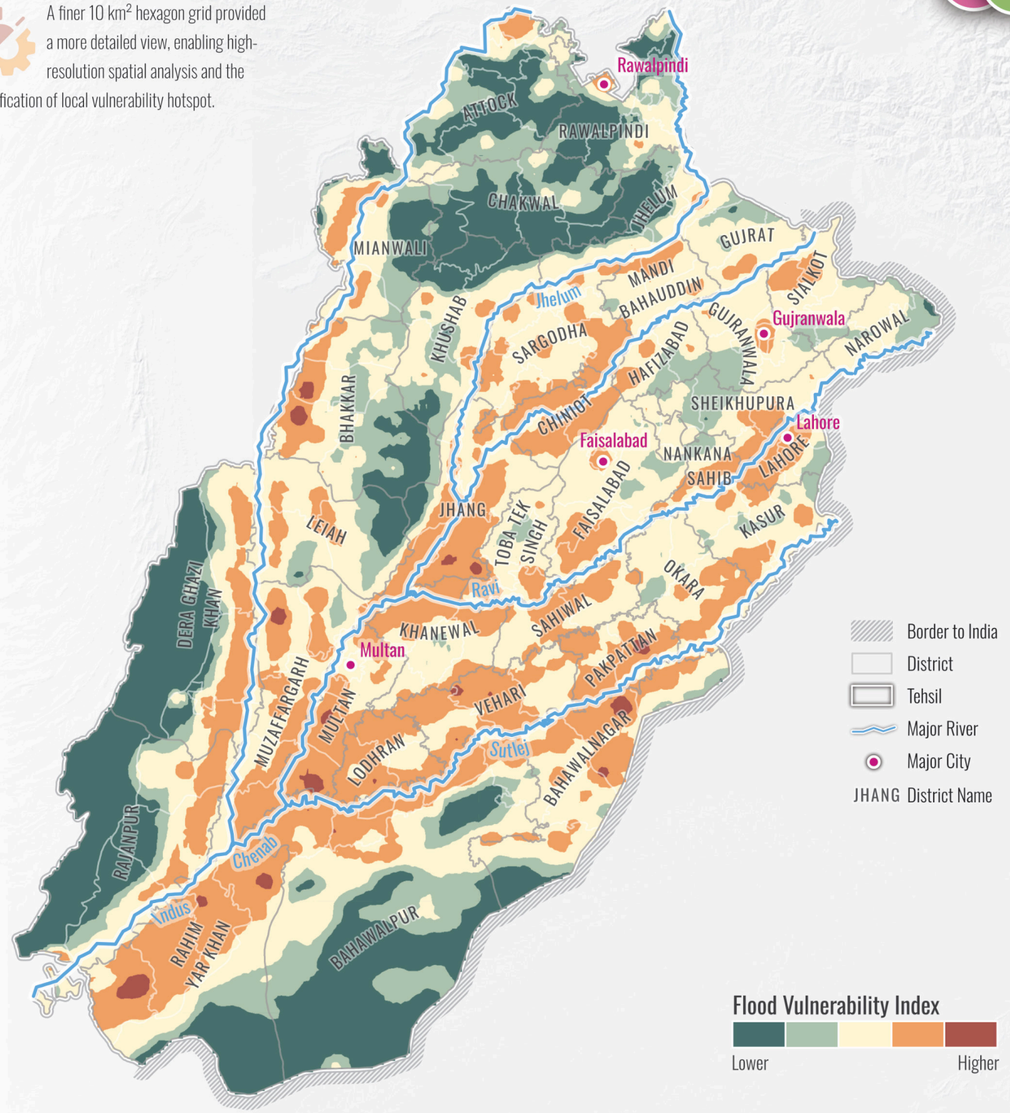

Map 5.4: FVI interpolated with a resolution of 10 km².

Flood Vulnerability, a holistic view of FPC, PSC, and CCC

The background indicates flood-prone (FPC) areas, while the half circles provide insight into human exposure (PSC, CCC). Tehsils with the highest FVI value are labeled with their first three letters.

How to read

Lower Population Susceptibility, higher Coping Capacity.

Higher Population Susceptibility, less Coping Capacity.

Border to India

Tehsil

Major River

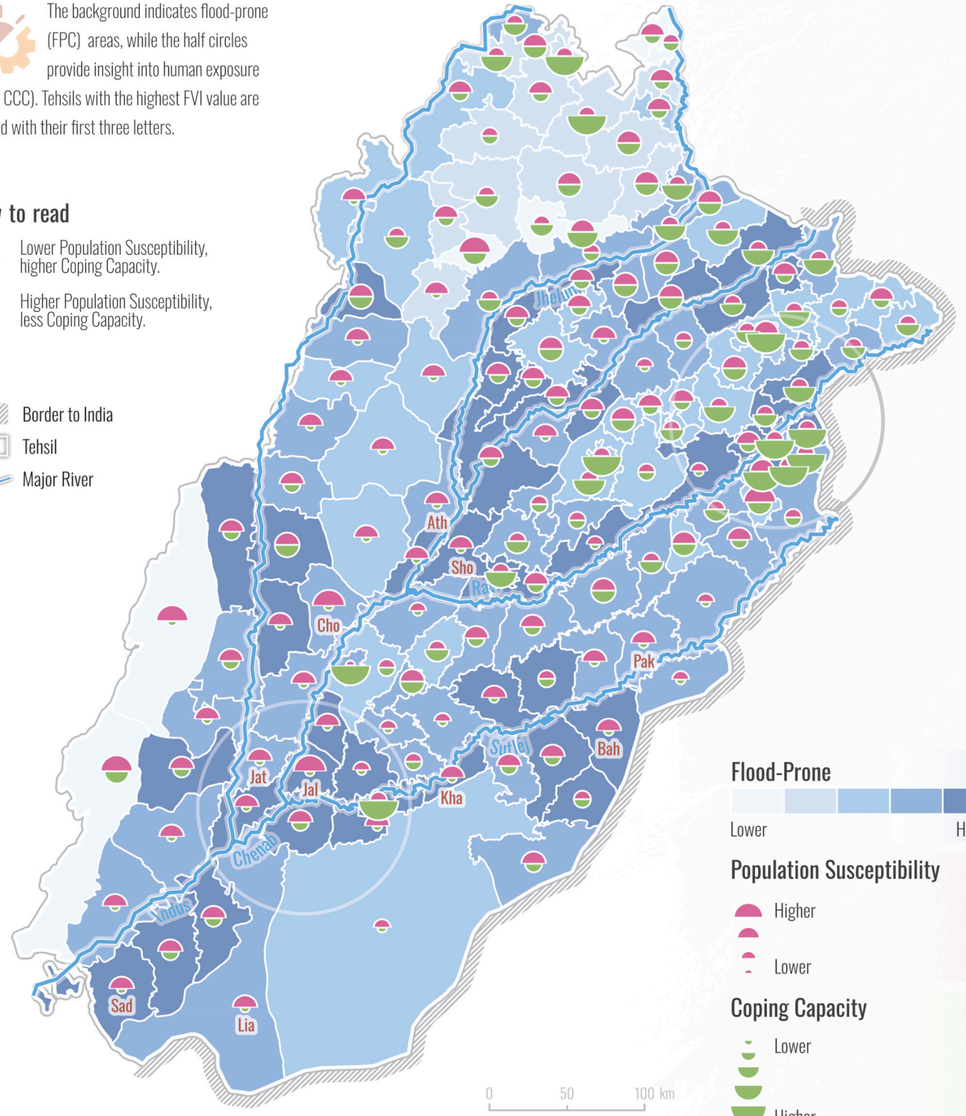

Flood-Prone

Lower — Higher

Population Susceptibility

Higher

Lower

Coping Capacity

Lower

Higher

Map 5.5: Flood vulnerability splitted into its three components (The top 10 Tehsils with the highest FVI score are labelled).

Altough flood-prone is high in the area of Lahore, the population suspectibility is low, as well as the coping capacity is high - making it less flood vulnerable.

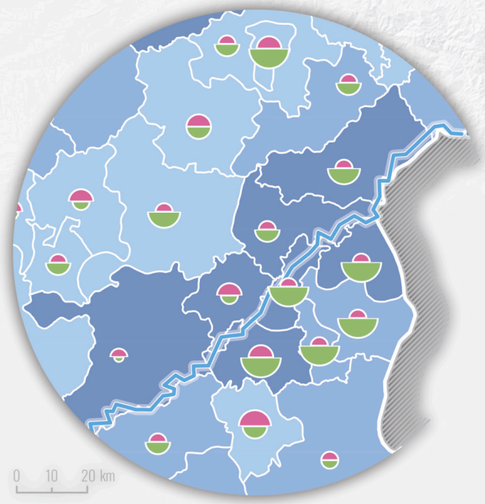

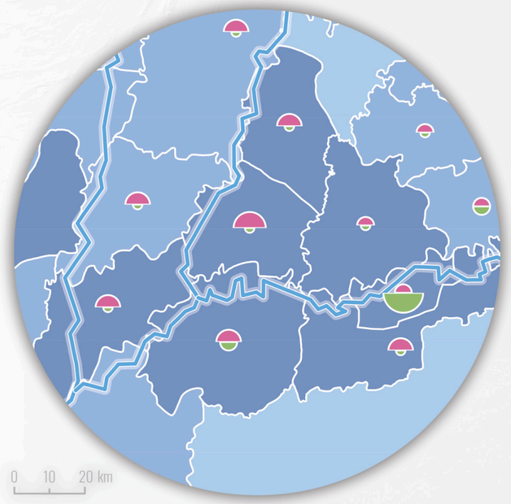

Jalalpur Pirwala has the highest FVI value. The area, as well as its adjocatning areas, are high in flood-prone.

Flood Vulnerability, a holistic view at FPC and people's vulnerability

The background represents flood-prone (FPC) areas in Punjab, calculated using a 100 km² hexagonal average and interpolated for a smoother representation. Wurman dots indicate the population at risk, derived from the average of 100 km² hexagons and calculated by dividing population susceptibility (PSC) by coping capacity (CCC).

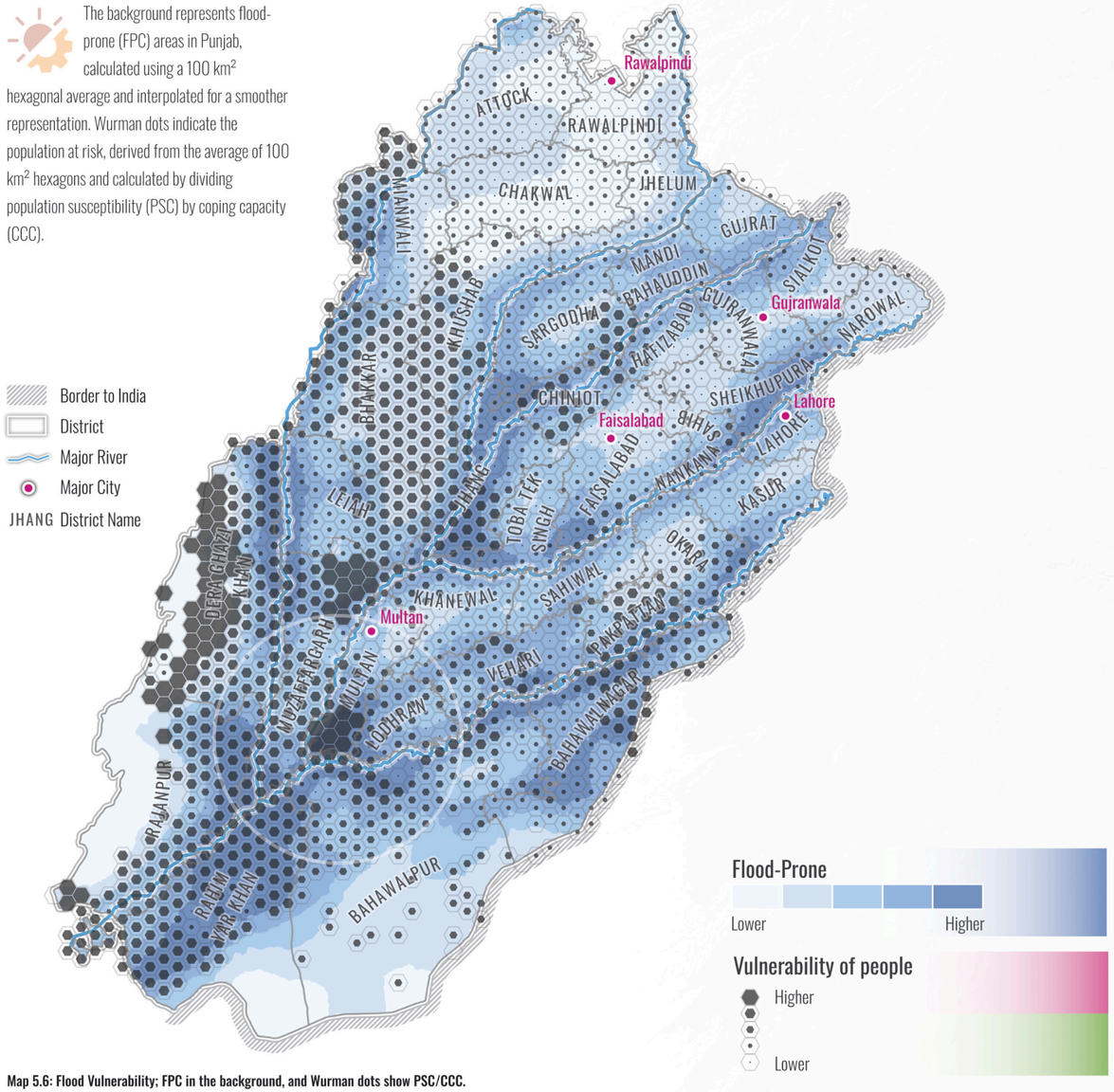

Border to India
District
Major River
Major City
JHANG District Name

Flood-Prone
Lower — Higher

Vulnerability of people
Higher
Lower

Map 5.6: Flood Vulnerability; FPC in the background, and Wurman dots show PSC/CCC.

Flood Vulnerability per 10 km²

A finer 10 km² hexagon grid provided a more detailed view, enabling high-resolution spatial analysis and the identification of local vulnerability hotspot. The estimated number of people affected is also visualized. Here at the hotpot region of Jalalpur Pirwala.

District
Buildings
JHANG District Name

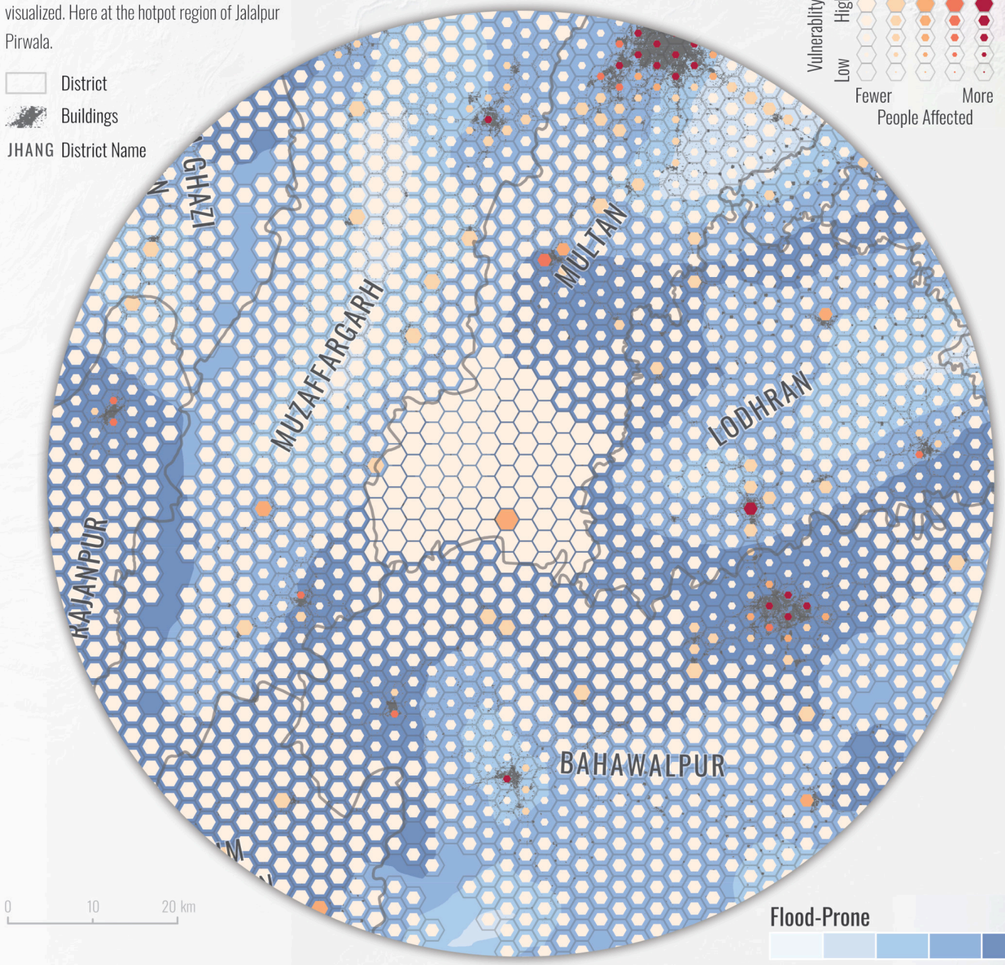

Vulnerability of people
Vulnerability: High / Low
Fewer — More
People Affected

Flood-Prone
Lower — Higher

Map 5.7: Flood Vulnerability; FPC in the background. Wurman dots show PSC/CCC, the color indicates people affected.

Discussion

The master's thesis deals with the flooding problem in Pakistan. The Punjab province was chosen as a study area, as this region is prone to flooding and people are yearly affected. To address these issues, the study developed a framework that aims to analyze the area with a multi-layer approach. In contrast to Ullah et al. (2024), this research not only concentrates on the identification of flood-prone areas but also takes the population into account. This Flood Vulnerability Index (FVI) framework consists of three components: the Flood-Prone Component (FPC), the Population Susceptibility Component (PSC), and the Coping Capacity Component (CCC). By integrating demographic and adaptive capacity factors, the study delivers insights that were not considered in previous studies in the Punjab region. Although the use of geospatial techniques, the Analytical Hierarchy Process (AHP), and the creation of user-friendly visualizations offer a practical way to evaluate the risk of flooding, some limitations must be considered. There are also some methodological points that must be discussed, which might have influenced the outcome of this study. Also, improvements are worth mentioning, which might pave the way for future research.

Data Sources, Processing, Resolution, Validation, and Scaling Issues

One thing that stood out was the huge study area, which has advantages and disadvantages. It has the benefit that a large area is covered by the assessment, but the analysis might not be able to capture small nuances. Classification of some parameters might be generalized, as the study areas are characterized by different topographic conditions. For example, Punjab reaches from high mountains in the north to flat terrain in the south. This results in a large range of values (e.g., meters in the Elevation), which can influence the classification and therefore, the outcome of the study. Nevertheless, the analysis provides general patterns of flood vulnerability. The determined hotspots can serve for future studies to analyze the most affected areas in greater detail. Future researchers can build on the results of this study and include data with higher resolution and more precise information in smaller and more localized study areas, as described below.

Existing limitations in the data and the processing must be discussed. The data for the health facilities and the rivers were obtained from OpenStreetMap (OSM). Although this data is freely available, the information is provided by users, and inaccuracies and gaps can occur. While Kablan et al (2017) uses census data based on sub-district level, the study uses a dasymetric mapping technique to enhance the data's localization of the PSC and the CCC. Future studies that might have access to data on the house survey level would provide better accuracy than the technique used in this study. Although the dasymetric mapping technique masked the census data to settlements, so as a proxy for where people live, each pixel in the administrative value still has the same value. However, as more precise data was not available, this technique still provided better precision in the FVI calculation than if the data had not been masked out. Had this not been done, each pixel of the whole administrative boundary would have had one pixel and would have distorted the results. The availability and up-to-date population data would improve future studies. As future studies might focus on smaller areas, highlighted as endangered areas in this study, it might be easier to obtain this data.

Resolution and the scaling of the data also have to be added to the consideration. All layers were scaled to 30m to guarantee consistency between the parameters. Although the 30m matched the resolution of the DEM, the Sentinel-1 and the Land Use Land Cover data had to be downscaled. Finer resolution of data might improve the accuracy of the study because smaller nuances in the topography might be captured. However, as discussed earlier, given the large study area, these nuances could be absorbed, and hence, higher resolution might be considered for smaller study areas. Furthermore, the use of 30m gives a good balance of computational efficiency and spatial resolution. What really has to be pointed out here is the precipitation data. This data was available with a resolution of 4 km and had to be upscaled. The data was processed with interpolation and resampling, that it matches the 30m and ensures consistency between the data sets. Therefore, this coarse resolution might have gaps which might be important in some local conditions and cannot be excused by the size of the study area.
Nevertheless, it provided general patterns of the annual rainfall in the province. Despite the available resolution, rainfall is a driver of flooding (Bates et al., 2008), and hence, it should not be neglected, as it gives crucial information about where most rainfall fell.

Furthermore, methodological limitations exist. As the AHP is rated based on opinion, it is rated with subjectivity. The low consistency ratio of below 0.1 suggests consistency, but a different group of experts might assign different relative importance to the parameters. The robustness of the AHP could be assessed with Sensitivity Analysis (Ullah et al., 2024). A single-parameter sensitivity analysis (SPSA) could be performed to evaluate how each parameter layer influences the FVI, providing valuable information about their impact. While the map removal sensitivity analysis (MRSA) might assess the significance of each parameter when each layer is systematically removed at a time to determine whether significant changes occur in the model output. Moreover, the classification of the parameters was mostly based on literature and interval methods. Precise adjustment of the indicators based on fieldwork or discussion with locals might enhance the model further.

Another point worth mentioning is the limitations in the validation process. The result of the FPC was validated with multiple flooding extents derived from Sentinel-1 covering five years. Adding more years to the validation step might improve the representation of the flood-prone analysis and the validation result. Furthermore, validating the whole FVI results would provide valuable information about the model's reliability. Similar to Hoque et al. (2019) the results of the FVI could be evaluated by people in the study area. Based on a survey, people affected and the experts from Pakistan who rated the AHP would give important feedback on the accuracy of the model's mapping result.

Mapping Approaches, FVI, and User Testing Feedback

While Hoque et al. (2019), Ullah et al. (2024), Roy and Dhar (2024), and Mshelia et al. (2024) produced raster-based maps for visualizing flood-prone and vulnerable areas, this study developed different mapping approaches for visualizing flood vulnerability. The user testing concluded that the FVI aggregated to the Tehsils is easier to understand and good for comparing regions with others. However, it also created artificial boundaries. The interpolated FVI might be more precise, but different resolutions should be provided because data could be lost, or misleading information could be added in the interpolation step. One thing that stood out is that mapping the components separately gives more insight into vulnerability, but it is more complex to understand. Although different visualization approaches offer various ways of reading the analyzed vulnerability, the formula-based method needs some discussion. A challenge that emerged here is that the FVI model uses different dimensions. While the FPC covers the whole area, the PSC and CCC cover pixels where settlements are located. Thus, visualizing the components separately gives the possibility to avoid this problem. The pie charts, half-circles, and the Wurman dots present a good way of combining the thematic content and at the same time deliver important information about their interplay in flood vulnerability in the respective areas.

The user testing was conducted with a relatively small sample size (n=16), and no user from Punjab was included. Different user groups are important in the user testing. While the climate risk analyzers gave feedback on technical aspects, the user of the general public ensured that the maps are also understandable for a broader audience. Also, if they are usually not in touch with such topics. Hence, adding an additional user group might enhance the findings. Cartographers will observe the maps with their professional perspective and provide information on cartographic rules. People in Punjab could be added to the general public group. They might look at the maps more specifically, due to their experiences, and different findings can be collected. Furthermore, only five maps were included in the user testing. Future studies, that also put effort into visual creation, might test the whole product. While the atlas was not tested in the user testing, the layout was discussed with experts in the atlas creation to ensure its correctness.

Overall, the mapping approaches were well received. Especially, the feedback from climate risk analysts was valuable, as they usually work with GIS outputs and pixel maps. They emphasize how important it is to find new ways of communicating and presenting the results. This study contributes to their research and can be directly used in flood management. Furthermore, the feedback highlighted a clear legend and additional text on how the data was processed and mapped. The user testing ensured that the final results are accurate, accessible, and understandable not only for decision makers but also for the public. Although the aggregation process from pixel maps to vector-based maps increases the readability, it also generalizes the results. Future studies might search for different mapping approaches or might focus more on the creation of an interactive pixel map. However, as the study's main focus lay in visualizing maps which are easy to understand and to interpret, the study's approach is still appropriate.

Conclusion

This study was motivated by the flood-danger in Punjab and the research gap which exists in the area. This issue was addressed in two parts. Firstly, flood vulnerable areas were identified and analyzed. For this, the study developed a Flood Vulnerability Index (FVI) which integrates various physical and environmental factors, and demographic and coping capacity parameters. Geospatial tools and an Analytical Hierarchy Process (AHP) were combined. The use of FVI's three components the study offered a multi-dimensional perspective of flood vulnerability. Secondly, the results obtained were visualized with different mapping approaches. The different visualization techniques were compiled to an atlas, making the results not only accessible for decision-makers, but also for a broader audience.

The atlas is not only a summary of the findings but also a practical product that translates the complex flood vulnerability assessments into accessible and clear visualizations. By following cartographic best practices and user-centered design principles, the atlas ensures that the information is understandable for diverse user groups, including authorities, researchers, and the general public. It supports decision-making processes and contributes to more effective communication about flood risk in Punjab.

The study followed a structured workflow for geospatial analysis and mapping creation. First, literature research on flooding was conducted and indicators identified. Seven parameters frame the Flood-Prone Component (FPC), including the Annual Rainfall, Distance to the River, Drainage Density, Elevation, Land Use Land Cover, Slope, and Topographic Wetness Index. Secondly, the Population Susceptibility Component (PSC) consists of four indicators, such as the Dependent Population, Disabled Population, Female Population, and Population Density. Lastly, two parameters, the Distance to Health Facilities and the Literacy Rate, create the Coping Capacity Component (CCC). This data was obtained from various open-data sources and platforms, such as Sentinel-1, ESA WorldCover, FABDEM, and OpenStreetMap. For every parameter a map was created, classified into 5 categories ranging from very low to very high, and weighed based on experts' opinion with the AHP. The participants consisted of eight experts in Pakistan and five climate risk analyzers from the United Nations University – Institute for Environment and Human Security (UNU-EHS). Pairwise comparison matrices helped with detecting the influence of each parameter. Furthermore, the consistency was determined. Each component map was then generated with an overlay analysis.

The research delivered methodical and thematic contributions to geospatial flood mapping. Furthermore, valuable results for the study program of geoinformatics, earth observation, geovisualization, and geocommunication were obtained. The FPC identified flood-prone areas, which lay generally in flat terrain near river basins. The PSC and the CCC determined regions where human susceptibility is high and coping capacity is lacking. However, the most important result of the study is the FVI itself and the different maps. Therefore, another contribution lies in the cartographic results. The different mapping approaches used, combined with the user testing, delivered valuable insights on how to create maps which are easy to understand while providing the required level of detail for decision making. The atlas created in this thesis thus provides legible visualization and tools for decision-making which are also understandable by non-experts.

At the same time, the study also delivers thematic contributions to the assessment and strategies for flooding. Using climate and environmental parameters, such as precipitation and elevation, the study not only determines current but also future flooding scenarios. By integrating population susceptibility and coping capacity, the study also offers another perspective of how the population might be affected. The major benefit of this study lies in the methodology which can be scaled to another region of the world. All data in this study was open access. If some data might be limited or not available, the FVI can be adopted for the respective area. Future study can build on the FVI framework to analyze flood vulnerabilities, especially when taking the limitations and improvements into account considered in Chapter 8. If data is available, information about housing quality, economic status and access to resources can draw a clearer picture of flood vulnerability. Taking these limitations and improvements into consideration, and adopting the framework to the study area, this study's methodology supports long-term climate planning and the analysis of risk induced by climate.

In summary, this study achieves its aims and delivered a useful contribution to flood assessment; especially its visualizations. The study not only deals with the methodical possibilities of mapping but also provides practical tools. The integration of geospatial analysis, with visual user-centered design enhances the potential of the study to serve as a model for future studies. The printed atlas and the digital product can help with decision making and to make communities more resilient and contribute to flood management and climate adaptation globally. While climate-related catastrophes arise and millions of people get affected, the need for frameworks like the study's grows too. Combining open access data, geodata data and user-centric design research is getting more and more important for building strong communities and to be prepared for the climate induced challenges we already face, and we will face in the coming years.

References

Ajtai, I. et al. (2023) 'Mapping social vulnerability to floods. A comprehensive framework using a vulnerability index approach and PCA analysis', Ecological Indicators, 154, p. 110838. Available at: https://doi.org/10.1016/j.ecolind.2023.110838.

Aldous, A. et al. (2011) 'Droughts, floods and freshwater ecosystems: evaluating climate change impacts and developing adaptation strategies', Marine and Freshwater Research, 62, pp. 223–231. Available at: https://doi.org/10.1071/MF09285.

Allafta, H. and Opp, C. (2021) 'GIS-based multi-criteria analysis for flood prone areas mapping in the trans-boundary Shatt Al-Arab basin, Iraq-Iran', Geomatics, Natural Hazards and Risk, 12(1), pp. 2087–2116. Available at: https://doi.org/10.1080/19475705.2021.1955755.

Arnell, N.W. and Gosling, S.N. (2013) 'The impacts of climate change on river flow regimes at the global scale', Journal of Hydrology, 486, pp. 351–364. Available at: https://doi.org/10.1016/j.jhydrol.2013.02.010.

Aydin, M.C. and Sevgi Birincioğlu, E. (2022) 'Flood risk analysis using gis-based analytical hierarchy process: a case study of Bitlis Province', Applied Water Science, 12(6), p. 122. Available at: https://doi.org/10.1007/s13201-022-01655-x.

Balica, S., Douben, N. and Wright, N. (2009) 'Flood vulnerability indices at varying spatial scales', Water science and technology : a journal of the International Association on Water Pollution Research, 60, pp. 2571–80. Available at: https://doi.org/10.2166/wst.2009.183.

Balica, S. and Wright, N. (2009) 'A network of knowledge on applying an indicator-based methodology for minimizing flood vulnerability', Hydrological Processes, 23, pp. 2983–2986. Available at: https://doi.org/10.1002/hyp.7424.

Balica, S. and Wright, N. (2010) 'Reducing the complexity of the flood vulnerability index', Environmental Hazards, 9(4), pp. 321–339. Available at: https://doi.org/10.3763/ehaz.2010.0043.

Bates, B. et al. (2008) 'Climate Change and Water. Technical Paper of the Intergovernmental Panel on Climate Change'.

Bathrellos, G.D. et al. (2016) 'Urban flood hazard assessment in the basin of Athens Metropolitan city, Greece', Environmental Earth Sciences, 75(4), p. 319. Available at: https://doi.org/10.1007/s12665-015-5157-1.

Bathrellos, G.D. et al. (2018) 'Temporal and Spatial Analysis of Flood Occurrences in the Drainage Basin of Pinios River (Thessaly, Central Greece)', Land, 7(3), p. 106. Available at: https://doi.org/10.3390/land7030106.

Beven, K.J. and Kirkby, M.J. (1979) 'A physically based, variable contributing area model of basin hydrology / Un modèle à base physique de zone d'appel variable de l'hydrologie du bassin versant', Hydrological Sciences Bulletin, 24(1), pp. 43–69. Available at: https://doi.org/10.1080/02626667909491834.

Brewer, C. (1999) Color Use Guidelines for Data Representation, Proceedings of the Section on Statistical Graphics.

Burayu, D.G., Karuppannan, S. and Shuniye, G. (2023) 'Identifying flood vulnerable and risk areas using the integration of analytical hierarchy process (AHP), GIS, and remote sensing: A case study of southern Oromia region', Urban Climate, 51, p. 101640. Available at: https://doi.org/10.1016/j.uclim.2023.101640.

Chen, F. et al. (2024) 'Pakistan's 2022 floods: Spatial distribution, causes and future trends from Sentinel-1 SAR observations', Remote Sensing of Environment, 304, p. 114055. Available at: https://doi.org/10.1016/j.rse.2024.114055.

CHRS (no date) CHRS Data Portal. Available at: https://chrsdata.eng.uci.edu/ (Accessed: 16 January 2025).

Connor, R. and Hiroki, K. (2005) 'Development of a method for assessing flood vulnerability', Water science and technology : a journal of the International Association on Water Pollution Research, 51, pp. 61–7. Available at: https://doi.org/10.2166/wst.2005.0109.

Copernicus Sentinel data, 2021-2024. Retrieved via Google Earth Engine. https://earthengine.google.com/.

Coveney, S. and Roberts, K. (2017) 'Lightweight UAV digital elevation models and orthoimagery for environmental applications: data accuracy evaluation and potential for river flood risk modelling', International Journal of Remote Sensing, 38(8–10), pp. 3159–3180. Available at: https://doi.org/10.1080/01431161.2017.1292074.

Cutter, S.L., Boruff, B.J. and Shirley, W.L. (2003) 'Social Vulnerability to Environmental Hazards', Social Science Quarterly, 84(2), pp. 242–261.

Eicher, C. and Brewer, C. (2001) 'Dasymetric Mapping and Areal Interpolation: Implementation and Evaluation', Cartography and Geographic Information Science - CARTOGR GEOGR INF SCI, 28, pp. 125–138. Available at: https://doi.org/10.1559/152304001782173727.

esri (no date a) Data classification methods. Available at: https://pro.arcgis.com/en/pro-app/latest/help/mapping/layer-properties/data-classification-methods.htm (Accessed: 7 February 2025).

esri (no date b) Distance Accumulation (Spatial Analyst). Available at: https://pro.arcgis.com/en/pro-app/3.2/tool-reference/spatial-analyst/distance-accumulation.htm (Accessed: 7 February 2025).

esri (no date c) Fill (Spatial Analyst)—ArcGIS Pro | Documentation. Available at: https://pro.arcgis.com/en/pro-app/latest/tool-reference/spatial-analyst/fill.htm (Accessed: 24 January 2025).

esri (no date d) Flow Accumulation (Spatial Analyst)—ArcGIS Pro | Documentation. Available at: https://pro.arcgis.com/en/pro-app/latest/tool-reference/spatial-analyst/flow-accumulation.htm (Accessed: 24 January 2025).

esri (no date e) Flow Direction (Spatial Analyst)—ArcGIS Pro | Documentation. Available at: https://pro.arcgis.com/en/pro-app/latest/tool-reference/spatial-analyst/flow-direction.htm (Accessed: 24 January 2025).

esri (no date f) Resample (Data Management)—ArcGIS Pro | Documentation. Available at: https://pro.arcgis.com/en/pro-app/3.2/tool-reference/data-management/resample.htm (Accessed: 24 January 2025).

esri (no date g) Slope (3D Analyst)—ArcGIS Pro | Documentation. Available at: https://pro.arcgis.com/en/pro-app/3.2/tool-reference/3d-analyst/slope.htm (Accessed: 24 January 2025).

Evers, M., Almoradie, A. and de Brito, M. (2018) 'Enhancing Flood Resilience Through Collaborative Modelling and Multi-criteria Decision Analysis (MCDA)', in Urban Book Series, pp. 221–236. Available at: https://doi.org/10.1007/978-3-319-68606-6_14.

Fernández, D.S. and Lutz, M.A. (2010) 'Urban flood hazard zoning in Tucumán Province, Argentina, using GIS and multicriteria decision analysis', Engineering Geology, 111(1), pp. 90–98. Available at: https://doi.org/10.1016/j.enggeo.2009.12.006.

Fernandez, P., Mourato, S. and Moreira, M. (2016) 'Social vulnerability assessment of flood risk using GIS-based multicriteria decision analysis. A case study of Vila Nova de Gaia (Portugal)', Geomatics, Natural Hazards and Risk [Preprint].

Ghorbani, S. et al. (2015) 'Delineation of groundwater potential zones using remote sensing and GIS-based data driven models', Geocarto International, 32. Available at: https://doi.org/10.1080/10106049.2015.1132481.

Gigović, L. et al. (2017) 'Application of GIS-Interval Rough AHP Methodology for Flood Hazard Mapping in Urban Areas', Water, 9, pp. 1–26. Available at: https://doi.org/10.3390/w9060360.

Hagenlocher, M. et al. (2016) 'Spatial assessment of social vulnerability in the context of landmines and explosive remnants of war in Battambang province, Cambodia', International Journal of Disaster Risk Reduction, 15, pp. 148–161. Available at: https://doi.org/10.1016/j.ijdrr.2015.11.003.

Hamidi, A.R. et al. (2022) 'Flood Exposure and Social Vulnerability Analysis in Rural Areas of Developing Countries: An Empirical Study of Charsadda District, Pakistan', Water, 14(7), p. 1176. Available at: https://doi.org/10.3390/w14071176.

Hawker, L. et al. (2022) 'A 30 m global map of elevation with forests and buildings removed', Environmental Research Letters, 17(2), p. 024016. Available at: https://doi.org/10.1088/1748-9326/ac4d4f.

Hoque, M.A.-A. et al. (2019) 'Assessing Spatial Flood Vulnerability at Kalapara Upazila in Bangladesh Using an Analytic Hierarchy Process', Sensors, 19(6), p. 1302. Available at: https://doi.org/10.3390/s19061302.

Hossain, Md.N. and Mumu, U.H. (2024) 'Flood susceptibility modelling of the Teesta River Basin through the AHP-MCDA process using GIS and remote sensing', Natural Hazards, 120(13), pp. 12137–12161. Available at: https://doi.org/10.1007/s11069-024-06677-z.

Huang, D. et al. (2012) 'An assessment of multidimensional flood vulnerability at the provincial scale in China based on the DEA method', Natural Hazards, 64. Available at: https://doi.org/10.1007/s11069-012-0323-1.

Ibrahim, M. et al. (2024) 'Flood vulnerability assessment in the flood prone area of Khyber Pakhtunkhwa, Pakistan', Frontiers in Environmental Science, 12, p. 13. Available at: https://doi.org/10.3389/fenvs.2024.1303976.

IPCC (2001) 'Climate Change 2001: Impacts, Adaptation, and Vulnerability'. Available at: https://www.ipcc.ch/site/assets/uploads/2018/03/WGII_TAR_full_report-2.pdf.

IPCC (2012) Managing the Risks of Extreme Events and Disasters to Advance Climate Change Adaptation: Special Report of the Intergovernmental Panel on Climate Change. 1st edn. Edited by C.B. Field et al. Cambridge University Press. Available at: https://doi.org/10.1017/CBO9781139177245.

IPCC (2014) Climate Change 2014: impacts, adaptation, and vulnerability Working Group II contribution to the fifth assessment report of the Intergovernmental panel on climate change. New York: Cambridge University Press, Cambridge, United Kingdom and New York, NY, USA, 1132 pp. ([Field, C.B., V.R. Barros, D.J. Dokken, K.J. Mach, M.D. Mastrandrea, T.E. Bilir, M. Chatterjee, K.L. Ebi, Y.O. Estrada, R.C. Genova, B. Girma, E.S. Kissel, A.N. Levy, S. MacCracken, P.R. Mastrandrea, and L.L. White (eds.)].).

IPCC (2022) Climate Change 2022: Impacts, Adaptation and Vulnerability. Contribution of Working Group II to the Sixth Assessment Report of the Intergovernmental Panel on Climate Change. ([H.-O. Pörtner, D.C. Roberts, M. Tignor, E.S. Poloczanska, K. Mintenbeck, A. Alegría, M. Craig, S. Langsdorf, S. Löschke, V. Möller, A. Okem, B. Rama (eds.)]. Cambridge University Press. Cambridge University Press, Cambridge, UK and New York, NY, USA, 3056 pp., doi:10.1017/9781009325844.). Available at: https://www.ipcc.ch/report/ar6/wg2/downloads/report/IPCC_AR6_WGII_FullReport.pdf.

Islamic Relief (2024) Pakistan Monsoon Floods 2024 Situation Report - August 29, 2024 - Pakistan. Available at: https://reliefweb.int/report/pakistan/pakistan-monsoon-floods-2024-situation-report-august-29-2024 (Accessed: 14 February 2025).

Jahandideh-Tehrani, M. et al. (2020) 'Hydrodynamic modelling of a flood-prone tidal river using the 1D model MIKE HYDRO River: calibration and sensitivity analysis', Environmental Monitoring and Assessment, 192(2), p. 97. Available at: https://doi.org/10.1007/s10661-019-8049-0.

Kabenge, M. et al. (2017) 'Characterizing flood hazard risk in data-scarce areas, using a remote sensing and GIS-based flood hazard index', Natural Hazards, 89(3), pp. 1369–1387. Available at: https://doi.org/10.1007/s11069-017-3024-y.

Kablan, M.K.A., Dongo, K. and Coulibaly, M. (2017) 'Assessment of Social Vulnerability to Flood in Urban Côte d'Ivoire Using the MOVE Framework', Water, 9(4), p. 292. Available at: https://doi.org/10.3390/w9040292.

Kara, R. and Singh, P. (2024) 'Flood assessment for Lower Godavari basin by using the application of GIS-based analytical hierarchy process', International Journal of System Assurance Engineering and Management [Preprint]. Available at: https://doi.org/10.1007/s13198-024-02595-2.

Kumar, V. et al. (2023) 'Comprehensive Overview of Flood Modeling Approaches: A Review of Recent Advances', Hydrology, 10(7), p. 141. Available at: https://doi.org/10.3390/hydrology10070141.

Kundzewicz, Z.W. et al. (2014) 'Flood risk and climate change: global and regional perspectives', Hydrological Sciences Journal, 59(1), pp. 1–28. Available at: https://doi.org/10.1080/02626667.2013.857411.

Latif, R.M.A. and He, J. (2025) 'Flood Susceptibility Mapping in Punjab, Pakistan: A Hybrid Approach Integrating Remote Sensing and Analytical Hierarchy Process', Atmosphere, 16(1), p. 22. Available at: https://doi.org/10.3390/atmos16010022.

Mojaddadi, H. et al. (2017) 'Ensemble machine-learning-based geospatial approach for flood risk assessment using multi-sensor remote-sensing data and GIS', Geomatics, Natural Hazards and Risk, 8(2), pp. 1080–1102. Available at: https://doi.org/10.1080/19475705.2017.1294113.

Molinari, D. et al. (2019) 'Validation of flood risk models: Current practice and possible improvements', International Journal of Disaster Risk Reduction, 33, pp. 441–448. Available at: https://doi.org/10.1016/j.ijdrr.2018.10.022.

Nasiri, H., Mohd Yusof, M.J. and Ali, T. (2016) 'An overview to flood vulnerability assessment methods', Sustainable Water Resources Management, 2. Available at: https://doi.org/10.1007/s40899-016-0051-x.

Neumayer, E. and Plümper, T. (2007) 'The Gendered Nature of Natural Disasters: The Impact of Catastrophic Events on the Gender Gap in Life Expectancy, 1981–2002', Annals of the Association of American Geographers, 97(3), pp. 551–566. Available at: https://doi.org/10.1111/j.1467-8306.2007.00563.x.

Ogato, G.S. et al. (2020) 'Geographic information system (GIS)-Based multicriteria analysis of flooding hazard and risk in Ambo Town and its watershed, West shoa zone, oromia regional State, Ethiopia', Journal of Hydrology: Regional Studies, 27, p. 100659. Available at: https://doi.org/10.1016/j.ejrh.2019.100659.

Ouma, Y.O. and Tateishi, R. (2014) 'Urban Flood Vulnerability and Risk Mapping Using Integrated Multi-Parametric AHP and GIS: Methodological Overview and Case Study Assessment', Water, 6(6), pp. 1515–1545. Available at: https://doi.org/10.3390/w6061515.

Owuor, S.O. et al. (2016) 'Groundwater recharge rates and surface runoff response to land use and land cover changes in semi-arid environments', Ecological Processes, 5(1), p. 16. Available at: https://doi.org/10.1186/s13717-016-0060-6.

Padhan, N. and Madheswaran, S. (2023) 'An integrated assessment of vulnerability to floods in coastal Odisha: a district-level analysis', Natural Hazards, 115(3), pp. 2351–2382. Available at: https://doi.org/10.1007/s11069-022-05641-z.

PBS (2023) Pakistan Bureau of Statistics, 7th Population and Housing Census - Detailed Results. Available at: https://www.pbs.gov.pk/digital-census/detailed-results (Accessed: 20 January 2025).

PMD (2024) Pakistan Meteorological Department - Pakistan Monsoon 2024 Analysis. Available at: https://cdpc.pmd.gov.pk/Monsoon_2024_update/Pakistan_Monsoon_2024_Rainfall_Update.pdf (Accessed: 15 February 2025).

Price, K., Jackson, C.R. and Parker, A.J. (2010) 'Variation of surficial soil hydraulic properties across land uses in the southern Blue Ridge Mountains, North Carolina, USA', Journal of Hydrology, 383(3), pp. 256–268. Available at: https://doi.org/10.1016/j.jhydrol.2009.12.041.

Proag, V. (2014) 'The Concept of Vulnerability and Resilience', Procedia Economics and Finance, 18, pp. 369–376. Available at: https://doi.org/10.1016/S2212-5671(14)00952-6.

Rahman, G. et al. (2017) 'Socio-Economic Damages caused by the 2014 Flood in Punjab Province, Pakistan', Proceedings of the Pakistan Academy of Sciences, 54, pp. 365–374.

Rahman, M. et al. (2019) 'Flood Susceptibility Assessment in Bangladesh Using Machine Learning and Multi-criteria Decision Analysis', Earth Systems and Environment, 3(3), pp. 585–601. Available at: https://doi.org/10.1007/s41748-019-00123-y.

Rentschler, J., Salhab, M. and Jafino, B.A. (2022) 'Flood exposure and poverty in 188 countries', Nature Communications, 13(1), p. 3527. Available at: https://doi.org/10.1038/s41467-022-30727-4.

Roy, A. and Dhar, S. (2024) 'Assessment of flood vulnerability and identification of flood footprint in Kelegħai River basin in India: a geo-spatial approach', Natural Hazards, 120. Available at: https://doi.org/10.1007/s11069-024-06411-9.

Saaty, R.W. (1987) 'The analytic hierarchy process—what it is and how it is used', Mathematical Modelling, 9(3), pp. 161–176. Available at: https://doi.org/10.1016/0270-0255(87)90473-8.

Saaty, T.L. (1990) 'How to make a decision: The analytic hierarchy process', European Journal of Operational Research, 48(1), pp. 9–26. Available at: https://doi.org/10.1016/0377-2217(90)90057-I.

Saaty, T.L. (1994) 'How to Make a Decision: The Analytic Hierarchy Process', Aestimum, 24. Available at: https://doi.org/10.13128/Aestimum-7138.

Sanders, B.F. et al. (2020) 'Collaborative Modeling With Fine-Resolution Data Enhances Flood Awareness, Minimizes Differences in Flood Perception, and Produces Actionable Flood Maps', Earth's Future, 8(1), p. e2019EF001391. Available at: https://doi.org/10.1029/2019EF001391.

Sanyal, J. and Lu, X.X. (2006) 'GIS-based flood hazard mapping at different administrative scales: A case study in Gangetic West Bengal, India', Singapore Journal of Tropical Geography, 27, pp. 207–220. Available at: https://doi.org/10.1111/j.1467-9493.2006.00254.x.

Subbarayan, S. and Saravanan, S. (2020) 'Modelling of Flood Susceptibility Based on GIS and Analytical Hierarchy Process—A Case Study of Adayar River Basin, Tamilnadu, India', in, pp. 91–110. Available at: https://doi.org/10.1007/978-981-32-9527-8_6.

Thomas, K. et al. (2018) 'Explaining differential vulnerability to climate change: A social science review', Wiley Interdisciplinary Reviews: Climate Change, 10, p. e565. Available at: https://doi.org/10.1002/wcc.565.

Ullah, N. et al. (2024) 'Geospatial analysis and AHP for flood risk mapping in Quetta, Pakistan: a tool for disaster management and mitigation', Applied Water Science, 14(11), p. 236. Available at: https://doi.org/10.1007/s13201-024-02293-1.

UNDP (2004) Reducing disaster risk a challenge for development. United Nations Development Programme Bureau for Crisis Prevention and Recovery. Edited by M. Pelling. New York: United Nations Development Programme.

UNDRR (2009) Definition: Exposure | UNDRR. Available at: https://www.undrr.org/terminology/exposure (Accessed: 1 December 2024).

UNISDR (2009) 'UNISDR terminology for disaster risk reduction'.

Waseem, H.B. and Rana, I.A. (2023) 'Floods in Pakistan: A state-of-the-art review', Natural Hazards Research, 3(3), pp. 359–373. Available at: https://doi.org/10.1016/j.nhres.2023.06.005.

WFP (2024) WFP Pakistan Floods Situation Report (August 2022 - December 2023) - Final report (January 2024) - Pakistan. Available at: https://reliefweb.int/report/pakistan/wfp-pakistan-floods-situation-report-august-2022-december-2023-final-report-january-2024 (Accessed: 14 February 2025).

Youssef, A. et al. (2021) 'The devastating flood in the arid region a consequence of rainfall and dam failure: Case study, Al-Lith flood on 23th November 2018, Kingdom of Saudi Arabia', Zeitschrift für Geomorphologie, 63. Available at: https://doi.org/10.1127/zfg/2021/0672.

Zanaga, D. et al. (2022) 'ESA WorldCover 10 m 2021 v200'. Zenodo. Available at: https://doi.org/10.5281/zenodo.7254221.

Zhran, M. et al. (2024) 'Exploring a GIS-based analytic hierarchy process for spatial flood risk assessment in Egypt: a case study of the Damietta branch', Environmental Sciences Europe, 36(1), p. 184. Available at: https://doi.org/10.1186/s12302-024-01001-9.

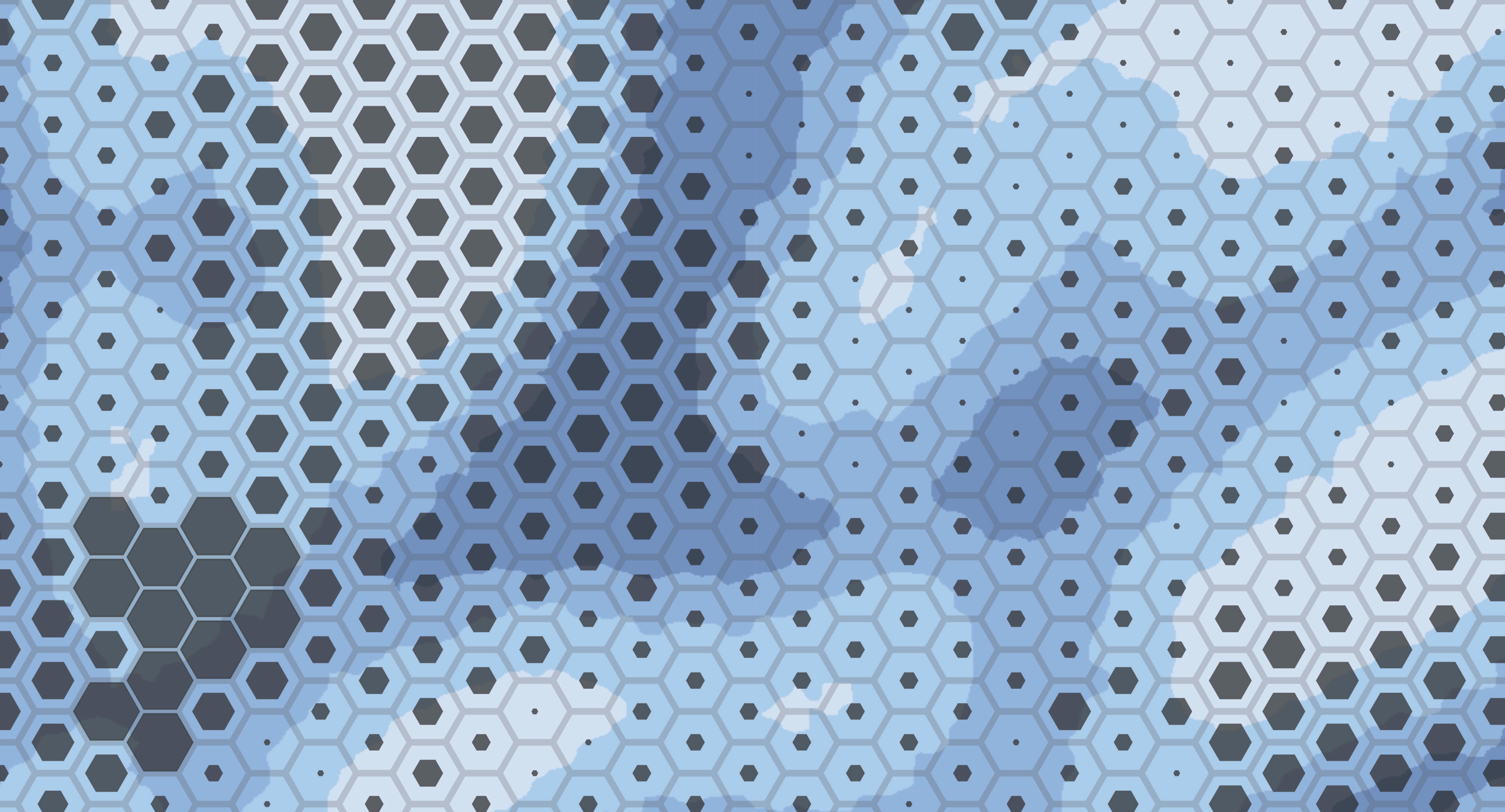

Flooding is one of the most destructive natural disasters, especially in regions with high population density like Punjab, Pakistan. This atlas presents a flood vulnerability framework, combining physical, environmental, and social factors to assess flood vulnerability and the impact on communities.

Gernot Nikolaus specializes in geospatial analysis, earth observation, and cartographic design.
With a master's thesis focusing on flood vulnerability in Punjab, Pakistan, Gernot aims to bring attention to climate change impacts through geospatial analysis and mapping techniques.

Message from the Author

This atlas was compiled as part of my master's thesis 'Flood Vulnerability in Punjab, Pakistan: A Geospatial Analysis and Cartographic Approach". Floods are one of the most severe catastrophic events, demanding human lives, leading to displacement, and the destruction of homes, infrastructure, and livelihoods.
Climate change exacerbates the frequency and intensity of such hazards - not only floods, but also others, such as droughts, sea level rise, and wildfires. While climate change is a global issue, it mainly affects the Global South. Millions of people are already forced to migrate due to hunger, conflict, and environmental collapse.
Everyone has the right to a safe, dignified life - something many of us take for granted because of the privileges we have been given.

I believe climate change is one of the greatest challenges of our era - and we are running out of time.
One of the barriers we face is the narrow-mindedness, denail, and indifference, especially those who think they are not affected. But we are all connected, and the suffering of others is not something we can afford to ignore.
The geospatial analysis was conducted, maps were created, and the atlas was compiled to support flood mitigation in Punjab, Pakistan, but also to raise awareness of climate impacts globally, through the lens of flooding. My hope is that it fosters understanding, empathy, and action.

Let us stop thinking only of ourselves, and instead be open to others - regardless of where they come from, their ethnicity, impairment, gender, sexual orientation, religion, or any other characteristics that make them who they are. We all share this planet, and we must care for it - and for each other - together.

Gernot Nikolaus

Palacký University Olomouc
PARIS LODRON UNIVERSITÄT SALZBURG
COPERNICUS MASTER IN DIGITAL EARTH
With the support of the Erasmus+ Programme of the European Union